PhD thesis

# Myocardial perfusion in heart disease

**Dr Kristopher D Knott**

**MRCP (UK) MBBS MA (Cantab)**

British Heart Foundation Clinical Research Training Fellow

Institute of Cardiovascular Science

University College London

**Supervisors**

Professor James Moon

Professor Sven Plein

**Declaration of originality**

I, Kristopher Knott, declare that the work presented in my thesis is my own. Where information has been derived from other sources, I confirm that this has been indicated in the thesis.

**Abstract**

**Heart disease:** Coronary heart disease is a major cause of mortality and morbidity in the UK and globally. It is managed with medical therapy and coronary revascularisation to reduce symptoms and reduce risk of major adverse cardiovascular events. When patients present with chest pain, it is important to risk stratify those that would most benefit from invasive coronary assessment and those that can be managed with medical therapy alone. Myocardial perfusion techniques have been developed in order to do this.

**Cardiovascular magnetic resonance (CMR) with stress perfusion:** CMR allows the non-invasive assessment of coronary artery disease (CAD). Under conditions of vasodilator stress, a gadolinium based contrast agent is injected and during the first pass through the left ventricle, perfusion defects can be observed. There is a strong evidence base for perfusion CMR but the technique is qualitative, relies on experienced operators and potentially misses globally low perfusion such as in cases of "balanced" ischaemia.

**Quantitative perfusion CMR:** In contrast, quantitative perfusion techniques allow the calculation of myocardial blood flow (MBF). It is more objective, less reliant on the expert observer and can give additional insights into microvascular disease and cardiomyopathy. As well as being less subjective, quantitative perfusion has other advantages for example it allows full assessment of ischaemic burden and may contain prognostic information that could be used to risk stratify and improve patient care. However, quantitative perfusion has been outside the realm of routine clinical practice due to difficulties in acquiring suitable data for full quantification and the laborious nature of analysing it.

**Perfusion mapping:** Peter Kellman, Hui Xue and colleagues at the National Institutes for Health, USA developed the "perfusion mapping" technique to address these limitations. Perfusion maps are generated automatically and inline during the CMR scan and each voxel encodes myocardial blood flow. This allows the instant quantification of MBF without complex

acquisition techniques and post processing. In this thesis I have taken perfusion mapping and deployed in the real-world at a scale an order of magnitude higher than prior quantitative perfusion studies, developing the evidence base for routine clinical use across a broad range of diseases and scenarios:

**In coronary artery disease:** I have shown that perfusion mapping is accurate to detect coronary artery stenosis as defined by 3D quantitative coronary angiography in a single centre, 50 patient study. Transmural and subendocardial perfusion are particularly sensitive to detect coronary stenoses with performances similar to expert readers. There is a high sensitivity and high negative predictive value making perfusion mapping a good "rule-out" test for coronary disease.

**Quantitative perfusion and prognosis:** I investigated whether stress MBF and myocardial perfusion reserve (MPR) calculated by perfusion mapping would encode prognostic information in a 1049 patient multi-centre study over a mean follow up time of 605 days. Both stress MBF and MPR were independently associated with death and major adverse cardiovascular events (MACE). The hazard ratio for MACE was 2.14 for each 1ml/g/min decrease in stress MBF and 1.74 for each unit decrease in MPR. This work can now be taken forward with prospective studies in order to better risk stratify patients, including those without perfusion defects on clinical read.

**Reference ranges and non-obstructive coronary disease:** I sought to determine the factors that contribute to perfusion in a multi-centre registry study. In patients with no obstructive coronary artery disease, stress MBF was reduced with age, diabetes, left ventricular hypertrophy (LVH) and the use of beta blockers. Rest MBF was influenced by sex (higher in females) and reduced with beta blockers. This study suggests patient factors beyond coronary artery disease (and therefore likely microvascular disease) should also be considered when interpreting quantitative perfusion studies.

**In cardiomyopathy:** I also investigated myocardial perfusion in cardiomyopathy looking at Fabry disease as an example disease. In a prospective, observational, single centre study of 44 patients and 27 controls I found Fabry patients had reduced perfusion (and therefore likely microvascular dysfunction), particularly in the subendocardium and was associated with left ventricular hypertrophy (LVH), glycophospholipid storage and scar. Perfusion was reduced even in patients without LVH suggesting it is an early disease marker.

In conclusion, in this thesis, I have developed an evidence base for quantitative perfusion CMR and demonstrated how it can be integrated into routine clinical care. Perfusion mapping is accurate for detecting coronary artery stenosis and encodes prognostic information. Further work in this area could enable patients to be risk stratified based on their myocardial perfusion in order to reduce the morbidity and mortality associated with epicardial and microvascular coronary artery disease. Following on from this work, two further British Heart Foundation Clinical Research Training Fellowships have been awarded to further investigate quantitative perfusion in patients following surgical revascularisation of coronary disease and in patients with hypertrophic cardiomyopathy.

**Impact statement**

In this thesis I have shown that:

**For single centres:** Quantitative perfusion can be readily integrated into routine clinical workflow; it is fast with no post processing and analysis required. Perfusion mapping can be relied upon for the accurate diagnosis of coronary artery disease and operators can have confidence in the results. Additional, prognostic information is provided alongside coronary disease assessment.

**For multi-centres:** Perfusion mapping allows the standardised analysis of myocardial perfusion, removing operator variability and therefore bias of centre size and expertise. There can be direct comparison between centres, allowing serial monitoring of patients.

**For patients:** Following perfusion CMR patients can be confidently diagnosed with coronary disease and have CAD more definitively ruled out if they have globally normal perfusion. They can greater understand their risk of a major adverse cardiovascular event depending on their myocardial perfusion. I performed the largest quantitative perfusion CMR study that looks at outcomes and the first multi-centre study in any modality of quantitative perfusion. For patients with Fabry disease specifically this was the first perfusion CMR study in Fabry disease, and the largest Fabry cohort studied with any perfusion modality. I have shown that myocardial perfusion is impaired in Fabry patients and thus microvascular dysfunction is a component in the pathophysiology of the disease. This may provide insights into other forms of cardiomyopathy going forward.

**For trials:** I have shown that quantitative perfusion is a new potential biomarker for clinical trials. Perfusion could be a drug target for macrovascular and microvascular disease and this work can be taken forward to see if patient outcomes can be improved by better targeting those with impaired perfusion.

**Acknowledgments**

I would like to thank all of the patients that consented to my study and to Barts Bioresource. Without their kind participation this thesis would not have been possible. The study would also not have been possible without the funding of the British Heart Foundation.

To James Moon, my supervisor, I will always be grateful for the training he has given me, the support through challenging times and the advice with the preparation of this thesis and the published manuscripts contributing to it. His inspiration and mentorship has been crucial during my research and I will take this forward into my future career.

I would also like to thank my second supervisor Sven Plein. He has always been available for advice and feedback and has been crucial throughout the project, providing additional guidance and support. I would also like to thank Peter Kellman, who has been like a third supervisor and friend, throughout the study. During our collaboration Peter has shown patience and kindness and has always been available to provide technical assistance and teaching during the research period. I am grateful for my friends and colleagues at Barts Heart Centre and University College London. To my peers Joao Augusto, Andreas Seraphim, Claudia Camaioni, Rebecca Hughes, Anish Bhuva, Paul Scully, Sabrina Nordin and Katia Menacho who have contributed directly and indirectly by helping create a fantastic work environment for us all to succeed. To my consultant mentors at Barts including Charlotte Manisty, Mark Westwood, Steffen Petersen and Thomas Treibel who have provided advice and support along the way. And to all of the radiographers at Barts and UCL, in particular Louise McGrath, Lizette Cash and Patricia Feuchter who trained me how to scan, supported me during the study and became friends. I am also grateful to the administrative staff who helped me book in study patients, often at short notice, and made the logistics of the study possible. Finally, I would like to thank my parents, Dave and Dawn, for always supporting me and my wife Venus for her love and support over the last 4 years.

# Contents

# List of tables

# List of figures

## Abbreviations

| | |
|---|---|
| ACS | Acute Coronary Syndrome |
| AF | Atrial Fibrillation |
| AI | Artificial Intelligence |
| AIF | Arterial Input Function |
| AUC | Area Under the Curve |
| BTEX | Blood Tissue Exchange |
| CABG | Coronary Artery Bypass Graft |
| CAD | Coronary Artery Disease |
| CCS | Chronic Coronary Syndromes |
| CER | Contrast Enhancement Ratio |
| CMR | Cardiovascular Magnetic Resonance |
| CNN | Convolution Neural Net |
| CFR | Coronary Flow Reserve |
| CMR | Cardiovascular Magnetic Resonance |
| CTCA | Computed Tomography Coronary Angiography |
| CVD | Cardiovascular Disease |
| DRA | Dark Rim Artefact |
| ECV | Extracellular Volume fraction |
| EDV | End Diastolic Volume |
| EF | Ejection Fraction |
| ERT | Enzyme Replacement Therapy |
| FD | Fabry Disease |
| FFR | Fractional Flow Reserve |
| Gd | Gadolinium |
| HCM | Hypertrophic Cardiomyopathy |
| HR | Hazard Ratio |
| HRA | Health Research Authority |
| IMR | Index of Microcirculatory Resistance |
| LGE | Late Gadolinium Enhancement |
| LVH | Left Ventricle Hypertrophy |
| MACE | Major Adverse Cardiovascular Events |
| MBF | Myocardial Blood Flow |
| MI | Myocardial Infarction |
| MICE | Multiple Imputation by Chained Equations |
| MOLLI | Modified Look Locker Inversion Recovery |
| MPR | Myocardial Perfusion Reserve |
| MPS | Myocardial Perfusion Scintigraphy |
| NHS REC | National Health Service Research Ethics Committee |
| PCI | Percutaneous Coronary Intervention |
| PET | Positron Emission Tomography |
| ROC | Receiver Operator Characteristic |
| QCA | Quantitative Coronary Angiography |
| SI | Signal Intensity |
| SPECT | Single Photo Emission Tomography |
| SSFP | Steady State Free Precession |
| T | Tesla |
| TIA | Transient Ischaemic Attack |

# 1. Introduction

The following review articles have been based on this introduction:
**Knott KD,** Fernandes JL, Moon JC. Automated Quantitative Stress Perfusion in a Clinical Routine. Magn Reson Imaging Clin N Am. 2019 Aug;27(3):507-520. doi: 10.1016/j.mric.2019.04.003. Epub 2019 May 13.
Seraphim A*, **Knott KD*,** Augusto J, Bhuva AN, Manisty C, Moon JC. Quantitative cardiac MRI. J Magn Reson Imaging. 2019 May 20. doi: 10.1002/jmri.26789. [Epub ahead of print] Review. ***Joint first author.**

## 1.1 The scale of the problem

Cardiovascular disease (CVD) is the leading cause of death globally (1). In the United Kingdom (UK) around 7 million people are living with CVD and each year 152,000 people die as a result of it (2). It is estimated that the associated total healthcare costs are around £9 billion annually (3). More recently, there have been improvements in the detection and treatment of CVD and these have resulted in falling rates of cardiovascular death over several decades, Figure 1.

Figure 1. Death rate from cardiovascular disease by gender, UK. The rates of death from cardiovascular disease are falling in the UK for men and women but remain high. *From the British Heart Foundation, UK factsheet, November 2018 (4).*

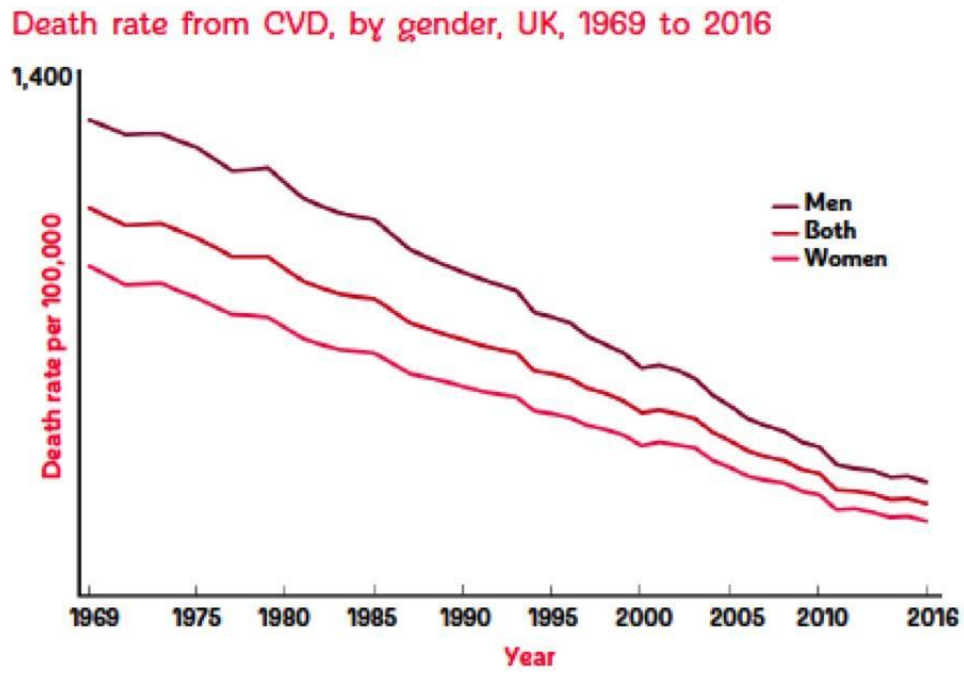

## 1.2 Coronary artery disease and the chronic coronary syndromes

CVD is a collection of diseases that affect the heart and circulatory system. The most common of these is coronary artery disease (CAD). CAD is the build-up of atheromatous plaque in the coronary arteries. This is a slow process, often building up over decades. It begins with lipid deposits in the arterial wall and the atheromatous cascade ultimately results in luminal narrowing. The luminal narrowing causes a mismatch between the myocardial blood supply and demand, particularly on exertion, causing chest pain (angina). Should the atherosclerotic plaque rupture, the subsequent thrombotic cascade results in heart attacks and death. Around 66,000 deaths are attributed to CAD each year in the UK (3).

There are treatment options available for CAD such as lifestyle changes, medical therapy and invasive interventional procedures. Aspirin and statins have been shown to reduce the rate of death and myocardial infarction when used for both primary and secondary prevention and form the mainstay of medical management (5–7). Obstructive CAD can also be treated invasively with percutaneous coronary intervention (PCI) or coronary artery bypass graft (CABG). In the context of myocardial infarction (typically plaque rupture with subsequent thrombotic occlusion of a coronary artery), urgent invasive revascularisation is lifesaving and recommended by all the major guidelines (8–11). However, more recent clinical trials have shown the need for caution with invasive management in patients with stable angina.

The most recent European Society of Cardiology (ESC) guidelines (12) make a distinction between acute coronary syndromes (ACS, including myocardial infarction and unstable angina) and chronic coronary syndromes. These chronic coronary syndromes (CCS), were previously labelled “stable CAD”, and are heterogenous and highlight the dynamic nature of coronary artery disease. They encompass the following clinical situations:

1. Patients with suspected CAD and stable symptoms
2. Patients with new onset heart failure or left ventricular (LV) impairment and suspected CAD
3. Patients < 1 year following ACS, with or without symptoms
4. Patients >1 year following ACS, with or without symptoms
5. Patients with angina and suspected microvascular dysfunction or vasospasm
6. Asymptomatic patients with CAD detected on screening.

The functional (haemodynamic) significance of the epicardial coronary lesion is also important in determining the appropriate management for the patient. This functional significance can be determined invasively by fractional flow reserve (FFR) by measuring the pressure proximal and distal to a lesion during vasodilator stress. It was shown in the multi-centre Fractional Flow reserve versus Angiography for Multivessel Evaluation (FAME) trial that performing PCI on a lesion with obstructive stenosis, as determined by FFR, resulted in a reduction in the composite endpoint of death, non-fatal MI and repeat revascularisation when compared to purely angiographically guided PCI (13,14). Performing PCI in addition to medical therapy may be superior to medical therapy alone in those with functionally significant disease (15). Additionally, intermediate coronary lesions have low event rates if there is no ischaemia (16,17). However, angiography and FFR uses ionising radiation, is invasive and consequently has risks associated with it (18,19). The Objective Randomised Blinded Investigation with optimal medical therapy or angioplasty in stable angina (ORBITA) study (20) compared PCI to a sham PCI procedure in patients with stable chest pain and found that there was no difference in a patient's symptoms or improvement in exercise tolerance between the groups at a follow up of 6 weeks. This suggests there is a significant placebo effect from PCI. Overall, non-invasive

testing is desirable to screen for those patients in which invasive management may be appropriate.

Patients with microvascular dysfunction often do not have flow-limiting epicardial coronary disease but disease of the coronary microcirculation. This may cause angina (which can mimic epicardial coronary disease), anxiety and potentially other psychological symptoms (21). Whilst invasive angiography and haemodynamic assessment can be useful in the work-up of these patients (22), the mainstay of treatment is lifestyle and medical therapy. Microvascular dysfunction is also thought to play a key role in the heart muscle diseases such as hypertrophic cardiomyopathy and Fabry disease although there is somewhat limited evidence in these rarer conditions.

In this thesis I will evaluate chronic coronary syndromes including CAD and microvascular dysfunction using non-invasive perfusion cardiovascular magnetic resonance (CMR) in various patient cohorts.

### 1.3 Non-invasive functional imaging in the real world

Non-invasive functional imaging techniques have been developed and are recommended in the contemporary clinical guidelines for the assessment of patients with suspected CAD / CCS (12,23,24). In Europe and the United States, the most widely available imaging modalities are cardiac computed tomography coronary angiography (CTCA), stress echocardiography (echo), cardiovascular magnetic resonance (CMR), single-photon emission computed tomography (SPECT) and positron emission tomography (PET). With the exception of CTCA, they assess CAD indirectly by observing perfusion (or ischaemia with stress echo) at the level of the myocardium. Each of these tests have high sensitivity and specificity for the detection of CAD in large clinical trials (25–29). CMR, SPECT and PET typically use a vasodilator stressor agent (such as adenosine) and a contrast agent to demonstrate areas of hypoperfused myocardium under conditions of maximal vasodilatation. The perfusion defects infer inducible ischaemia in the region of interest. In contrast, stress echo typically uses an inotropic agent such as dobutamine to demonstrate ischaemia directly. Non-invasive testing is recommended in international guidelines as the first line investigation in low to medium risk patients with suspected coronary artery disease (12,23,24).

There have been a multitude of studies demonstrating generally impressive results for non-invasive imaging in the diagnostic accuracy of CCS, and this would be expected to translate into substantial improvements in the management of patients. However, this has not always translated into real-world experience. Studies have found that non-invasive tests do not provide as much incremental improvement in evaluating CCS as would be expected from the randomised controlled trials above simple clinical risk assessment models. A real-world registry study included 398,978 patients from 663 hospitals attending for invasive coronary angiography of which 83.9% had a prior non-invasive test (68.6% positive) (30). Patients with

a positive non-invasive test had only a slightly higher prevalence of obstructive coronary disease (deemed >50% stenosis in a major coronary artery) - 41.0% vs 35.0%. There was only minimal incremental benefit of adding non-invasive testing over Framingham risk score, clinical risk factors and symptoms (C-statistic 0.761 vs 0.764 with the additional ischaemia test) and a positive non-invasive test was less associated with CAD than major clinical risk factors. However, this study was limited by including resting electrocardiogram and resting echocardiogram in the non-invasive testing models and the non-randomised nature of the study. In another large registry study of 549,078 patients in 224 hospitals, those with the most non-invasive imaging tests had the highest rates of admission, coronary angiograms and revascularisation (31). Readmission for acute myocardial infarction did not differ between those who had non-invasive testing and those that didn't. In that study over 96% of the testing was performed with SPECT and stress echo.

### 1.3.1 Cardiovascular magnetic resonance

CMR with stress perfusion assesses the first myocardial passage of a gadolinium based contrast agent during vasodilator stress (and repeated at rest) to detect myocardial hypoperfusion. From when it was initially described in 1990, it has now been validated against angiography (32–34) and invasive FFR (35–38) in numerous clinical trials. A normal perfusion CMR scan is reassuring, with a low subsequent cardiovascular event rate (39–41). The Cardiovascular magnetic resonance and single-photon emission computed tomography or the diagnosis of coronary heart disease (CE-MARC) trial prospectively enrolled 752 patients with suspected angina and at least one cardiovascular risk factor for perfusion CMR, SPECT and invasive coronary angiography. They demonstrated that CMR was superior to SPECT in detecting coronary artery disease (26). In a five year follow up study of the original CE-MARC cohort, an

abnormal CMR was found to be a stronger predictor of MACE than SPECT, independent of cardiovascular risk factors (42).

More recently, the magnetic resonance perfusion or fractional flow reserve in coronary disease (MR inform) trial prospectively randomised 918 patients with stable angina and at least 2 cardiovascular risk factors to a perfusion CMR or an invasive FFR guided management strategy (43). Patients with > 6% ischaemia on CMR (>1 myocardial segment) or an FFR of <0.8 were revascularized. The investigators found a CMR guided approach was non-inferior to an FFR guided approach in regard to major adverse cardiovascular events (MACE) at one year. There were fewer revascularisations in the CMR group and no difference in percentage of patients free from angina between the groups.

Another large study that looked at outcomes following CMR was the Clinical Impact of Stress CMR Perfusion Imaging in the United States (SPINS) trial (44). This was a 13 (USA-based) centre registry study of 2,349 patients, which followed up patients for 4 years after the perfusion CMR. They found that in those patients without ischaemia or infarction, the rate of adverse cardiovascular outcomes (cardiovascular death or non-fatal MI) was very low (<1%) and that perfusion CMR was a cost-effective test in these patients.

Additional advantages of CMR include the modality using no ionising radiation, having unlimited imaging planes (allowing imaging regardless of patient anatomy or body habitus), it enables optimal assessment of cardiac systolic function (using cine imaging for chamber volume analysis) and tissue characterisation including detecting myocardial infarction and viability assessment (using the delayed enhancement technique) (45–47). Consequently, in the UK, the field of CMR has been growing at the expense of nuclear ischaemia testing.

In usual clinical practice, CMR with stress perfusion involves the acquisition of three short axis left ventricle (LV) slices (basal, mid and apical) and occasionally a long axis view at stress and at rest during the first pass of a gadolinium based contrast agent (48). The reporting physician

compares the stress and rest images for each slice and notes the presence of reversible "perfusion defects" which are areas of myocardial hypoperfusion present at stress but not at rest. The amount of myocardial ischaemia can be estimated using the American Heart Association segment model (49). The LV is divided into 17 segments – 6 basal, 6 mid, 4 apical, plus the apical cap. The proportion of hypoperfused segments gives an estimation of LV ischaemia, with each segment representing approximately 6% myocardial ischaemia. Figure 2 shows an example of perfusion CMR images for a patient with right coronary artery stenosis. Perfusion CMR is highly operator dependent and requires a high level of expertise with level 3 accredited operators (the highest European Association of Cardiovascular Imaging, EACVI, accreditation) performing significantly better at identifying CAD than level 2 and level 1 operators (50). Furthermore, simply adjusting the window-level of the images can alter the apparent extent of hypoperfusion, which can lead to underestimating or overestimating the degree of ischaemia. There is also the possibility of missing truly "balanced" ischaemia (ischaemia in all 3 coronary vessels) which would cause global hypoperfusion rather than a relative perfusion defect. A more robust alternative is fully quantitative perfusion CMR where absolute blood flow is quantified in the myocardium.

Figure 2. Perfusion CMR for a patient with obstructive right coronary artery stenosis. The basal, mid and apical LV slices (left to right) are shown under conditions of vasodilator stress (A) and rest (B). The inferior perfusion defect can be visually appreciated (black arrows) in the basal and mid slices.

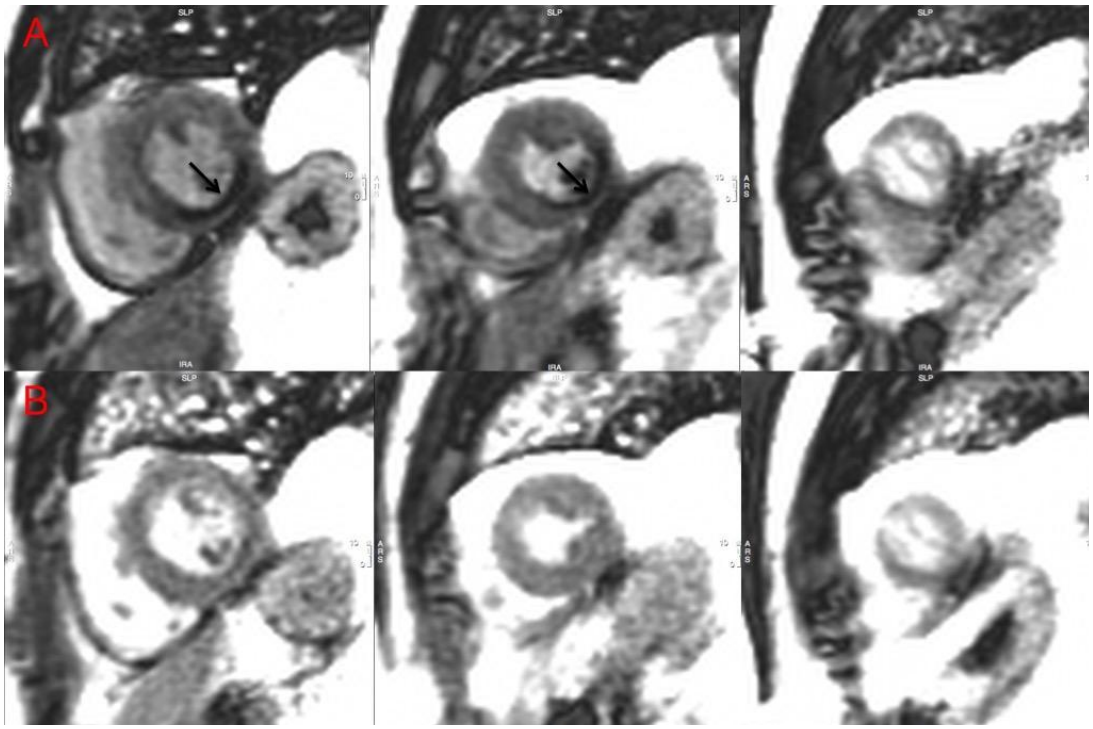

The diagnostic performance of CMR has been compared to coronary angiography in several single centre (34,51,52) and a few multi-centre studies (53,54). The majority of those comparing CMR with MPS have been single centre (26,55,56). These studies are potentially subject to "Expert Centre Bias". This is the phenomenon in which a centre shows that one modality is superior to another but at least some of the difference may be explained by the lack of expertise in the other modality, the use of out-dated equipment or image analysis software (57,58). For example the sensitivity and specificity of SPECT was 66.5% and 82.6% respectively in CE-MARC compared to 90% and 86% respectively in a 202 patient single centre study in 1996 (59).

Meta-analyses have been performed which show that perfusion CMR is highly accurate for the detection of CAD (35,38) . However, there are several limitations with combining the studies in the meta-analyses due to the considerable heterogeneity with the studies. For example, in their meta-analysis, Hamon et al. found that the concentration of gadolinium used varied from 0.025 to 0.15mmol/kg. There is currently no consensus of the most appropriate dose and two studies have found conflicting results. The first found that a dose of 0.05mmol/kg was at least as efficacious as higher doses (0.15mmol/kg) (53). The second, Magnetic Resonance Imaging for Myocardial Perfusion Assessment in Coronary artery disease trial (MR IMPACT), showed the most efficacious dose was 0.1mmol/kg (the highest dose used in the study) (60). There is also a variation in the clinical protocol used in perfusion studies. The most "real-world" setting would be to use a multiparametric CMR approach (a combination of cine, scar imaging in addition to the perfusion). This has been shown to improve the diagnostic accuracy of coronary artery disease (52,61,62). This is not done in all trials with some considering only the stress and rest perfusion components of the CMR scan and so could potentially have reduced the pooled accuracy in meta-analyses.

Furthermore, there is much heterogeneity in the stress protocol. In perfusion CMR, one of 3 main stressor agents are chosen - adenosine, dipyridamole and regadenoson. It has been suggested that adenosine is superior to dipyridamole but there is limited evidence and further work is needed (35).

The SCMR have produced guidelines (48) on the standardisation of perfusion CMR but within this there is uncertainty and scope for variation. The protocol at Barts Heart Centre involves an adenosine infusion at a rate of 140mcg/kg/min for 4 minutes which should be increased to 175mcg/kg/min if there are no symptoms and no heart rate response (increase by 10 beats per minute, bpm) after 2 minutes. However haemodynamic response to adenosine correlates poorly with stress myocardial blood flow (63). This calls into question the appropriateness of using haemodynamic and symptom assessment to ensure adequacy of adenosine stress.

Medication may also impact the adequacy of vasodilator stress. Studies have shown that beta adrenoreceptor blockade reduces the extent and severity of perfusion defects in MPS studies (64) and for this reason they may be withheld for 3-5 days prior to the scan in some centres. This may be the case with other anti-anginal agents such as calcium channel blockers and nitrates (65). Such studies have not taken place for CMR but similar effects may occur. Medications are not routinely halted before perfusion CMR and in the literature to date a variety of protocols regarding medication suspension have been used.

Splenic switch off is a useful sign of stress adequacy (66). Adenosine and dipyridamole (but not regadenoson) reduces splenic blood flow, in contrast to the increase in myocardial blood flow, and the spleen darkens in adequately stressed patients. The splenic switch off sign has not been used routinely in clinical trials, and so the sensitivity of the test may have been underestimated in these trials compared to contemporary practice in real world centres in which the splenic switch off sign is routinely used to assess stress adequacy. There are drawbacks to the splenic switch off sign. It is only possible to see splenic switch off during the

scan once the contrast has been administered so does not allow for further or increased stressor dose during the scan.

Further heterogeneity exists in the variety of scanner vendors, magnetic field strength (1.5 vs 3 Tesla, T), perfusion sequence and post-processing software. The technique is qualitative (a relative difference in perfusion is appreciated) and reliant on operator experience and familiarity with the local setup. To gain this clinical experience and attain results as impressive as the trials therefore is problematic, particularly in low volume centres.

### 1.3.2 Myocardial Perfusion Scintigraphy

Myocardial Perfusion Scintigraphy (MPS) with Single Photon Emission Computed Tomography (SPECT) was the first widely available imaging test used to non-invasively assess coronary disease. Early studies in the 1980s showed good sensitivity and specificity for the detection of coronary artery disease (25,67,68), comparable to recent CMR and stress echo data. Typically, a radio-isotope is injected and myocardial uptake compared under conditions of stress and rest. The heterogeneity of approaches is particularly varied. There are a multitude of stressor agents, radionuclear isotopes, stress durations, analysis approaches and analysis software.

The choice of stressor agent employed is typically the same as CMR (adenosine, dipyridamole or regadenoson) but also exercise can be used. Although not directly compared, a number of studies have shown high diagnostic accuracy with each of them (e.g. (69–71)). Caution should be used in pooling accuracy across each of these. A potential benefit of MPS is the ability to use exercise as a stressor which is more straightforward and physiological than with other modalities. It is important to ensure the exercise is sufficient as sub-maximal exercise can reduce the sensitivity of the test (67). Combining exercise and adenosine may reduce side effects but does not improve the sensitivity and may improve scan tolerance (72). Rather than

a contrast agent, MPS uses a radio-isotope which is taken up by the myocardium. The choice of radio-isotope is most commonly thallium, MIBI or tetrofosmin. They all have similar sensitivities when compared head to head but there are some technical differences between them (73). The methodology of the MPS in any given centre may deviate from the trial protocols due to the heterogeneity in approach.

Referral bias is prominent in many MPS studies and may therefore influence study outcomes and the conclusions drawn from them. For example, many of the studies only perform the gold standard test of invasive angiography on patients who have an abnormal MPS. The sensitivity of the test is therefore artificially increased and the specificity decreased, but this may reflect real world experience. One trial where referral bias was minimised was the CE-MARC trial (26) in which all patients had MPS, CMR and invasive coronary angiography. This may in part explain why the diagnostic accuracy of MPS was lower in this study than other studies (74). A large study in which only patients with abnormal MPS had coronary angiography had a sensitivity of 98% and specificity of 13%. However, once corrected for referral bias, this changed to 65-67% and 67-75% respectively (depending on methodology of correction) (75). Therefore, the real-world sensitivity and specificity of MPS is likely to be somewhat lower than the clinical trials. With advances in technology, the most up to date MPS scans involve latest generation cameras, reconstruction, attenuation and resolution correction algorithms (76). However not all centres have such techniques and technology available. Older studies using out-dated equipment, compared to new technology (such as CMR) in more modern studies may under-estimate the diagnostic capabilities of up to date MPS techniques.

### 1.3.3 Stress echocardiography

While vasodilator stress echocardiography is possible, the most common stressor agents are dobutamine or exercise. Rather than vasodilate and create perfusion mismatches in regions

supplied by stenosed epicardial coronary arteries, they work by increasing myocardial oxygen demand and inducing wall motion abnormalities. Viability information can also be obtained: If the myocardium is hypokinetic at rest but improves with low-dose dobutamine it is likely to be viable (77,78), known as the biphasic response to stress. The trial data for sensitivity, specificity and accuracy is comparable to other imaging modalities and there are similar biases in the studies which should influence their interpretation.

First of all there is some heterogeneity in protocol and image analysis. There are however, international society guidelines which can be followed such as the European Association of Echocardiography and AHA guidelines (79,80) to minimise this heterogeneity. Dobutamine is infused at an increasing concentration at 3-minute intervals (5 to 40 mcg/kg/min) and if target heart rate (85% maximal) is not attained atropine may also be given. At each stage of the test a visual assessment is made as to whether the myocardium is normokinetic, hypokinetic, akinetic or dyskinetic. Image quality and image interpretation is variable. One study estimated that the image quality in up to 30% of exercise stress echoes was suboptimal (81). One way to improve image quality and increase sensitivity and specificity is to use contrast (82). This adds heterogeneity to studies and is not routinely done at all centres.

There is a wide range of variability in the exercise protocol performed. Some centres use a modified Bruce protocol, others supine bicycle. Therefore, the level of exercise achieved may be variable and comparing studies is problematic. It is also vital to ensure a patient remains under exercise conditions when they move from treadmill to couch in exercise treadmill tests and acquire images as quickly as possible. Despite these limitations, studies have compared exercise and dobutamine stress to a gold standard of coronary angiography and shown them to have high sensitivity, specificity and diagnostic accuracy (83,84).

There are again biases in the data which impact on the real-world applicability. Some of these are the same as other functional tests for example the gold standard has generally been visual assessment at coronary angiography (83,84). Whether this biases in favour or against stress echo is questionable. Also the studies have been predominantly single centre with the associated problems of generalisability (29,85–88)

There are also more general issues with the applicability of the trial results. In some patient groups stress echo has been found to be less reliable. For example in akinetic myocardial segments the sensitivity of stress echo to predict viability falls significantly and may be as low as 68% (89). Sensitivity also falls in patients with impaired LV function although may still be preferable to MPS due to its higher positive predictive value (90). In summary, although the sensitivity, specificity and accuracy in an optimised patient population are high, this is unlikely to be the case in the real world.

### 1.3.4 Positron Emission Tomography

Cardiac PET perfusion is accurate in detecting functionally significant coronary artery disease (91–93). Perhaps the unique feature for PET has been accurate quantification of myocardial perfusion and not solely rely on a purely visual assessment. Quantitative PET has also shown the prognostic value of myocardial perfusion reserve in large cohorts of patients (94–96). PET relies on the principle of coincidence detection of pairs of high-energy photons produced from the annihilation of an emitted positron with a free electrode. With hybrid CT technology, there is the ability to correct for attenuation and scatter which often causes artefact in MPS (97). Similar to other technologies, there are technical features that can improve image quality including filtered-back projection and iterative reconstruction approaches. In general, PET takes place in expert centres due to the limited availability of PET and centralisation of scanners due to requirements for on-site cyclotrons or large-scale production of tracers.

Similar to other functional modalities, there is a substantial heterogeneity to the approach and trial data and a number of pitfalls are those shared with other imaging modalities. For example, the choice of vasodilator stressor agent (similar to CMR and SPECT), whether to hold medication prior to the scan and the gold standard to which PET has been assessed has typically been visual assessment of invasive coronary angiography (92,93). The choice of tracer is more complex and depends on a variety of factors.

The main tracers in clinical use are $^{15}$O-water, $^{82}$Rb and $^{13}$N-ammonia. $^{15}$O-water and $^{13}$N-ammonia require an on-site cyclotron (98,99). Previously this has been prohibitive but with more widespread use of PET in oncology studies this is becoming more widely available. However, $^{15}$O-water requires more specialist processing. $^{82}$Rb can be produced in a generator off-site with a good shelf life of around 5 weeks. However, large batches are produced requiring the site to have high patient numbers (98). The tracers are also interpreted depending on whether they are suited to qualitative perfusion defects or quantitative perfusion (100). $^{15}$O-water has a high extraction fraction so is highly accurate for myocardial blood flow quantification, but the short half-life and fast tissue washout prevent qualitative assessment. $^{13}$N-ammonia allows better qualitative assessment whilst allowing good quantitative perfusion (although not as accurate as $^{15}$O-water). $^{82}$Rb is the most generally available tracer but has a shorter half-life than $^{13}$N-ammonia with a consequent reduction in visual image quality and with a lower extraction fraction reducing the accuracy of quantitative perfusion.

For PET studies using tracers in which quantitative myocardial perfusion is performed, there is considerable heterogeneity between software packages. Monroy-Gonzalez et al analysed the scans of 91 patients with normal perfusion, reversible perfusion defects and fixed perfusion defects using three widely used and clinically available software packages (101). There were considerable differences with the calculated myocardial blood flow (MBF) between software

packages, particularly in the patients with reversible perfusion defects and normal perfusion. There are also heterogeneities in MBF depending on the tissue model used to quantify perfusion (102,103). This has implications when making diagnoses of coronary artery disease based on absolute cut-off values for MBF.

### 1.3.5 Cardiac CT

In the UK and worldwide, there remains a debate around the importance of ischaemia testing as a first line investigation for chest pain. An alternative viewpoint is that an anatomical test should be used initially. Unlike the previously discussed imaging modalities, cardiac CT is an anatomical rather than functional test for the presence of obstructive coronary artery disease. A coronary calcium score can give important prognostic information (104–106) and the coronary angiogram can show the presence of obstructive coronary artery disease. The relative cost-effectiveness, availability and high negative predictive value (107,108) have resulted in the National Institute for Health and Clinical excellence (NICE) in the UK recommending it as the first line investigation for all patients presenting with typical and atypical angina and functional tests only if there is diagnostic uncertainty (24). This differs somewhat from the European Society of Cardiology guidelines whereby the recommendation for cardiac CT remains first line only for patients at low or intermediate risk of coronary artery disease and they continue to recommend functional test for patients at intermediate risk (109). Sensitivity and specificity for the detection of coronary artery disease has been shown to be extremely high in a number of clinical trials, 94-100% and 89-91% respectively in meta-analyses (110–112) and this contributed to the increased interest in the field. However, there are a number of inherent biases in the trial data that reduce its generalisability and

applicability. The biases are similar yet subtly different to those for the functional ischaemia tests.

First of all, it is unsurprising that the apparent sensitivity and specificity of cardiac CT is higher than functional imaging modalities due to the fact that we are comparing an anatomical test to the gold standard of invasive coronary angiography which is also an anatomical test. Again, we have a problem of using a poor gold standard but for cardiac CT this results in a positive bias in favour of CT compared to the negative bias seen with functional tests. Meta-analyses of CT studies use visual assessment of invasive coronary angiography or quantitative coronary angiography (QCA), typically with a cut off of 50-70% stenosis being called positive. FFR has not been commonly used as the gold standard comparator and so the presence of disease may be there, but the lesion felt not to be functionally significant at invasive angiography and so does not change management of the patient. Intermediate stenoses may or may not be flow limiting and this is difficult to determine from visual analysis. One study that did use FFR as a gold standard was the NXT study (113). Diagnostic accuracy of cardiac CT with and without CT-FFR was compared to a gold standard of invasive coronary angiography. The sensitivity for cardiac CT remained high at 94% but specificity dropped to 34%. The values for CT-FFR were 86% and 79% respectively, indicating the additional value of the functional assessment.

The next bias with cardiac CT is using trial data focusing on low-intermediate risk patients with a potentially lower prevalence of flow-limiting coronary artery disease and extrapolating the results to higher risk populations. For example the EVINCI trial found cardiac CT to be more accurate than functional imaging tests (114) in a low CAD prevalence European population. The problem with this is that the diagnostic accuracy is very high in low risk patients, but this is not necessarily the case with the higher risk patients. High-risk patients may have abnormal findings on CTCA which are either artefactual, precluding sufficient analysis or are not functionally significant. For example the prospective multicentre imaging

study for evaluation of chest pain (PROMISE) trial randomised patients with no history of coronary disease attending chest pain clinic to either an anatomical imaging strategy with cardiac CT or a functional imaging strategy (115). They demonstrated that there were more invasive angiograms performed in patients who were investigated with CT than those with a functional test but there was no difference in cardiovascular outcomes. In a large real world patient population including low and high risk patients, the diagnostic accuracy may be significantly lower than what is seen in trials with a lower prevalence of coronary artery disease.

Similarly, despite the apparent greater detection of coronary artery disease, the prospective longitudinal trial of FFR CT: outcome and resource impacts (PLATFORM) trial randomised patients to CT or CT derived FFR to compare the percentage of patients with no obstructive coronary disease at angiography (116). The study showed that 85.9% of those referred for a coronary angiogram following an abnormal CT coronary angiogram had no obstructive coronary artery disease. This compared to 7.7% in the group with the additional functional imaging component. CT stress perfusion has also been developed in which the passage of contrast is observed during vasodilator stress (117). This technique, when used in combination with CTCA is potentially more accurate than CT FFR when compared to invasive FFR at the expense of a higher radiation dose (118).

Finally, similar to functional imaging, the technology available is different in the typical real-world centres compared to expert centres. As for other imaging modalities there are a number of vendors, scanner models and post-processing software. This makes extrapolating the data from these centres to the general cardiology community problematic.

### 1.3.6 Summary

Despite excellent clinical trial evidence of non-invasive imaging in the detection of coronary artery disease it is not always mirrored by real world performance. This is mostly down to

inherent bias in clinical trial data, variability in protocol, image acquisition and post-processing and the use of sub-optimal gold standards. In order to improve real world performance, it is important to standardise protocols, make image analysis less subjective, ensure patients are sufficiently stressed, design clinical trials to minimise bias and to compare like with like. Practical ways that this could be done would be to produce Society guidelines for the standardisation of stress imaging protocols. This would allow greater comparison between centres and better generalisability of study results. An example of standardising image analysis would be to make non-invasive imaging techniques more quantitative. This would remove the subjective element of image analysis. For example, CT-FFR and CT perfusion (including quantitative perfusion) data is promising and provides a more objective way of assessing coronary anatomy. Another example is quantitative perfusion CMR which has historically been solely a research tool. In the field of stress echo, strain imaging during stress has shown promise in improving the diagnostic accuracy and may make the analysis more objective (119). Furthermore, contrast should be used routinely and perhaps with 3D stress echo becoming more widely available, image acquisition time will be reduced improving quality of assessment. In the field of PET there is increasing interest in newer 18F labelled tracers which hope to combine the image quality and perfusion quantification without the need for an on-site cyclotron (120).

Multi-centre studies with outcome data are required for each imaging strategy. The MR INFORM is one such trial in CMR, which compared outcomes for patients undergoing an invasive FFR strategy of perfusion CMR (43). Major adverse cardiovascular end-points were not significantly different in those managed according to a functional imaging or invasive angiography with FFR strategy. Similarly, in CT, the coronary CT angiography and 5-year risk of myocardial infarction (SCOT-HEART) trial has shown that patients managed with a CTCA in addition to standard care had a lower rate of death or non-fatal MI at 5 years compared with

standard care alone, without increasing the rate of coronary angiography (121). However, in the symptoms and quality of life analysis of patients in the SCOT-HEART trial, Williams et al. found that those patients in the CT arm had less marked improvements in symptoms and quality of life compared to the patients treated with the standard of care (122). The reasons for this were not elucidated in the trial but it is plausible that there were some patients who had anginal symptoms due to microvascular dysfunction and vasospastic which was not detected by the CT scan. It's possible that these patients had anti-anginal therapy discontinued as there was no obstructive epicardial disease seen on CT. Non-invasive functional testing could potentially identify reduced myocardial perfusion in this group of patients which would allow targeted therapy.

In this thesis, I will attempt to improve the non-invasive assessment of patients with CCS by addressing some of the limitations in CMR perfusion. I will develop an evidence base for quantitative CMR in the diagnosis of coronary artery disease and the investigation of microvascular dysfunction and will investigate where there is useful prognostic data in fully quantitative perfusion with respect to patient outcome.

### 1.4 The advantages of fully quantitative perfusion in CAD

Fully quantitative perfusion has been well established and well validated in the PET literature conferring advantages in the diagnosis of CAD but also extending beyond this. Quantitative PET perfusion was shown by Gould et al to be highly sensitive and specific for the detection of CAD (123). The coronary flow reserve (CFR, the ratio of stress myocardial blood flow to rest myocardial blood flow) was deemed abnormal if less than 3.0 and 95% specific and 100% sensitive for the detection of CAD in a 50 patient cohort. Furthermore, quantitative PET perfusion has been validated against FFR. In 104 patients at moderate risk of CAD, absolute quantification had a significantly higher positive predictive value, negative predictive value and diagnostic accuracy for the detection of functionally significant stenoses in comparison with standard PET perfusion (124). The inter-observer variability of perfusion assessment was also lower with absolute quantification. Quantitative perfusion in CMR has been shown to be non-inferior to expert clinical observers (level 3) and superior to level 1 and level 2 operators (50).

In patients with multi-vessel coronary atherosclerosis, quantitative perfusion is advantageous. PET studies have found that it is possible to appreciate more extensive ischaemia with quantitative techniques than with qualitative approaches in patients with multi-vessel disease (125). Similarly, in CMR, the myocardial blood flow (MBF) and the myocardial perfusion reserve (MPR, stress MBF to rest MBF, which is similar to CFR in PET studies) has been shown to effectively discriminate between single and three-vessel disease in a way that was not possible with qualitative perfusion (126), in an influential but small study of 30 patients. In summary, more extensive CAD is better characterised with quantitative perfusion which may lead to more appropriate patient management.

### 1.5 Advantages of quantitative perfusion beyond obstructive CAD

Beyond the investigation of potentially obstructive CAD, quantitative analysis has additional advantages over qualitative perfusion. There is important prognostic information encoded in the stress MBF and the perfusion reserve, which is likely to be related to the extended spectrum of CCS. This has been studied with PET previously. In a 256 patient study referred for ammonia PET perfusion for standard clinical indications, the cohort included 150 patients with known CAD and the entire cohort was followed up for a mean of 5.5 years (94). The rates of death and major adverse cardiovascular events (MACE) were higher in patients with a CFR less than 2 than in patients with a CFR greater than 2. This was true for patients with perfusion defects indicative of obstructive coronary disease and for those without. Patients with perfusion defects and a CFR <2 had worse outcomes than those with a CFR >2. Similarly patients with no perfusion defects but a CFR <2 did worse than those with a CFR >2.

Myocardial perfusion is also important in patients with non-ischaemic cardiomyopathies. Neglia et al. prospectively recruited 67 patients with LV impairment to undergo PET perfusion imaging (127). Following a mean of 45 months follow up, they found that patients with the most severely impaired stress MBF (≤ 1.36 ml/g/min) and rest MBF (≤ 0.65ml/g/min) had the worst outcomes. These patients had a relative risk of death or progression of heart failure of 3.5 and 3.3 compared to those with stress MBF > 1.36 ml/g/min and rest MBF > 0.65ml/g/min respectively. The five-year event free survival was 35.8% in patients with stress MBF ≤ 1.36 ml/g/min compared to 79% in those with MBF > 1.36ml/g/min. Following multiple linear regression, they found that stress MBF, resting heart rate and end diastolic volumes were independently associated with outcome.

Myocardial perfusion is also impaired in other cardiomyopathies. For example, patients with hypertrophic cardiomyopathy (HCM) commonly have symptoms including chest pain and have

electrocardiogram (ECG) abnormalities such as deep T wave inversion, which are often associated with ischaemia. This may at least in part be related to microvascular dysfunction (128) and acute and chronic ischaemic injury is seen at autopsy (129). Perfusion abnormalities have been seen with SPECT and are associated with syncope, cardiac arrest and ventricular arrhythmias in young patients (130). Patients with HCM have impaired stress perfusion compared to healthy controls (see example Figure 3). These perfusion abnormalities are associated with areas of fibrosis and hypertrophied myocardium but may also be present in non-hypertrophied segments (131). Furthermore, perfusion is an independent predictor of death and adverse cardiovascular events in HCM. In a prospective cohort study, Cecchi et al enrolled 51 HCM patients and 12 controls with atypical chest pain for quantitative PET perfusion (132). They found that following a mean follow up of 8.1 years, those with the most severely impaired perfusion had a higher incidence of death, progression in New York Heart Association (NYHA) functional class or sustained ventricular arrhythmias than those with less pronounced perfusion abnormalities.

Similarly, perfusion is affected in other cardiomyopathies that have a hypertrophic phenotype. Fabry disease (FD) is a multi-system disorder that occurs due to a defect in the alpha-galactosidase enzyme. An inability to break down sphingolipids results in accumulation in tissues such as the brain, kidneys and the heart (133). Cardiac sphingolipid accumulation occurs slowly over decades and ultimately can result in heart failure, arrhythmia and death. CMR has been used to investigate the pathological processes occurring in the myocardium. Sphingolipids accumulate in the myocardium and over time there is inflammation, LVH and eventually fibrosis. The sphingolipid accumulation can be detected with CMR as low myocardial native T1, the LV mass measured with cine imaging, the inflammation as high myocardial T2 and scar with LGE and extracellular volume fraction (ECV) (134,135). There have been PET studies in which perfusion has been shown to be impaired in FD and perfusion

has not been shown to change in response to alpha-galactosidase enzyme replacement therapy (ERT) (136). No studies have looked at the relationship between perfusion and the other disease processes in FD, which is possible with multiparametric CMR.

Figure 3. CMR with stress perfusion for a patient with apical HCM. The 2 chamber, base, mid and apical LV slices are shown at stress (A) and rest (B). There is a circumferential perfusion defect in the hypertrophied apex (arrows).

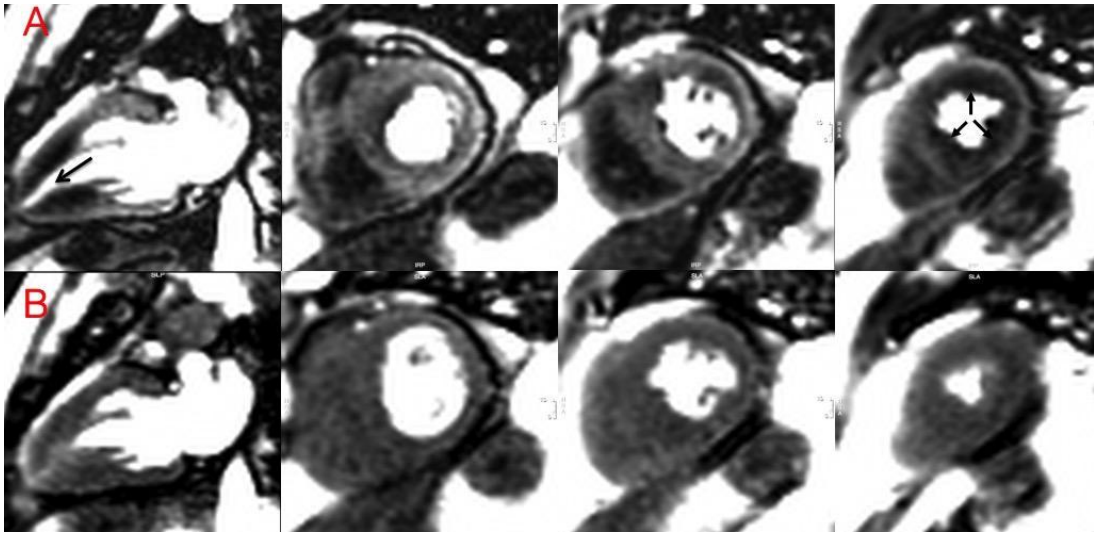

## 1.6 Methods of quantifying perfusion CMR

### 1.6.1 Semi quantitative perfusion

In order to improve upon the subjective nature of CMR perfusion imaging, semi-quantitative CMR techniques were first developed. These techniques rely on the measurement of signal intensity (SI) in the myocardium during the first pass of contrast. The analysis requires the use of dedicated software. Signal intensity-time curves are plotted for each myocardial segment and give a semi-quantitative assessment of myocardial perfusion. There are many different semi-quantitative methods including the contrast enhancement ratio (CER), the myocardial-to-LV upslope index ratio and upslope integral ratio (137).

The CER is calculated for each myocardial segment according to the following equation, where the $SI_{peak}$ is the maximum signal intensity measured during the passage of contrast in the region of interest and the $SI_{baseline}$ is the mean baseline SI measurement:

$$CER = (SI_{peak} - SI_{baseline}) / SI_{baseline}$$

The myocardial to LV upslope is calculated by dividing the initial upslope of the myocardial time-signal intensity curve by the initial upslope of the LV blood pool myocardial time-signal intensity curve (51):

$$\text{Myocardial to LV upslope index} = \text{Upslope } SI_{myocardium} / \text{Upslope } SI_{blood}$$

The upslope integral ratio is the area under the curve of the upslope of the myocardial SI-time for the region of the myocardium, having adjusted for the baseline (138):

$$\text{Upslope integral ratio} = \text{Area under the curve (upslope} - \text{baseline)}$$

These methods have been compared to absolute MBF quantification in patients using PET perfusion (51) and invasive angiography (139) and in animal models using microspheres (137).

Semi-quantitative perfusion has given mixed results in clinical studies. Schwitter et al. compared the myocardial LV upslope index to PET and quantitative angiography. Against the gold standard of PET, it performed well with a sensitivity, specificity and area under the curve (AUC) of 91%, 94% and 93% respectively for the detection of CAD. Compared to quantitative angiography (diameter stenosis >50%) the diagnostic performance remained high but lower than the PET comparison - 87%, 85% and 91% for sensitivity, specificity and AUC respectively (51).

Mordini et al. also compared semi-quantitative perfusion CMR to quantitative coronary angiography with inferior results (139). They found that the sensitivity, specificity and AUC for the CER method was 57%, 91% and 78% respectively, LV to myocardial upslope method 87%, 68% and 82% respectively and the upslope integral ratio 83%, 68% and 75% respectively.

At low MBF values all of the semi-quantitative perfusion methods have a linear relationship with absolute blood flow as measured with microspheres in animal studies (137). However, as the absolute flow increases (such as during exercise or with vasodilator, hyperaemic flow), the semi-quantitative methods all underestimate flow and the linear relationship is lost (Figure 4). Of these, the most robust semi-quantitative method appeared to be the upslope integral ratio, which maintains the linear relationship with flow until an MBF of around 3ml/g/min. However above this rate, flow is underestimated. The CER and the LV to myocardial upslope ratio methods perform even less well. They begin to underestimate absolute MBF from 1ml/g/min.

Figure 4. The relationship between semi-quantitative perfusion analysis and absolute blood flow as measured using microspheres in a canine model. Each of the semi-quantitative techniques maintain a linear relationship until 1ml/g/min after which point the CER and myocardial to LV upslope ratio lose this linearity. The upslope integral method performs best, but only up until flow rates of around 3ml/g/min. From Christian et al (137).

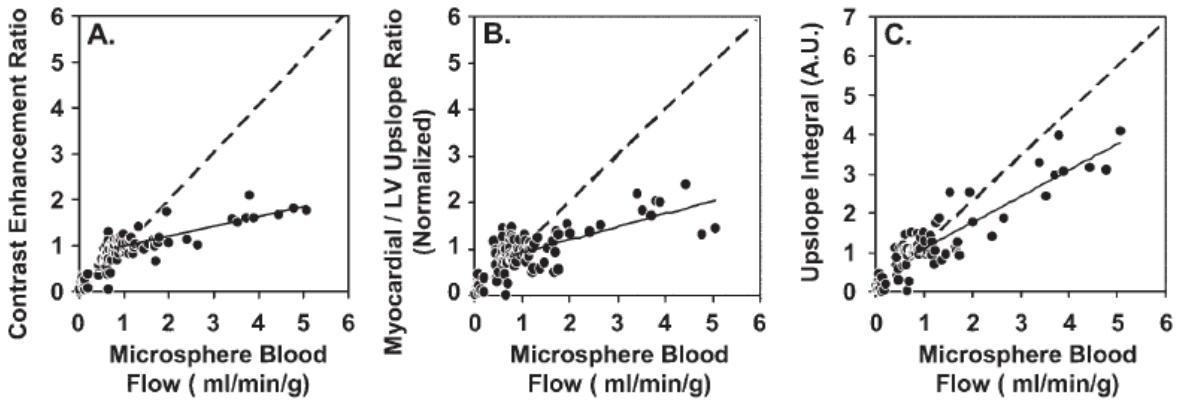


Practically, the procedure for semi-quantitative perfusion calculation is time consuming and complex. Endocardial and epicardial contours are traced on each LV short axis perfusion slice and adjusted for each phase (typically at least 50 phases). This can make the analysis of each scan laborious and puts the process beyond routine clinical use (see Figure 5).

In summary, the non-linear relationship between semi-quantitative perfusion and absolute MBF with the underestimation of hyperaemic flow and the time taken to perform the analysis make semi-quantitative assessment of perfusion not enough of an incremental improvement relative to qualitative approaches to be integrated into routine clinical practice.

Figure 5. An example of semi-quantitative perfusion analysis for a patient with RCA stenosis. Epicardial (green) and endocardial (red) contours are manually drawn on each slice and for each phase (A). Slide B demonstrates that the signal intensity in the remote myocardium (purple arrow and purple curve) is higher than in the ischaemic segment (blue arrow, blue curve). Following semi-quantitative analysis with the contrast enhancement ratio, a bulls-eye plot for each AHA demonstrates the impaired perfusion inferiorly.

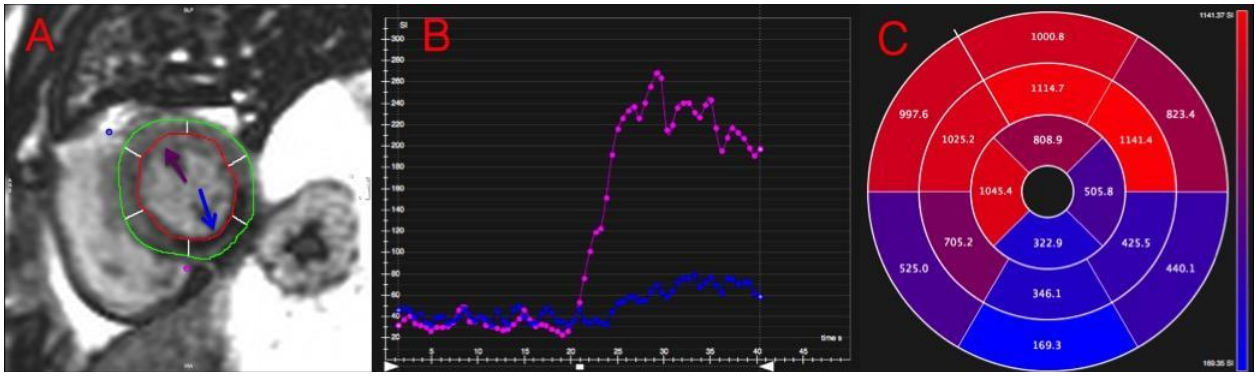


1.6.2 Absolute quantification of perfusion with CMR

To improve the accuracy of perfusion quantification, absolute quantitative CMR methods have been developed. The absolute quantification of perfusion has several challenges and is significantly more technically difficult than semi-quantitative approaches. Multiple steps are required; the first is the accurate measurement of the arterial input function (AIF), which is the concentration of contrast delivered to the myocardium over time. Typically this is measured from the LV blood pool or sometimes the aortic root. It is also necessary to accurately measure the myocardial response to the contrast bolus, ideally at the same time as the AIF. After these measurements are made there is a final deconvolution step in which the measured contrast concentration in the myocardium can be converted to an absolute MBF (140).

In order to elicit a measurable myocardial response (with adequate signal to noise), a high concentration of contrast is required. However, during the first pass, gadolinium is very

concentrated in the blood pool, resulting in T1, T2 and T2* loss. At high concentrations in the blood pool, there is thus a non-linearity between the signal intensity and gadolinium concentration (141). These effects are less significant at the lower concentrations of gadolinium passage through the myocardium. Consequently, it is not possible to optimise a single measurement (read-out) technique for both the AIF and myocardium. Quantifying perfusion using a single bolus of high concentration gadolinium is thus a complex process.

To overcome these challenges, two approaches have been developed to ensure accurate measurement of the AIF and the myocardial response to gadolinium. They are the "dual bolus, single sequence" and "single bolus, dual sequence" techniques and both correlate well with absolute MBF measured using microspheres in animal models (142).

The dual bolus single sequence approach involves the administration of an initial low dose of contrast which is used to accurately measure the AIF. The low dose allows the linear association between the SI and the gadolinium concentration in the blood pool. Subsequently, a second, higher, dose of contrast is administered to elicit a measurable myocardial response (137). This approach has practical limitations. Firstly it takes longer, requiring 2 acquisitions each for stress and rest. It is also cumbersome for use in clinical practice in that it is difficult to fit into a departmental workflow, which largely has prevented it from being used at scale routinely.

An alternative is the single bolus, dual sequence approach. As the name suggests, this approach uses two sequences; one sequence to measure the AIF and a second sequence to measure the myocardial response to a single, high concentration contrast bolus. Initially described by Gatehouse et al, the technique uses a low resolution, short pre-pulse delay, gradient echo sequence acquired immediately after the R wave to measure LV blood pool signal (the AIF) followed by a long recovery delay, high resolution gradient echo or balanced SSFP readout to measure the myocardial signal (143). The higher resolution sequence is optimised for the

myocardium and allows multi-slice coverage of the LV, in the same way as a standard perfusion sequence. This approach is advantageous as a single contrast bolus is used and requires no modification to the perfusion protocol for the clinical workflow in contrast to the dual bolus approach. Also, only one acquisition is required for stress and rest.

As well as measuring the AIF and myocardial signal, additional steps are required to develop a high quality, quantitative sequence that is equally robust for clinical care. This includes ensuring there is adequate temporal and spatial resolution to detect perfusion defects, the ability to convert SI into gadolinium concentration and the use of a suitable model of the myocardium in order that the gadolinium concentration can be converted into the MBF. There are several models of blood myocardial contrast exchange that have been used in quantitative perfusion (144). Increasing model sophistication requires increasing computational power but is potentially more accurate. However, in trials to date, the approaches have not been standardised and there are a variety of different approaches available, which has made comparisons between them difficult (145,146).

The first fully quantitative CMR studies utilised the dual bolus method. In dog models, it was found that there was a good correlation between fully quantitative MBF and microspheres up to flow rates of 5ml/g/min for vasodilator stress and rest perfusion (137). An advantage of CMR over PET is the superior spatial resolution. This enables transmural gradients in flow to be appreciated in CMR where it has not been possible with PET. Christian et al found a high correlation between microspheres and perfusion CMR for endocardial and epicardial flow with r=0.92 and r=0.95 respectively (137). Similarly, for the dual sequence method, there is a high correlation between fully quantitative perfusion CMR and microspheres. One study found r=0.91 for transmural, r=0.89 for endocardial and r=0.92 for epicardial flow (Figure 6) (144).

Figure 6. Correlation between MBF measure by single and dual-bolus perfusion CMR and microspheres. Correlation between MBF measured by single and dual-bolus perfusion CMR and microspheres. From Christian et al (142).

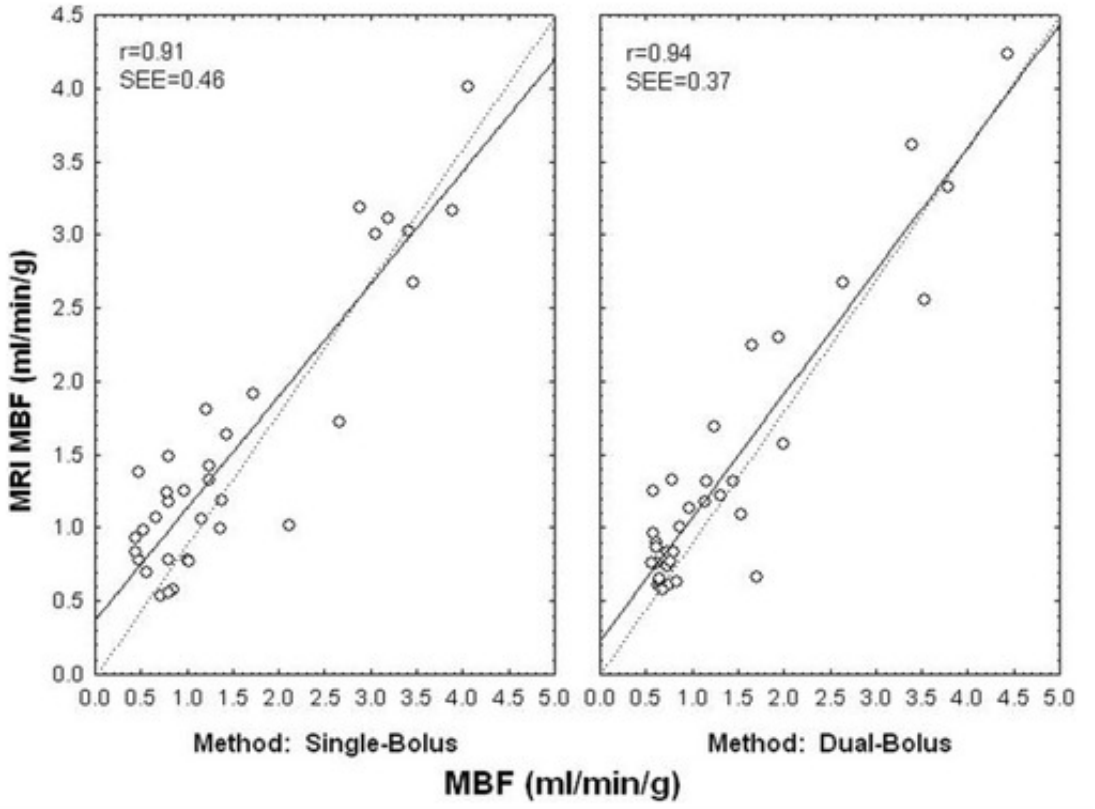


Quantitative perfusion has also been compared to invasive angiography and FFR with good diagnostic accuracy at 1.5 and 3T (147,148). It also has a higher diagnostic accuracy than semi-quantitative CMR perfusion compared to QCA (139). In the few studies against PET, CMR demonstrated similar accuracy for the detection of significant coronary artery disease. However, depending on the CMR quantification method, the absolute MBF correlation is somewhat variable (149,150).

As well as the technical challenges in the acquisition of data in which fully quantitative perfusion can be calculated, there are also challenges in the post-processing and analysis of

results. In a similar way to the semi-quantitative perfusion analysis, both the dual bolus and dual sequence techniques require considerable post-processing, which is time consuming. For a typical study, LV endocardial and epicardial borders would need to be manually traced for each of the 50 stress and rest measurements on each of the 3 LV slices. This analysis, which could take around one hour per scan, is not convenient or practical for routine clinical use. This has meant that despite the technological advances, CMR with stress perfusion has remained a qualitative technique and quantitative analysis has not been incorporated into clinical care.

In summary, a quantitative stress perfusion technique robust for clinical practice requires the following:

a) Precise measurement of the arterial input function (AIF)
b) Precise measurement of myocardial enhancement curves
c) Sufficient temporal-spatial resolution to detect disease
d) The ability to convert signals above into contrast concentrations [Gd]
e) A model of blood myocardium contrast behaviour.
f) The computing power to solve the model to derive myocardial blood flow

In order for this to be useful to clinical care, the above should be done with sufficient accuracy, without significant time penalty and in a generalisable way. Within each stage there are additional requirements and complications. There is the requirement to image extremely fast, every heartbeat for at least 3 slices to achieve good spatial resolution across the myocardium. The images should be motion corrected to improve patient experience (by allowing them to breathe freely during the acquisition) and accuracy. This also facilitates automation and allows for segmentation of the blood pool and also the myocardium without the need for manual contours of each measurement. To make quantitative perfusion available clinically, the

quantitative process would need to occur without user input. It should also permit quality control overview by the reporting physician without necessarily being present for the scan. For example through the additional display of quality control outputs such as displaying the AIF curves, heart rate and ECG triggering during the acquisition and the rates and depths of breathing of the patient. Finally the quantitative output should be displayed in a standardised format for clinicians to allow easy interpretation.

### 1.6.3 Myocardial perfusion mapping

The concept of parametric mapping has matured in recent years with the publications of consensus statement documents detailing the use for parameters such as T1, T2 and T2* time (151). Essentially, the parameter (for example T1) is encoded in each voxel (three-dimensional pixel) in a map. This allows absolute quantification of the parameter in a region of interest without the need for reference tissue simply by drawing a region of interest on the map using any analysis software available to the clinician. Furthermore, the production of suitable colour look up tables enables the easy appreciation of normality and abnormality if it is designed so that the colour changes outside the upper and lower limit of normal. A major step forward in quantitative perfusion is myocardial perfusion mapping (152). In the perfusion maps, each voxel encodes myocardial blood flow in ml/g/min and can be outputted for stress and rest.

Kellman and colleagues developed the perfusion mapping technique which they implemented using the Gadgetron framework (153). They recognised that fully automatic, in-line reconstruction of quantitative perfusion maps was essential for adoption in a clinical workflow. As mentioned previously, developing a sequence optimised for perfusion quantification is technically challenging. The approach taken in perfusion mapping is as follows:

1. Saturation Pre-pulse: A new, 90 degree pre-pulse with higher efficiency saturation preparation was incorporated which was based on the latest SASHA refinement work T1-mapping implementation (154).

2. A dual-sequence, single bolus approach: The sequence acquires low resolution blood pool images to derive the AIF curve (143). The AIF acquisition was modified to optimise the linearity, reduce biases, and minimise duration by incorporating parallel imaging, raw filtering, adaptive coil combining, and acquiring 2 echoes. The reconstruction estimates and corrects for T2* losses (Figure 7) to avoid clipping, and uses a Bloch calculation to further linearise for saturation recovery (155).

3. Read-out imaging reconstruction approaches: Parallel image reconstruction, raw filtering, adaptive coil combination, signal to noise ratio (SNR) unit scaling, surface coil intensity correction (156–160).

4. Advanced motion correction (MOCO): Latest generation MOCO using non-rigid image registration and an iterative approach to deal with changing contrast. The initial MOCO applied to free breathing late enhancement (161,162) was improved for perfusion with time varying contrast (163), and subsequently revised for T1 mapping to incorporate a synthetic reference approach (164). The implementation used an iterative scheme incorporating concepts from each of these approaches (155) which is based on T1 mapping and real-time cine approaches.

5. Automatic blood pool detection: Initial implementation of a semi quantitative method using automatic blood pool segmentation (155,163). This is based on blood pool detection for synthetic ECV mapping (165) and have been improved and optimised for the low resolution blood pool images in the current in-line implementation which used a dedicated dual sequence for deriving the AIF (166).

6. Gadolinium look-up table: A per-readout level Bloch simulation to correlate signal intensity saturation recovery (SR)/ proton density (PD) vs Gd concentration. This is computed

from exact imaging sequence parameters and passed on to the Gadgetron on-the-fly and based on inline Bloch simulation first used inline for the dark blood LGE approach (167). Look-up tables are calculated on-the-fly in the image reconstruction (155).

7. Model selection: There are multiple potential tissue models that can be used to estimate myocardial blood flow. A pixel level deconvolution using a model free, Fermi and two compartment exponential approach were all considered but ultimately a more sophisticated model was selected – the blood-tissue exchange (BTEX) model which is more physiological (166,168,169).

8. Analysis method: Partial differential equation solution of tracer kinetics for 4 unknown parameters from the BTEX model: F: myocardial blood flow (ml/g/min), V: plasma volume (ml/g), Visf: nominal interstitial volume (ml/g), PS: symmetric permeability-surface-area-product (ml/min/g)

9. Analysis implementation: The image reconstruction and calculation of quantitative perfusion maps is implemented using the Gadgetron architecture software framework (153).

In summary, the AIF is measured through the acquisition of low-resolution images immediately after the R wave. T2* loss is minimised by using a short readout, wide bandwidth and short duration radiofrequency pulse and 2 echoes acquired to directly estimate and correct for T2* decay. Latest generation respiratory MOCO is applied and the blood pool automatically segmented in order to extract the AIF. The signal is then converted to a gadolinium concentration using Bloch signal calculations. The myocardial imaging is performed using a single shot gradient echo or balanced SSFP readout. Following MOCO and normalisation for surface coil intensity, the signal intensity in the myocardium is converted to a gadolinium concentration. Finally absolute myocardial blood flow is calculated for each voxel of tissue using the BTEX model.

The outcome is a dual sequence approach in which "standard" perfusion images are outputted alongside perfusion maps automatically and inline at the scanner with no user input required (Figure 8). An additional advantage is that a single bolus of contrast is required which is easier for clinical workflow and the sequence is completely free-breathing which is more tolerable for patients. Furthermore, by using the Gadgetron framework, which is open source and potentially deployable by all scanner manufacturers, this approach raises the possibility of a standardised approach to image reconstruction and analysis across healthcare systems. Initial validation work has been promising. It has been found to have a similar intra-subject coefficient of variation to PET (around 8-12%) (170) which is clinically acceptable. Also, perfusion mapping has recently been validated against PET, demonstrating good correlation at a regional and global level in patients with suspected coronary artery disease (150). Consequently, for the first time quantitative perfusion CMR is possible, within the clinical workflow, with minimal analysis time and requiring no post processing (see example Figure 9 and Figure10). Theoretically there should not be a significant difference in values obtained by scanning at 1.5 vs 3T or between scanners, but this has not been investigated in phantom models or volunteers. Whilst minor adjustments in the sequence to provide additional data (e.g. pulmonary transit time and integration of artificial intelligence analysis) are anticipated, major changes to the sequence are unlikely.

Artefacts may arise due to factors such motion correction failure, miss-identification of the LV blood pool for the AIF assessment and ECG miss-triggering. Although it is not possible to adjust the maps subsequently, in clinical practice, there are quality control. These include blood pool identification images outputted to demonstrate correct identification of the LV blood pool, AIF graphs to show the AIF curve, heart rate ECG trigger graphs on the scanner as well as the perfusion map outputs. This allows the reporting clinician to interrogate the raw data from which the maps are created and have confidence in the perfusion maps outputted.

Figure 7. Arterial input function estimation. In (A) the signal intensity is plotted for the first and second echoes, and following correction for T2* loss. The gadolinium concentration over time is then calculated (B).

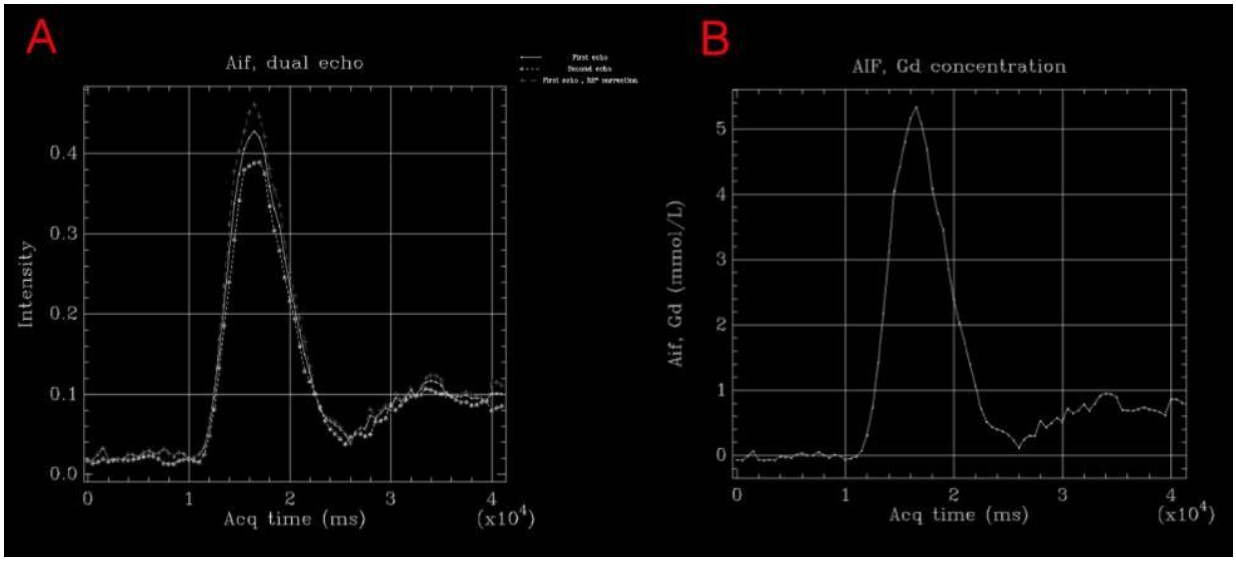


Figure 8. A summary of perfusion mapping. A summary of perfusion mapping. The outcome is a standard perfusion image alongside a perfusion map. From Kellman et al (154).

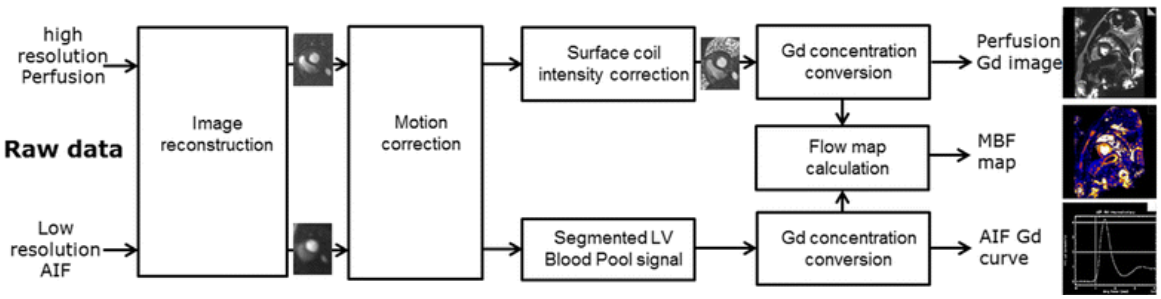

Figure 9. Example perfusion maps for a patient with RCA disease (same patient as Figure 2). The stress maps (A) and rest maps (B) are demonstrated. The MBF in the hypoperfused myocardium is 0.60 ml/g/min, compared to 3.22 ml/g/min in the remote myocardium and 1.00 ml/g/min at rest.

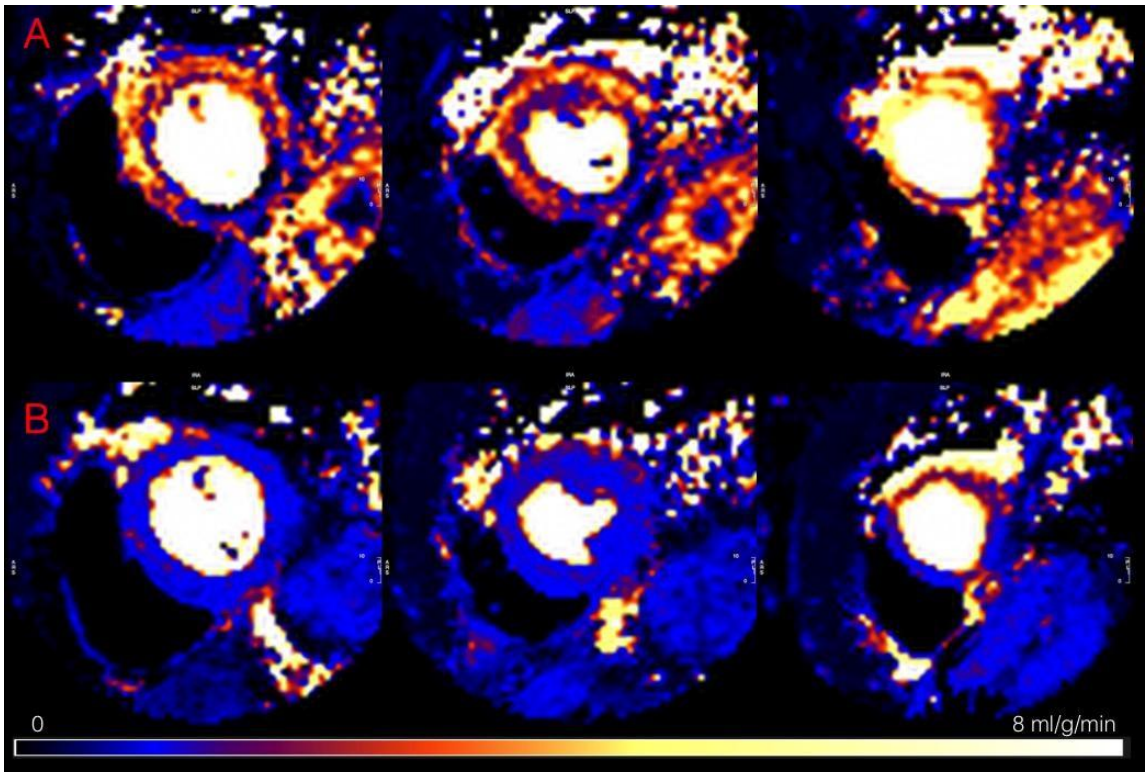


Figure 10. Perfusion maps for a patient with apical HCM (same patient as Figure 3) for stress (A) and rest (B). The MBF is as low as 0.40 ml/g/min in the apex, 1.84 ml/g/min in remote myocardium and 0.96 ml/g/min at rest.

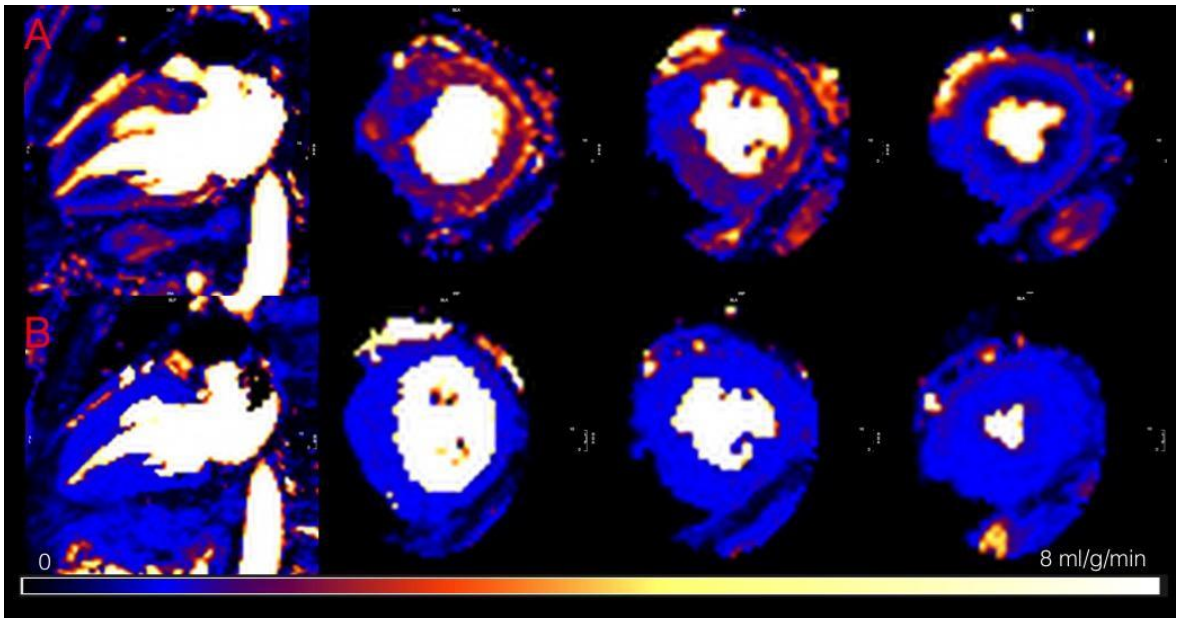

## 1.7 Outstanding questions for quantitative CMR perfusion

Although there have been considerable advances with quantitative perfusion there remain outstanding issues. These include the establishment of normal ranges, the need to understand how factors such as ageing and the presence of comorbidity affects perfusion, the validation of the technique in epicardial coronary artery disease and microvascular dysfunction and to determine whether there is prognostic information included in perfusion. By beginning to answer these questions, it is possible to facilitate the technique in clinical practice.

# 2. Research aims and objectives

## 2.1 Hypothesis

- Quantitative perfusion assessment, with perfusion mapping, can be used to accurately diagnose coronary stenoses in patients with suspected coronary artery disease.
- Perfusion mapping can detect patients with reduced stress MBF and MPR and these patients are at increased risk of major adverse cardiovascular events.
- Myocardial perfusion is affected by physiological (e.g. ageing) and pathological factors (e.g. co-morbidity) in the absence of obstructive coronary artery disease.
- Quantitative perfusion may be abnormal in heart muscle disease including Fabry disease cardiomyopathy, even before overt hypertrophy and is associated with other markers of disease severity.

## 2.2 Aims

- To determine the diagnostic accuracy of perfusion mapping in CAD in comparison to invasive coronary angiography.
- To investigate whether patients with reduced stress MBF and MPR have an increased risk of death and major adverse cardiovascular events.
- To assess the effects of patient factors on myocardial perfusion in the absence of obstructive epicardial coronary artery disease in patients referred for CMR scans.
- To study the determinants of myocardial perfusion in Fabry disease.

# 3. Methods

## 3.1 Ethical approval

Upon starting the project, I sought ethical approval for the prospective recruitment of participants to the study. Whilst prospective CMR research studies were being performed at Barts, there were no prospective studies using stress perfusion and so new ethics were required. The stages included local Barts Heart Centre peer review, University College London / University College London Hospital sponsorship (16/0782) and ultimately approval from the UK National Health Service Research Ethics Committee (NHS REC) and Health Research Authority (HRA). Integrated research application system ID 217617, research ethics committee reference 17/SC/0077. Study title: An observational cohort study to investigate the accuracy and reproducibility of myocardial perfusion mapping in the assessment of coronary artery disease and cardiomyopathy. This study conformed to the Declaration of Helsinki and all participants gave written informed consent to participate.

Additionally an application was granted by the Barts BioResource to use CMR and registry data from the Barts Cardiovascular Registry (BCR). This is a sub-study within the BCR (IRAS ID 143355, REC reference 14/EE/0007). Similarly, all participants gave written informed consent to participate.

## 3.2 Study outline

The study included prospectively recruited patient cohorts, which included healthy volunteers and patients with coronary artery disease and cardiomyopathy. There were also cohorts of patients clinically referred for perfusion CMR with suspected coronary artery disease within the BCR. Our collaborators at the Royal Free Hospital and Leeds University were simultaneously

investigating perfusion mapping and so some aspects of quantitative perfusion (repeatability, assessment of multi-vessel coronary disease) are not part of this thesis but were contributed to as a co-author.

### 3.2.1 General inclusion and exclusion criteria.

The general study inclusion criteria were:

- Age over 18 years
- The ability to consent for a CMR study.

The exclusion criteria were:

- Pregnancy or breastfeeding
- Renal impairment with an eGFR <30ml/min, preventing the administration of a gadolinium-based contrast agent
- Severe asthma or chronic obstructive pulmonary disease preventing administration of adenosine
- Significant cardiac conduction disease (second or third degree atrio-ventricular block) preventing administration of adenosine
- A non-MRI conditional cardiac implantable electronic device.

### 3.2.2 Healthy controls

All healthy controls were recruited for a perfusion CMR. In addition to the above, additional exclusion criteria were:

- Cardiovascular risk factors including hypertension, diabetes mellitus, dyslipidaemia and smoking.
- Known coronary artery disease (including previous PCI or CABG).
- A diagnosis of cardiomyopathy (dilated, amyloid, hypertrophic or arrhythmogenic)

### 3.2.3 Coronary artery disease

50 patients were prospectively recruited from the coronary angiogram (+/- PCI) waiting list at Barts Heart Centre. They had a history of chest pain and suspected coronary artery disease. They were deemed of sufficient risk of CAD to warrant invasive coronary angiography by their clinical team and were recruited from the angiography waiting lists. All patients had a stress perfusion CMR (with automated inline perfusion mapping) before coronary angiography. Patients were excluded from the study if they had a history of previous coronary artery bypass grafting (CABG), chronic kidney disease with a eGFR <30mmol/l, cardiomyopathy (hypertrophic, arrhythmogenic, dilated, amyloid cardiomyopathy), contraindication to MRI or contraindication to adenosine.

### 3.2.3 Real-world cohorts

Since 2016, the perfusion mapping sequence has been implemented on the clinical scanners at Barts Heart Centre. Over 1300 patients have been scanned clinically and recruited to the Barts Cardiovascular Registry (BCR). Those with known cardiomyopathy (amyloid, hypertrophic or arrhythmogenic) were excluded. There were two real-world cohorts studied. The first were all comers that underwent stress perfusion CMR and consented to the BCR were included in the study. A similar cohort of patients were included from the RFH and the same exclusion criteria were applied.

In the second real-world cohort, patients referred for perfusion CMR at five centres: Barts Heart Centre (BHC), United Kingdom (UK); St Luca Hospital Milan, Italy (Milan); University of Leeds, UK (Leeds); Harefield Hospital, UK (HH); Royal Free Hospital, UK (RFH) between May 2016 and December 2019 were recruited. All patients had undergone contemporaneous invasive or computed tomography coronary angiography (CTCA), without interval coronary event or intervention within 6 months. Patients with coronary artery disease (diameter stenosis on coronary angiography >50%), previous coronary revascularisation or cardiomyopathy (hypertrophic, arrhythmogenic, dilated, amyloid) were excluded. In addition, patients with

previous infarction / scar (ischaemic or non-ischaemic aetiology) seen with late gadolinium enhancement were excluded. Patient demographic data and medication were documented from the medical notes. This cohort was used to determine the factors influencing perfusion in the absence of obstructive coronary artery disease.

### 3.2.4 Fabry disease

Patients with Fabry disease were recruited from the Fabry clinic at the Royal Free Hospital or cardiomyopathy clinic at Barts Heart Centre. All patients had confirmed Fabry disease on genetic mutation analysis. All patients who attended these clinics were eligible for recruitment and they were approached to under CMR including stress perfusion analysis. 44 patients with Fabry disease were recruited. The patient's cardiovascular history, symptoms and FD treatment status were assessed with a questionnaire at the time of CMR..  In addition to the general exclusion criteria above, Fabry patients with known coronary artery disease were excluded.

## 3.3 CMR scan

Prospective CMR scanning was performed at 1.5 Tesla (Aera, Siemens Healthcare, Erlangen, Germany) and based on a standard clinical perfusion approach (48), Figure 11. Details of a the standard CMR scan for all prospectively recruited patients:

### 3.3.1 Pilot imaging

Each study began with single shot pilot images. The sequence parameters were as follows: repetition time (TR): 2.67ms, echo time (TE): 1.2ms, slice thickness: 8mm, field of view (FOV): 360 x 360mm, read matrix: 256, flip angle 80°.

### 3.3.2 Cine imaging

Following acquisition of pilot imaging, balanced steady state free precession (SSFP) cine images were acquired. The views acquired were 2 chamber, 4 chamber, 3 chamber, coronal left ventricle outflow tract (LVOT) and short axis aortic valve. Following stress perfusion, an LV short axis cine stack was acquired. Typical parameters were: TE: 1.1ms, TR: 2.66ms, in-plane pixel size 1.8 x 1.8mm, slice thickness 8mm, flip angle (FA) 72°. The standard approach was retrospective gating with end-expiratory breath-holding but this was optimised in cases of arrhythmia and instead a prospective acquisition was used.

### 3.3.3 T1 and T2 mapping – cardiomyopathy cohort

T1 mapping was performed before and after contrast administration in the Fabry disease cohort. The T1 sequence used was a balanced SSFP based modified look-locker inversion recovery (MOLLI) sequence (171). The pre-contrast MOLLI used was the 5s(3s)3s variant which means that there is an inversion with a 5 second acquisition, followed by 3 seconds recovery, followed by another inversion with 3 seconds of image acquisition. The post-contrast MOLLI was 4s(1s)3s(1s)2s – inversion with 4 seconds image acquisition, 1 second recovery, second inversion with 3 seconds acquisition and 1 second recovery and finally an inversion with 2

seconds acquisition. The MOLLI sequence has additional features including motion correction (MOCO), phase sensitive inversion recovery (PSIR) and error maps (highlighting areas of increased pixel standard deviation). Synthetic extracellular volume fraction (ECV) maps were outputted inline from the pre and post contrast T1 maps (165).

T2 mapping was performed before contrast administration. The sequence was a balanced SSFP with 3 single shot images acquired at increasing T2 preparation times (0ms, 25ms, 55ms). Typical imaging parameters were: TR = 2.4ms, TE = 1ms, FA = 70°, read matrix 192; slice thickness 8mm; field of view 360 x 360 mm.

3.3.4 Perfusion imaging

Perfusion images were acquired for 3 short axis LV slices. The same slice position was used for stress and rest perfusion. The sequence was a dual-sequence, saturation recovery (SR) sequence acquired during the first pass of a gadolinium based contrast agent (152). Low-resolution images of the blood pool are acquired immediately after the R wave trigger (from the most basal LV slice) in order for the AIF to be measured, using a single shot, gradient echo readout. Typical AIF parameters are listed in Table 1. Short readout, wide bandwidth, short duration RF pulses minimise T2* losses. A two echo acquisition allowed an improved estimation T2* during first pass of contrast. At the start of the scan, proton density (PD) weighted images are acquired to correct for surface coil variation and correct for AIF noise. The acquisition is accelerated with parallel imaging.

Table 1. Typical parameters of the AIF sequence. Adapted from Kellman et al 2017 (152). Abbreviations: FLASH – fast low angle shot, TE – echo time, TR – repetition time, FA – flip angle, FOV – field of view, PE – phase encoding, TI – inversion time, SR – saturation recovery.

| | **FLASH** |
|---|---|
| TE | 0.76 & 1.76 ms |
| TR | 2.45 ms |
| FA | 5° |
| Matrix | 64x48 |
| FOV | 360x270x10 $mm^3$ |
| Phase Encoding order | Linear |
| Parallel imaging | TPAT3 |
| TI | 23.8ms |
| SR prep | 6-pulse |
| Imaging duration | 42ms |
| Total duration | 68.2ms |

The myocardial sequence uses the same saturation preparation pulse sequence as the AIF. There is a trigger delay (TD) and single shot balanced SSFP readout. Parallel imaging also speeds up the acquisition. For typical parameters see Table 2.

Table 2. Typical sequence parameters for the myocardial sequence. Abbreviations: SSFP – steady state free precession, TE – echo time, TR – repetition time, FA – flip angle, FOV – field of view, PE – phase encoding, TS – saturation delay, SR – saturation recovery.

| | **SSFP** |
|---|---|
| TE | 1.04ms |
| TR | 2.5ms |
| FA | 50° |
| Matrix | 192x111 (1.9x2.4mm$^2$) |
| Partial Fourier | 3/4 |
| FOV (typical) | 360x270x8mm$^3$ |
| PE order | Linear |
| Parallel imaging | TPAT3 |
| TS | 105ms |
| SR prep | 5-pulse |
| Imaging duration | 70ms |
| Total duration | 142ms/slice |
| 3 slices + AIF | 495ms |

Myocardial blood flow maps were created automatically and inline at the scanner using the Gadgetron framework (153). The BTEX model (172) was used to calculate the MBF for each pixel based on the AIF and the myocardial response.

### 3.3.5 Late gadolinium enhancement

A gadolinium based contrast agent, Gadoterate meglumine (Dotarem, Guerbet, S.A. France). Was administered in two split boluses at time of stress and rest perfusion. The total dose was 0.1mmol/kg and each 0.05mmol/kg bolus was given through a power injector at a rate of 4ml/s followed by a 25ml saline flush and LGE was performed 5-15 minutes after contrast administration. The sequence is a free-breathing MOCO single shot, balanced SSFP, inversion recovery sequence with 8 repeated measurements (averages). Magnitude and PSIR reconstructions were used. Image parameters were modified according to each patient and the inversion time (TI) manually set to null the myocardium, typically between 300 and 400ms. Typical image parameters were: FOV 360 x 270mm$^2$, spatial resolution 1.4 x 1.9 x 8mm, matrix size 256 x 144, TE 1.2ms, TR 2.8ms.

Figure 11. The CMR protocol used during subject scanning. Abbreviations: Ch- Chamber, SAX – short axis, MOLLI – modified look Locker lnversion recovery

| | Notes |
|---|---|
| ***Sequence*** | |
| Localisers | |
| White and black blood axis stack, | |
| 2Ch, SAX pilots | |
| Long axis cines - 2CH , 4CH, and 3CH | |
| Native T1 mapping: MOLLI 5s(3s)5s<br>- Basal, mid and apical SAX slices | Cardiomyopathy scans<br>Repeat if artefacts or gating error |
| T2 mapping:<br>- Basal, mid and apical SAX slices | Cardiomyopathy scans<br>Repeat if artefacts or gating error |
| SSFP Perfusion test | Repeat if artefacts |
| **Adenosine stress** | |
| Start adenosine infusion | 140mcg/kg/min for 4 minutes, if no symptom / heart rate response, increase to 175 and then 210mcg/kg/min |
| Adenosine stress perfusion: base, mid, apex | SSFP sequence |
| Short axis stack cines | |
| **At 10 mins post stress perfusion:** | |
| Rest perfusion: base, mid apex | Same slice positions as stress |
| EGE (2CH, 4CH) | |
| LVOT cine, aortic valve cines | |
| **Late enhancement imaging (LGE)** | |
| 3 x Long Axis LGE (2CH, 4CH and 3CH), SAX | |
| **At 15 mins post rest perfusion:** | |
| Post contrast T1 mapping: MOLLI 4s(1s)3s(1s)2s<br>- Basal, mid and apical SAX slices (3 slices) | Cardiomyopathy scans<br>Same FOV size as pre contrast T1 map |
| **Finish** | |

## 3.4 CMR image analysis

### 3.4.1 Parametric map analysis

CMR images were predominately analysed using commercially available software (CVI42, Calgary, Canada). Parametric map analysis (stress and rest perfusion, T1, T2 and ECV) was performed in a dedicated analysis module. Endocardial and epicardial contours were manually traced, the superior and inferior RV insertion points identified on each short axis slice and the mitral valve plane and cardiac apex were drawn on a long axis reference image. The contours were offset by 10% to minimise contamination (e.g. blood pool / pericardium) and therefore partial volume effects. From these contours a polar map is produced where each AHA segment (except the apical cap) demonstrates the parameter measured (for example MBF or T1). Global "mean" values were also calculated using the analysis module. An example of perfusion map analysis is shown in Figure 12.

During the progression of the project, advances were made in the perfusion maps generation. Automatically contoured perfusion maps using an artificial intelligence (AI) approach, without the need for user interaction were produced for all patients in the outcome cohort, Figure 13. The AI tool performs automatic segmentation LV myocardium using a convolution neural net (CNN) approach (173). The LV cavity and myocardium were delineated and the epicardial fat and papillary muscles were excluded. The global MBF was then calculated as a mean of the pixel values. The automatically contoured perfusion maps were visually checked for errors.

### 3.4.2 LV volume analysis

LV volume analysis was performed by manually contouring the endocardial borders in end diastole and systole. Papillary muscles were excluded. LV mass analysis was performed by contouring the epicardial and endocardial borders at end diastole. Papillary muscles were included in LV mass.

3.4.3 Late gadolinium enhancement (LGE) analysis

The presence or absence of LGE was noted on read of the images. Where relevant, LGE was quantified using a dedicated analysis module in CVI42 using a semi-automated method. The "remote" myocardium, free of LGE, was identified with a manually drawn region of interest. Pixels greater than 5 standard deviations above the remote myocardium were automatically detected as positive for LGE. LGE is then quantified on a global and segmental basis.

Figure 12. Example of manual perfusion maps analysis. The endocardial (red) and epicardial contours are manually drawn and RV insertion points identified. A 10% offset was then applied. The MBF for each segment was then recorded.

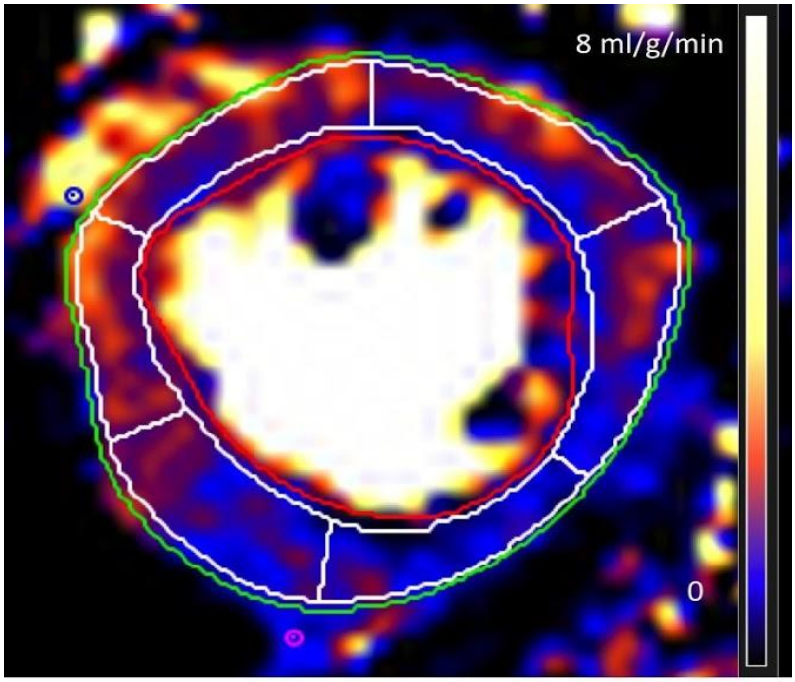

Figure 13. Automatically contoured perfusion maps using artificial intelligence. Basal, mid and apical short axis stress perfusion maps (left to right) for a patient in the outcome cohort. The yellow and green contours demonstrate the first and second myocardial segments for each slice respectively. This allows appreciation of errors in the AI algorithm. Global and regional perfusion can then be documented.

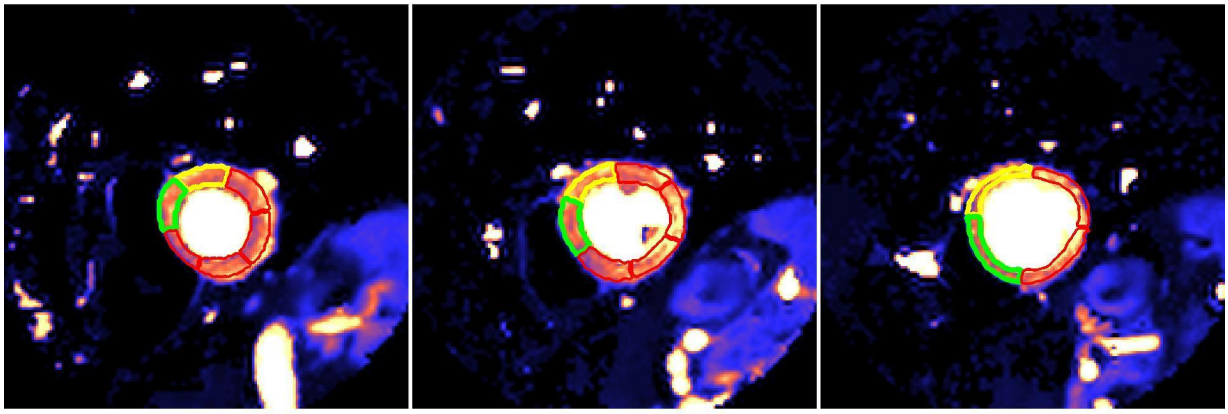

### 3.5 Invasive coronary angiography

In the prospective coronary artery disease perfusion mapping validation study, invasive angiography was performed in accordance with standard clinical practice. The major epicardial vessels and large side branches (intermediate, large diagonal and large obtuse marginal) with visual luminal stenosis >30% were reconstructed based on the angiographic data using three-dimensional quantitative coronary angiography (3D QCA) methodology (174). This was performed using specialised software (QAngio XA 3D RE, Medis Specials by, Leiden, the Netherlands). Two end-diastolic angiographic projections (>25 degrees apart) with no overlap or foreshortening of the segment of interest were selected for analysis to allow accurate delineation of the lumen silhouette. The analysis was performed by a single operator blinded to CMR data, Dr Anantharaman Ramasamy under the supervision of Dr Christos Bourantas who ensured internal quality control.

### 3.6 Registry cohorts

A high proportion of patients attending Barts Heart Centre for a clinical CMR scan are recruited to the Barts cardiovascular registry (BCR). Similar registries are in place with our collaborators. The BCR is a research, audit and educational health resource sponsored by Barts Health NHS Trust (REC reference 14 / EE / 0007). It includes a database of patient data, blood samples and / or soft tissue samples. All patients who attend Barts Heart Centre for a scan (e.g. echocardiogram, CMR, CT), invasive investigation or clinic appointment are potentially recruited. Participants provide written, informed consent to participate and have the option of withdrawing consent at any time. Patients are often recruited whilst waiting for their CMR scan. All patients attending BHC are eligible for recruitment. There are currently >20,000 patients in the registry and patients who had a perfusion CMR including perfusion mapping were included in the cohort studied here.

Demographic details (age, sex, height, weight, body surface area), CMR details (LV volumes, LV ejection fraction, LGE and perfusion defects) and co-morbidities (including previous coronary revascularisation, hypertension, dyslipidaemia, diabetes mellitus, smoking, cancer) were documented from the clinical notes.

All-cause mortality was identified through a search of the NHS spine records system. Major adverse cardiovascular events (MACE) were determined through thorough review of the medical records. MACE events included myocardial infarction, stroke, heart failure and coronary revascularisation. Early revascularisation events (< 90 days after CMR) were excluded to prevent the inclusion of events occurring as a result of the CMR.

### 3.7 Statistical analysis

Statistical analysis was performed in SPSS (IBM SPSS statistics, Version 25.0). Numerical variables are presented as mean ± standard deviation or median (interquartile range) depending on the normality of the data. Categorical variables are presented as absolute values and percentages. Comparison between numerical variables was performed using an independent t-test or Mann Whitney U test. The chi-square test was used for categorical variables. A p value of $<0.05$ and was considered statistically significant.

In the coronary artery disease chapter, receiver operator characteristic (ROC) curves were calculated to determine the accuracy of the perfusion maps in detecting a coronary artery stenosis. The area under the curve (AUC) of ROC curves were compared using the method of DeLong et al. (175).

In the perfusion in non-obstructive coronary disease and the Fabry disease chapters, a simple linear regression analysis was performed to determine the factors that contribute to stress MBF. Subsequently, the variables that were significantly associated were used in a multiple linear regression analysis. A mixed effects linear regression model controlled for subject dependency in the segmental perfusion analysis of the Fabry cohort.

In the outcome cohort, Cox hazard regression analysis was performed to determine whether perfusion was associated with death and MACE adjusting for demographics, CMR parameters and co-morbidities. A sensitivity analysis using a penalised model was performed to obtain Firth's bias-adjusted estimates to ensure there was no bias in the estimated coefficient. Kaplan Meier survival estimates were then plotted for the upper and lower $50^{th}$ percentiles of stress MBF and MPR. Harrel's C indices compared stress MBF and MPR in their association with outcome.

# 4. Results 1. Perfusion mapping in coronary artery disease

The following manuscript is based on this chapter:

"Quantitative myocardial perfusion in coronary artery disease: a perfusion mapping study".

**Knott KD,** Camaioni C, Ramasamy A, Augusto JA, Bhuva AN, Xue H, Manisty C,

Hughes RK, Brown LAE, Amersey R, Bourantas C, Kellman P, Plein S, Moon JC.

J Magn Reson Imaging. 2019 Jan 25. doi: 10.1002/jmri.26668.

## 4.1 Summary

This study was the first to use the fully quantitative perfusion mapping CMR technique in patients with coronary artery disease planned for invasive coronary angiography. I investigated the diagnostic performance of perfusion mapping in detecting obstructive CAD in patients scheduled to undergo coronary angiography.

This observational cohort study included 50 patients who underwent CMR with perfusion mapping and invasive coronary angiography and a comparator group (n=24) of healthy volunteers that had perfusion CMR alone. Receiver operator characteristic curves were calculated for stress MBF and myocardial perfusion reserve to diagnose severe (>70%) stenoses as measured by three-dimensional quantitative coronary angiography (3D QCA). The diagnostic performance of transmyocardial, subendocardial and subepicardial MBF were evaluated. For this chapter, I obtained ethics, recruited all of the patients and volunteers and personally scanned them prior to angiography. I analysed the CMR data, performed the statistical analysis and drafted the chapter and manuscript.

Patients with suspected CAD had lower stress MBF and MPR than volunteers even in vessels with <50% stenosis (2.00 vs 3.08ml/g/min respectively). As stenosis severity increased (<50%, 50-70%, >70%), MBF and MPR decreased. To diagnose the most severe stenoses (>70%), endocardial and transmyocardial stress MBF out-performed MPR (area under the curve 0.92 (95% CI 0.86-0.97) vs 0.90 (95% CI 0.84-0.95) and 0.80 (95% CI 0.72-0.87) respectively). An endocardial threshold of MBF of 1.31ml/g/min provided a per coronary artery sensitivity, specificity, positive predictive value (PPV) and negative predictive value (NPV) of 90%, 82%, 50% and 98%, with a per-patient diagnostic performance of 100%, 66%, 57% and 100% respectively.

In conclusion, perfusion mapping has high accuracy for the detection of severe coronary artery disease. In particular it has a high sensitivity and NPV making it a good test to “rule-out” CAD.

## 4.2 Introduction

Non-invasive imaging allows the detection of CAD by identifying areas of the myocardium that are relatively hypoperfused during vasodilator stress (28,34,35). Employing a non-invasive imaging strategy as the first line investigation potentially reduces the rates of unnecessary invasive coronary angiography (and the associated complications) and allows targeted invasive strategies in which the intervention is applied to the coronary artery which supplies the area of hypoperfused myocardium. However, false negative non-invasive tests can also be harmful and prevent the invasive assessment of potentially significant coronary artery disease. It is therefore essential that the non-invasive test is highly accurate to be useful clinically (31).

Whereas the standard first past stress perfusion CMR used clinically is well validated, there is a high level of operator dependence and the potential to miss balanced ischaemia. In contrast, quantifying myocardial blood flow (MBF) has the potential to be less operator dependent (126) and to more accurately detect more extensive ischaemia (125) but has not been as well validated in clinical practice.

Developing quantitative perfusion CMR for clinical use has been challenging and labour intensive as highlighted in chapter 2. These problems have limited the uptake of quantitative perfusion in clinical care, despite the potential benefits. Off-line techniques are improving and reducing the work of the operator, but operator input and the requirement to import images to custom tools is still holding back the field and this has also limited clinical uptake (176).

Perfusion mapping (152) solves many of these problems due to its automated nature and pictorial display of myocardial blood flow (MBF) in a colour map (Figure 14). Perfusion mapping shows a good correlation with quantitative PET (150,177).

In order to validate the technique for clinical practice, we investigated the diagnostic performance of perfusion mapping in patients suspected of having coronary disease and scheduled for invasive coronary angiography.

Figure 14. Example of perfusion maps in health and coronary artery disease. Stress (A-C) and rest (E-G) perfusion maps for a 64 year-old healthy volunteer and a patient with 80% stenosis of the LCx and occlusion of the RCA (I-K, M-O) respectively. The polar maps (L and P) indicate that the patient's stress MBF is lowest in the RCA territory (0.96ml/g/min) and 2.09-2.70ml/g/min in remote myocardium. The volunteer's stress MBF is 2.43-3.17ml/g/min and rest MBF 0.42-0.79ml/g/min.

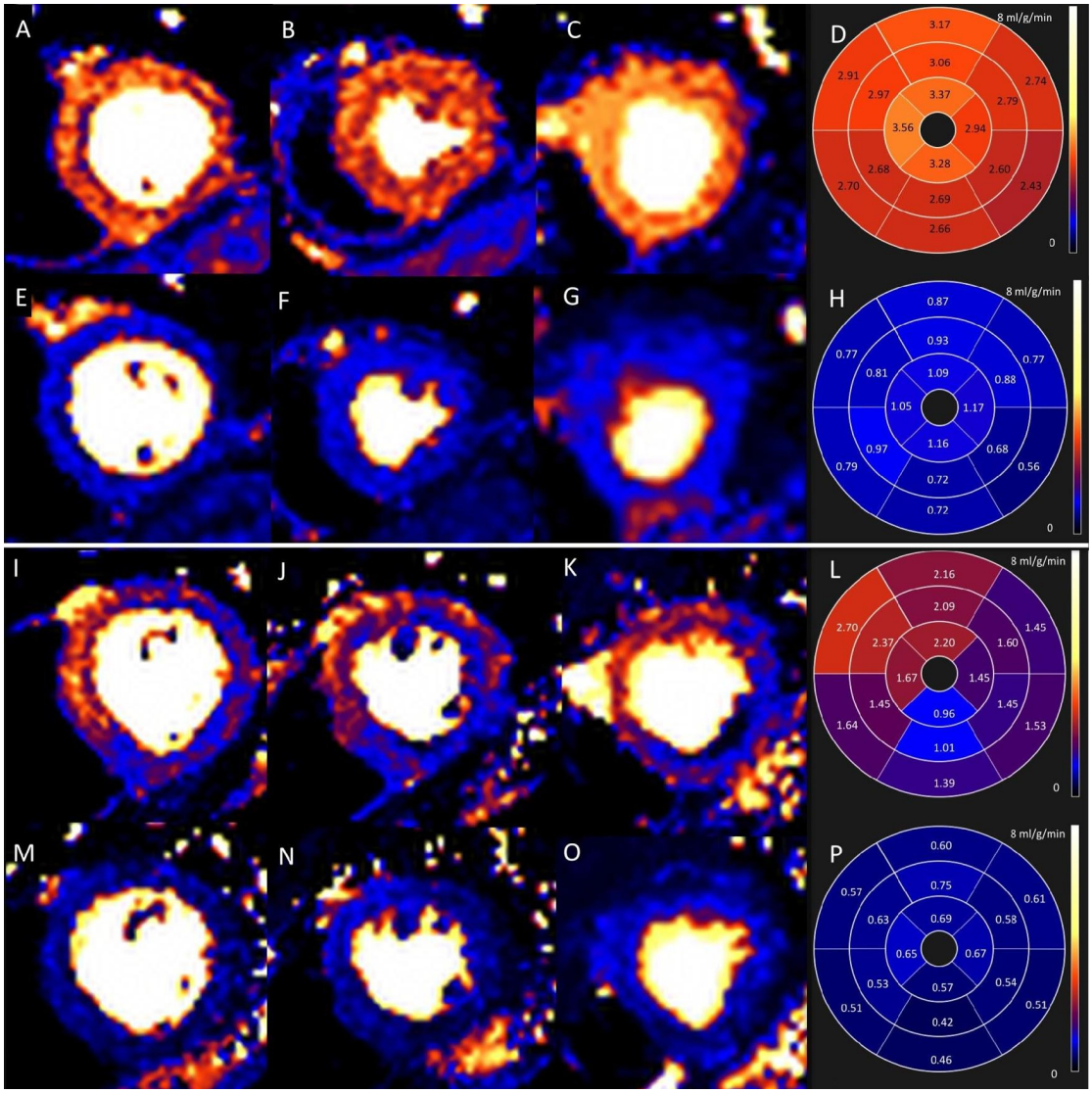

## 4.3 Methods

Patients were prospectively recruited from the coronary angiogram (+/- PCI) waiting list at Barts Heart Centre. They had a history of chest pain and suspected coronary artery disease. In total 50 patients were recruited. All patients had a stress perfusion CMR (with automated inline perfusion mapping) before coronary angiography. Patients were excluded from the study if they had a history of previous coronary artery bypass grafting (CABG), chronic kidney disease with an eGFR <30mmol/l, cardiomyopathy (hypertrophic, arrhythmogenic, dilated, amyloid cardiomyopathy), contraindication to MRI or contraindication to adenosine. A healthy volunteer cohort of 24 individuals was simultaneously recruited.

*CMR studies*

All CMR scans were performed at 1.5T using a standard protocol (48). The protocol included cine imaging, stress and rest perfusion (with perfusion mapping) and late gadolinium enhancement (LGE) imaging, see chapter 3 for the full CMR protocol. Perfusion mapping was performed as previously described in the methods chapter (152) producing three short axis LV slices at stress and rest.

The perfusion maps were analysed using CVI42. The LV endo- and epicardial borders were manually contoured. A 10% offset from the epicardium and endocardium was applied. Segmental flow according to the American Heart Association (AHA) 17 segment model, minus the apical cap, was documented (49), Figure 15. The epicardial and endocardial borders were also offset in CVI42 by 50% sequentially to determine the endocardial and epicardial MBF respectively for each segment (Figure 16). The coronary artery territories were defined as:

Left Anterior Descending (LAD) - segments 1, 2, 7, 8, 13, 14

Left Circumflex (LCx)- segments 5, 6, 11, 12, 16

Right Coronary Artery (RCA) - segments 3, 4, 9, 10, 15

The mean MBF of the two adjacent myocardial segments with the lowest flow in each coronary territory was recorded. This was to ensure that there was no bias against distal coronary stenosis. For example the flow in a coronary artery territory with a distal stenosis could be artificially increased by the normal flow values from myocardium supplied by territories proximal to the stenosis. Using the mean of the lowest two segments has been a standard analysis approach in other perfusion studies (148). The MBF was calculated in this way for each coronary territory at stress and rest and the ratio of these gave the MPR. Segments with subendocardial and transmural LGE suggesting previous myocardial infarction in these segments were excluded.

Additionally, the data was analysed on a per-patient basis where the lowest (mean of the lowest 2 adjacent segments) MBF/MPR in any coronary territory was considered.

*Invasive angiography*

Invasive coronary angiography was performed by the patient's cardiologist using a standard approach. Subsequently, the angiograms were analysed offline as described previously with three-dimensional quantitative coronary angiography (3D QCA) (174) in dedicated software (QAngio XA 3D RE, Medis, Leiden, the Netherlands). The large epicardial vessels including side branches (such as intermediate, large diagonal and large obtuse marginal) with visual luminal stenosis >30% were reconstructed in the software. The branches were attributed to the coronary territory as per the AHA segment diagram (Figure 15). Two end-diastolic images of each vessel (>25 degrees apart) with no overlapping or foreshortening of the segment of interest were selected to allow accurate contouring of the lumen silhouette. The lumen centreline and borders were automatically detected by the software and manual adjustments were made if necessary by an interventional cardiologist blinded to the CMR results. For each coronary stenosis the diameter stenosis (DS) was calculated. The lesions were grouped into three DS groups: <50% (mild), 50-70% (moderate) and >70% (severe).

*Statistical analysis*

Numerical values were compared using an independent sample t-test and categorical variables compared using the chi-square test. P values <0.05 were considered statistically significant. To determine the accuracy of perfusion mapping in determining a coronary artery stenosis >70%, receiver operator characteristic (ROC) curves were calculated. From the ROC curves, the sensitivity, specificity, positive predictive value (PPV) and negative predictive value (NPV) of the perfusion maps for diagnosing a patient with CAD was calculated. The area under the curve (AUC) of the ROC curves were compared according to DeLong et al. (175).

Figure 15. The American Heart Association (AHA) segment model demonstrating the myocardium supplied by each coronary artery (minus the apical cap). Red – left anterior descending (LAD), blue – left circumflex (LCx), yellow – right coronary artery (RCA).

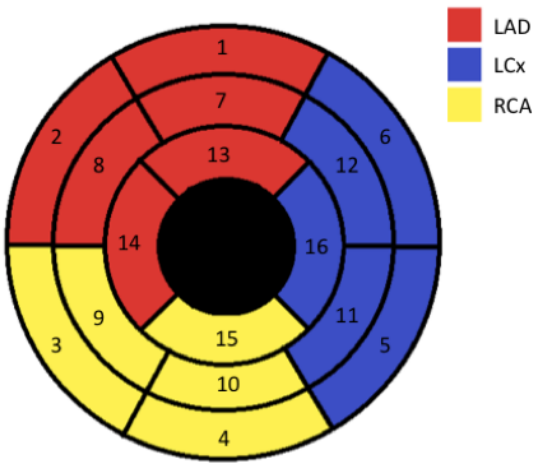

Figure 16. Perfusion map analysis. An example of perfusion map analysis for a single mid LV slice. Endocardial and epicardial borders were manually traced, RV insertion points identified and the LV segmented. Left panel- the borders are offset by 10% to minimise partial volume effects at the blood-myocardial and myocardial-pericardial borders. Right panel - the epicardial border is offset by 50% to measure endocardial flow.

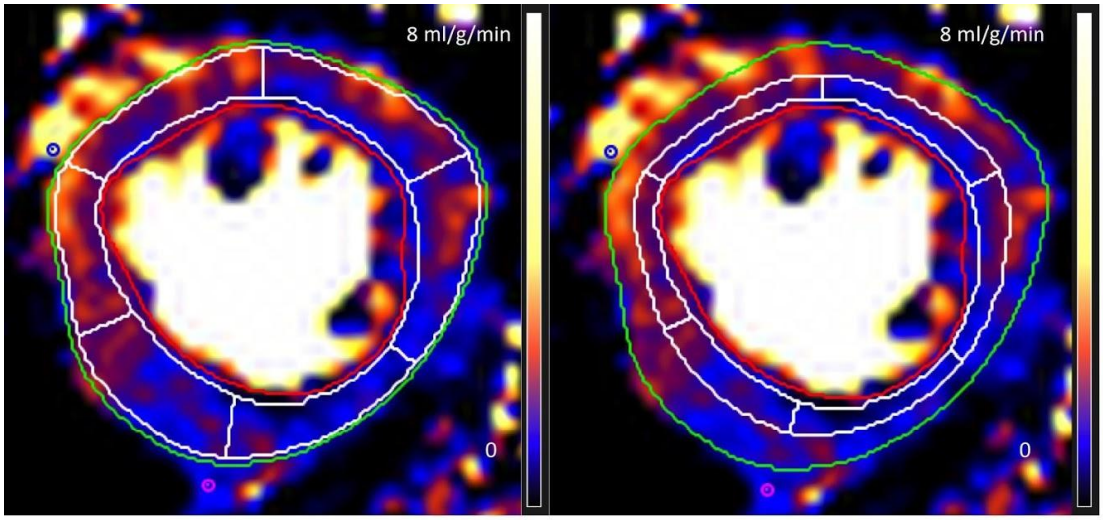

## 4.4 Results

50 patients were recruited. All patients underwent a research perfusion CMR and invasive coronary angiogram. Baseline patient and volunteer characteristics are shown in Table 3. Patients were older (58.2 vs 37.3 years, p<0.0001), a higher proportion was male (87% vs 50%, p=0.003) and had more comorbidities than volunteers.

Perfusion mapping analysis was possible in all 150 coronary territories but 3D QCA analysis was not performed in 28 vessels due to technical limitations with inadequate images for analysis due to the problems with the acquisition. Reasons for this included there not being two views at least 25 degrees apart, foreshortened images or images that overlapped in the segment of interest. Therefore in total, 122 vessels and their corresponding myocardial territories were included in the final analysis. The diameter stenosis was <50% in 81 vessels, 50-70% in 20 vessels and >70% in 21 vessels. 18 patients (36%) had at least 1 vessel with a severe stenosis (>70%). In the volunteer cohort, all 72 coronary territories were analysed by perfusion mapping.

Volunteers had higher stress MBF and MPR than patients even in the myocardial segments of patients supplied by vessels that were angiographically unobstructed (DS <50% stenosis). The global MBF was 3.07ml/g/min in healthy volunteers compared to 2.00ml/g/min in patients with DS <50%. The MBF and MPR fell with increasing severity of stenosis (Figure 17). Rest MBF was not significantly different between volunteers (0.86ml/g/min) and the remote myocardium (0.80ml/g/min, p=0.32) or ischaemic myocardium of patients (0.77ml/g/min, p=0.24).

The diagnostic accuracy of endocardial stress MBF, transmyocardial stress MBF and MPR for detecting a >70% coronary artery stenosis was calculated from receiver operating characteristic (ROC) curves using the patient data (Figure 18), excluding segments with infarction, detected from LGE (8 myocardial territories). The most accurate was endocardial stress MBF (AUC 0.92,

95% CI 0.87-0.97) although not statistically significantly different (p=0.051) from transmyocardial stress MBF (AUC 0.90, 95% CI 0.84-0.95). MPR was less accurate (AUC 0.81, 95% CI 0.71-0.91) than either endocardial (p=0.01) or transmyocardial (p=0.04) stress MBF.

The ROC curves were used to determine the optimal diagnostic threshold for transmyocardial stress MBF, endocardial MBF and MPR. For endocardial stress MBF, the optimal threshold on a per vessel basis was 1.31ml/g/min with sensitivity, specificity, PPV and NPV of 90%, 85%, 55% and 98% respectively. For transmyocardial MBF the optimal threshold was 1.50ml/g/min with sensitivity, specificity, PPV and NPV of 90%, 78%, 47% and 97%, respectively.

A per-patient based analysis (rather than a single coronary vessel basis) was also performed. The optimal value for endocardial stress MBF was <1.31ml/g/min with sensitivity, specificity, PPV and NPV of 100%, 74%, 73% and 100% respectively. With a transmyocardial stress MBF of <1.5ml/g/min in any coronary territory, the sensitivity, specificity, PPV and NPV was 100%, 70%, 70% and 100%, respectively.

Table 3. Patient and volunteer characteristics. Patients were significantly older, a greater proportion were male and they had more co-morbidities than the volunteers.

| | Patients (n=50) | Volunteers (n=24) | p-value |
|---|---|---|---|
| Age (years) | 58.2 | 37.3 | **<0.0001** |
| Gender (% male) | 86 | 50 | **0.003** |
| Height (cm) | 172 | 173 | 0.556 |
| Weight (kg) | 83 | 77 | 0.083 |
| BSA | 1.99 | 1.92 | 0.181 |
| LVEDV (ml) | 145 | 153 | 0.389 |
| LV mass (g) | 116 | 103 | 0.090 |
| EF (%) | 66 | 66 | 0.924 |
| Diabetes (%) | 16 | 0 | **0.004** |
| Hypertension (%) | 58 | 0 | **<0.0001** |
| Hypercholesterolemia (%) | 68 | 0 | **<0.0001** |
| Smoker (%) | 46 | 0 | **<0.0001** |
| AF (%) | 6 | 0 | 0.226 |

Figure 17. MBF (blue bars) and MPR (red bars) in volunteers and patients according to coronary vessel stenosis. Stress MBF (blue) is lower for patients than volunteers (p<0.001), even in territories supplied by vessels with <50% stenosis. Stress MBF is significantly lower in the myocardium supplied by vessels with >70% stenosis than <50% (p<0.001) and 50-70% stenosis (p<0.001). MPR (red) is lower in patients than volunteers (p=0.009). MPR is lower in the myocardium supplied by vessels with >70% stenosis than <50% (p<0.001) and 50-70% stenosis (p=0.03).

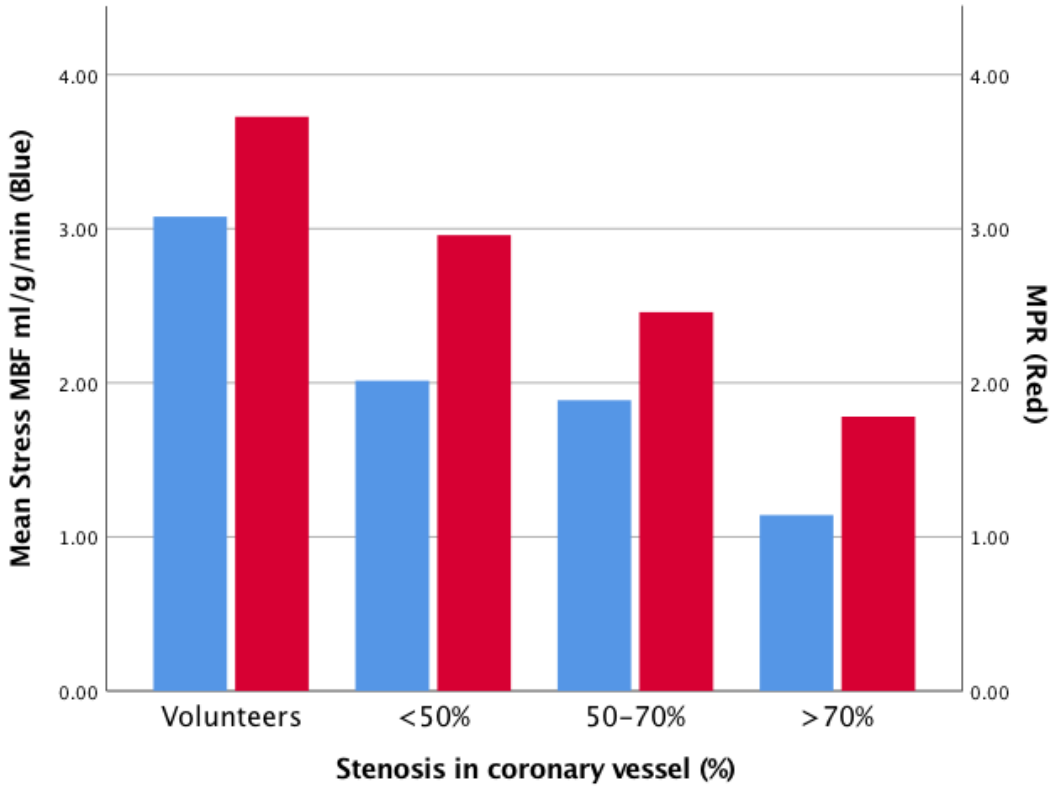

Figure 18. Receiver operating characteristic curves for MBF and MPR diagnosing coronary stenosis. The curves plot sensitivity against 1- specificity for transmyocardial MBF (red), sub-endocardial MBF (blue) and MPR (green) in diagnosing a coronary stenosis >70%. Endocardial stress and transmyocardial stress are superior to MPR (p=0.01 and p=0.04 respectively).

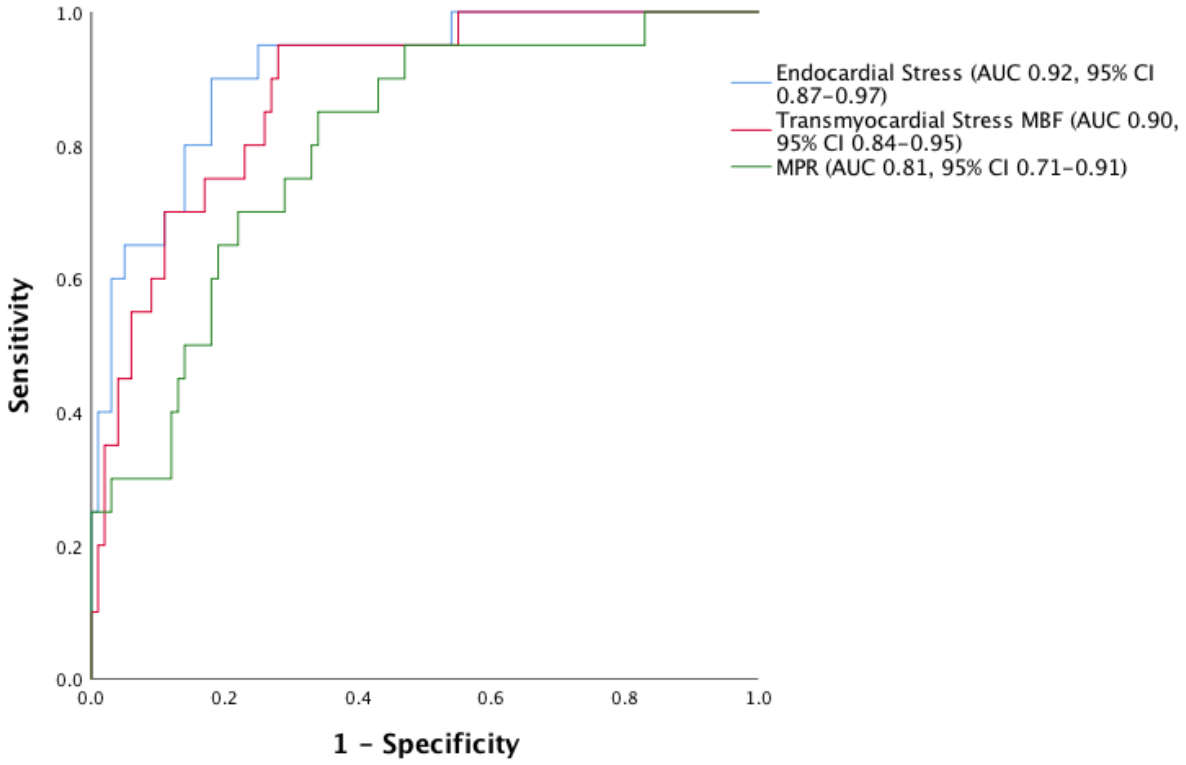

## 4.5 Discussion

This study shows that CMR perfusion mapping is accurate for the detection of coronary artery disease and it can be easily performed within a routine clinical workflow. I found that stress MBF (both endocardial and transmyocardial) were more accurate than myocardial perfusion reserve in these cases. Overall, the technique was highly sensitive, had good specificity and a high NPV on a coronary territory and whole patient basis. I found that if the MBF was >1.5ml/g/min in every myocardial territory, there was no significant obstructive CAD. We could immediately visualise this on the colour perfusion maps, which allows the clinician to quickly and easily rule out significant CAD.

An advantage of absolute perfusion quantification is that it takes away the subjective interpretation of perfusion CMR. The disadvantage with dual-sequence quantitative perfusion was the time-consuming post-processing required. With perfusion mapping, this is eliminated and a step forward. Also, the technique uses a single contrast bolus which is much more acceptable clinically as opposed to dual bolus techniques which can be cumbersome for the radiographer or technician performing the scan. These factors mean that perfusion mapping is easy to introduce into clinical CMR with minimal changes needed from standard practice. It is also important that we have shown that perfusion mapping has a high diagnostic accuracy. In this study we have found similar accuracies for perfusion mapping in the diagnosis of CAD to expert visual reads in studies such as CE-MARC (26). These are significant improvements on the quantitative perfusion techniques to date.

The principle of parametric mapping has expanded greatly over the last few years. Essentially, a colour map is output in which each pixel encodes a parameter. In much the same way that T1 and T2 mapping have provided great insight into characterising the myocardium (151), perfusion mapping permits instant visualisation of tissue perfusion without the need for a reference comparator. In our study we have found a high NPV, which, assuming there is an

appropriate colour look up table, a readily appreciable normal scan. The finding is also consistent with the PET literature where normal quantitative perfusion has a high NPV (178). The values that we have found in our study are reassuringly consistent with those seen in the PET literature (for both healthy volunteers and coronary artery disease patients) (178). This is despite an expected variation in the MBF and MPR parameters due to the heterogeneity involved with any non-invasive test, including variations in study protocols, sequences and tracers.

Whether the stress MBF or the MPR (the ability to increase the stress perfusion from the rest perfusion baseline) is a better myocardial biomarker of occlusive epicardial CAD has been hotly debated and contentious with inconsistent results. Some studies have found MPR to be a better predictor but in our study (and also other studies (178).), the opposite was the case. We found that it is the peak stress MBF that was the most accurate for the diagnosis of CAD. MPR may be inferior in the detection of CAD because the denominator of MPR – rest flow is independently regulated through the autonomic nervous system and is likely influenced by factors such as gender, resting heart rate, contractility and wall stress that are not related to peak flow. Therefore, the peak MBF may be normal, but if the rest MBF is (for example) high, perhaps due to an elevated resting heart rate secondary to anxiety the MPR would be abnormally low. In our study we did not find MPR to indicate a higher likelihood of coronary stenoses than MBF. Obstructive epicardial coronary artery disease reduces the peak stress MBF and this can be seen on the perfusion maps. However epicardial flow is not the only determinant of myocardial perfusion and so MBF/MPR is not specific to CAD. This would explain the lower specificity and PPV (85% and 55% respectively for endocardial MBF) that we found in the study, compared to the sensitivity and NPV (90% and 98% respectively) in our study. Other explanations that could lead to 'False positives' using a fixed threshold approach to perfusion map analysis include microvascular disease (179), submaximal response to adenosine or a combination of these

factors.  Also, epicardial CAD and microvascular disease may co-exist and this has been shown in other quantitative studies. For example it has been shown using PET that perfusion falls with an increasing coronary calcium score (180). In our study population we had patients who had single vessel CAD but reduced myocardial perfusion in multiple coronary artery territories. It is conceivable that as well as the occlusive CAD they also had co-existent microvascular dysfunction. Such a scenario would result in a false positive if the results were considered on a per vessel analysis but a true positive on a per patient analysis.

The difference in stress MBF between patients with a DS <50% and volunteers is interesting and may be explained by microvascular disease. The patients had co-morbidities including cardiovascular risk factors (including coronary disease) and smoking history. They were also older than the volunteers. Elucidating what MBF values are “normal” in patients with co-morbidities is also necessary to avoid false positives.

The study is limited by the small sample size (n=50) and in the absence of power calculations the results are hypothesis generating and require further trials to validate the findings. The reference standard used was QCA rather than a functional reference of FFR which, although better than a purely visual assessment, is a limitation. Furthermore, the total atheroma burden was not quantified and only focal stenoses were assessed. It is possible additional insights can be gained from total atheroma burden on MBF.

### 4.6 Conclusion

In summary, we have shown that stress perfusion cardiovascular magnetic resonance imaging with automated inline perfusion mapping is accurate (against 3D QCA analysis of invasive coronary angiography) for the detection of epicardial occlusive coronary artery disease and can be implemented relatively easily into the clinical workflow. It has a high sensitivity, and high negative predictive value which make it a good test to rule out obstructive CAD. If a patient has a

normal perfusion map (in which all pixels encode an MBF above the normal cut-off values) with a suitable look up table, a clinician can quickly rule out CAD.

# 5. Results 2 - The prognostic significance of myocardial perfusion

The following publication is based on this chapter:

The Prognostic Significance of Quantitative Myocardial Perfusion – an Artificial Intelligence Based Approach Using Perfusion Mapping

**Knott KD,** Seraphim A, Augusto JB, Xue H, Chako L, Aung N, Petersen SE, Cooper JA, Manisty C, Bhuva AN, Kotecha T, Bourantas CV, Davies RH, Brown LAE, Plein S, Fontana M, Kellman P, Moon JC. Circulation. 2020 Feb 14. doi: 10.1161/CIRCULATIONAHA.119.044666.

## 5.1 Summary

In this study I investigated the relationship of myocardial perfusion to patient outcome in patients referred for CMR.

As myocardial perfusion represents the blood that ultimately reaches the myocardium, it is determined by a combination of flow down the epicardial coronary arteries and the microvascular circulation. I sought to determine whether the patients' stress MBF and myocardial perfusion reserve were prognostic, over and above conventional risk factors.

This was a two-centre study of patients who were referred for a clinical CMR to investigate potential coronary artery disease. Perfusion maps were performed for all patients and the maps were analysed automatically using an artificial intelligence (AI) approach to derive the global stress MBF and MPR. To determine the associations of stress MBF and MPR with death and major adverse cardiovascular events (MACE) having adjusted for conventional risk factors, cox proportional hazard models were performed. The MACE events recorded were myocardial infarction, stroke, heart failure hospitalisation, late revascularisation and death.

In this study we followed up 1049 patients for a median of 605 days (interquartile range 464-814 days). During the period of follow up there were 42 (4.0%) deaths and 183 MACE events in 174 (16.6%) patients. Even after adjusting for other conventional risk factors, stress MBF and MPR were independently associated with both death and MACE. The adjusted hazard ratio (HR) for a 1ml/g/min decrease in stress MBF ratio was 1.93 (95% CI 1.08-3.48, P=0.028) for death and 2.14 (95% CI 1.58-2.90, P<0.0001) for MACE. The adjusted HR for a 1 unit decrease in MPR was 2.45 (95% CI 1.42-4.24, P=0.001) for death and 1.74 (95% CI 1.36-2.22, P<0.0001) for MACE. Even if there was no history of CAD and no perfusion defects on clinical read (n=783) perfusion was still prognostic. MPR was independently associated with both death and MACE, whereas stress MBF was independently associated with MACE only.

In conclusion, in this study I have shown that reduced myocardial perfusion provides a strong, incremental predictor of adverse cardiovascular outcomes. Going forward, further studies are required to see whether impaired perfusion can be treated and modify future cardiovascular risk and reduce events.

For this chapter I submitted an ethics request to the Barts Bioresource, compiled the list of patients, determined the patient risk factors for the majority of patients and searched the NHS spine for deaths and the patient record for MACE events. I then performed the statistical analysis and drafted the chapter and manuscript.

## 5.2 Introduction

The chronic coronary syndromes (CCS) are a heterogeneous group of cardiovascular disorders including large vessel or epicardial coronary artery disease (CAD) and microvascular dysfunction (12). These conditions both adversely affect the amount of blood that perfuses the myocardium and are associated with adverse outcomes (181). Investigations are often required to diagnose and tailor appropriate therapy to patients with CCS. A non-invasive risk-stratification test is desirable particularly if it provides prognostic information to the clinician. Non-invasive tests for cardiovascular risk stratification in symptomatic and asymptomatic patients have been developed. Quantitative cardiac PET has been the most developed technique used to quantify the MBF at stress and rest and therefore the MPR. Myocardial perfusion has been shown to be prognostic in PET studies in patients with suspected CAD (94–96,182) and also in patients with cardiomyopathy (132).

The latest iterations of the perfusion mapping technique use artificial intelligence (AI) to automatically segment the maps providing immediate global and regional quantification. AI has been used in CMR for volume analysis to enable widespread, precision measurement (183), but has not been applied to perfusion imaging before.

In this two-centre study we investigated whether quantitative perfusion biomarkers (stress MBF and MPR) were associated with adverse outcomes in all-comers referred for perfusion CMR.

## 5.3 Methods

*Patients*

Included in the study were consecutive patients referred for stress perfusion CMR at Barts Heart Centre (BHC) and the Royal Free Hospital (RFH), London, UK. Patients were aged over 18 years and recruited from March 2016 to August 2018.

The cardiovascular risk factors were documented from the patients' electronic record and from the NHS spine. The risk factors recorded were hypertension, diabetes mellitus, dyslipidaemia, previous revascularisation (including PCI or CABG), atrial fibrillation (AF), stroke or transient ischaemic attack (TIA), smoking status and history of cancer. The follow up outcomes recorded were all cause mortality and major adverse cardiovascular events (MACE). MACE events included myocardial infarction, stroke, heart failure admission, revascularisation (>90 days following CMR) and deaths. Early revascularisation (<90 days) were excluded to prevent bias from the ischaemia on the CMR resulting in a MACE event. A committee (authors KK, AS, JA) who were blinded to the quantitative perfusion data adjudicated the MACE events. Death was ascertained from a query of the NHS spine. Other events were reviewed and agreed upon following review of the clinical notes, (clinic letters, discharge summaries and GP records). Clinicians treating the patients were not involved in event adjudication.

*Cardiovascular Magnetic Resonance Scan*

The CMR scans were performed at 1.5 (Aera) or 3 Tesla (Prisma, Siemens Healthcare, Erlangen, Germany) according to a standard clinical approach (48). The stress and rest quantitative perfusion maps were immediately generated at the time of the scan (152).

*Image analysis*

The clinical CMR images were analysed by a European Association of Cardiovascular Imaging accredited cardiologist. The LV volumes (systolic and diastolic) and ejection fraction were calculated for each patient. It was documented whether late gadolinium enhancement (LGE)

was present and whether it was infarct pattern (subendocardial, coronary distribution) or non-infarct pattern (mid-myocardial or subepicardial).

Three LV short axis (base, mid and apex) perfusion maps were generated at stress and rest (152). The analysis of the perfusion maps was performed using an AI tool. Using a convolution neural network (CNN) approach the tool automatically segmented the LV cavity and myocardium. The AI excluded papillary muscles and epicardial fat (184). The average pixel value across all 3 short axis slices was used to determine the global MBF. Subsequently the MPR was calculated as the stress MBF divided by the rest MBF. An advantage of the AI approach is that the contouring was performed without bias and in a blinded fashion to other CMR and MACE outcome data. For an example of the AI contouring see Figure 19. The contoured perfusion maps were checked subsequently as a quality control mechanism to ensure there were no significant errors with the maps. If errors were observed the maps were discarded from analysis (for examples of reconstruction errors, see Figure 20). The errors were due to the AI incorrectly identifying sites other than the LV blood pool for arterial input function analysis, ECG miss-triggering or motion correction errors. The myocardial blood flow calculation would be highly inaccurate in these cases and so they were not used in the analysis. Once the AI contouring had been performed, it was not possible to make further manual adjustments to the contours. For each patient the stress MBF, rest MBF and MPR was recorded.

*Statistical analysis*

To compare means either the student T-test (if normally distributed) or Mann Whitney U test (if not normally distributed) were used for continuous variables and the chi-square test was used for categorical variables (2-sided Fisher exact test).

To determine the association of myocardial perfusion (stress MBF, MPR) with outcome (death and MACE) cox proportional hazard regression analyses was performed. The model adjusted for age, sex, co-morbidities (previous revascularisation, CAD, hypertension, dyslipidaemia,

diabetes mellitus, AF, stroke / TIA, smoking and cancer) and CMR parameters (EDV, LVEF, LGE). As the event rates were relatively low and there were a large number of variables, a sensitivity analysis was additionally performed to obtain Firth's bias-adjusted estimates (185). Kaplan Meier survival estimates were calculated for the stress MBF and MPR. In this analysis the data was censured at the date of death, MACE or last follow up. To compare the ability of stress MBF and MPR to predict outcome Harrel's C-indices were calculated.

Shoenfeld residuals were used to test the proportionality assumptions for each variable using a Bonferroni corrected significance level of $p<0.0008$. Plotting deviance residuals against each predictor variable and assessing the locally estimated scatterplot smoothing (LOESS) curve assessed functional form. To ensure that missing data did not affect results, models were run with and without imputation of missing data. As the models gave similar results, only complete case results are presented.

Figure 19. AI automatic segmentation of stress perfusion maps. The analysis was performed with no user input and demonstrated for two different patients. Three short axis (base, mid and apical) left ventricle slices are shown for a 76-year-old male with dyslipidaemia and no MACE (A) and a 64-year-old female with hypertension and atrial fibrillation who died within 24 months of the scan (B). Stress myocardial blood flow was 2.25ml/g/min in (A) and 1.52ml/g/min (B). The myocardium is additionally segmented as per the American Heart Association model with the first segment from each slice outlined in yellow and the second in green.

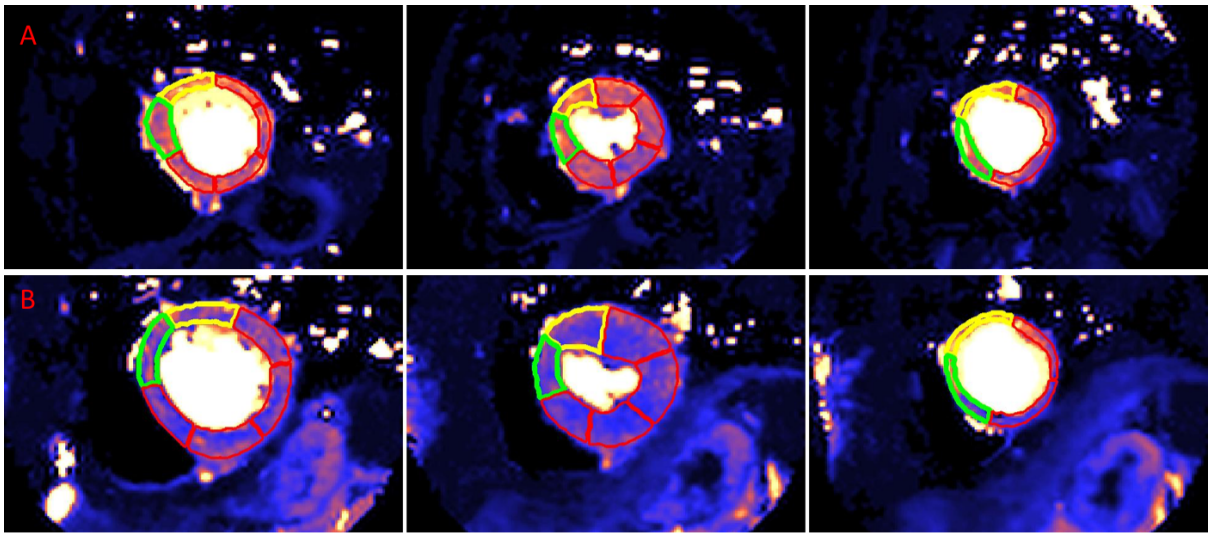

Figure 20. Examples of reconstruction errors. Examples of perfusion map reconstruction errors for 5 different patients (A-E) compared to a correct reconstruction (F). As a result, the LV myocardium is visually highly artefactual and the segmentation unreliable.

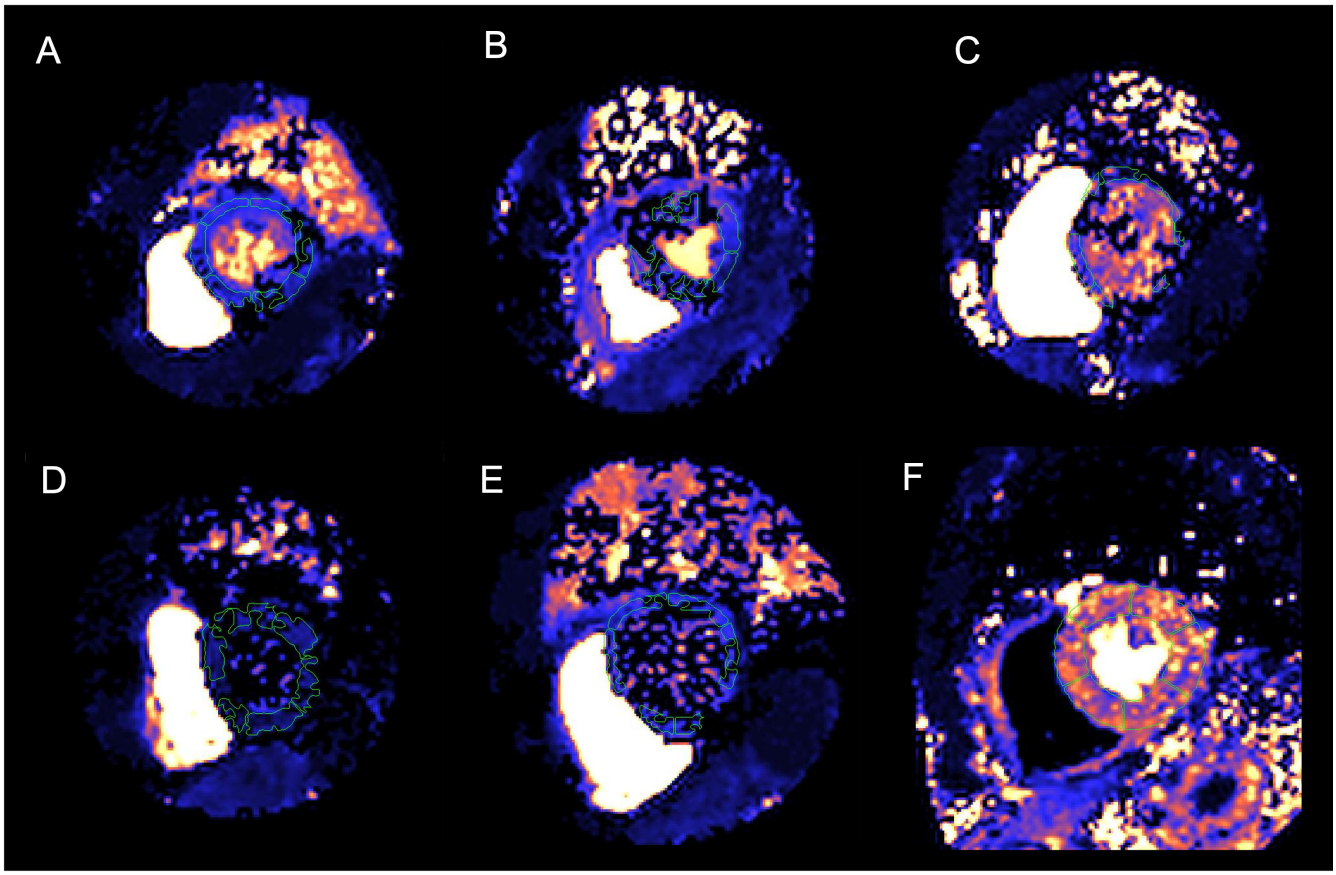

## 5.4 Results

*Patient demographics, comorbidities and CMR parameters*

In total 1356 patients were referred for stress perfusion CMR between September 2016 and August 2018 at BHC and the RFH. There were 143 patients who were excluded based on the exclusion criteria. 45 (3%) patients were excluded due to lack of stress response (determined by change in heart rate, symptoms, splenic switch off). In 15 cases (1%) there were significant perfusion map errors preventing analysis (see Figure 20). There were 104 patients (8%) who were lost to follow up. These patients were referred for CMR from local district general hospitals who were not follow up by Barts Health / Royal Free and did not have accessible GP records. In total 1049 patients were included in the final analysis (889 BHC, 160 from RFH, Figure 21). Rest perfusion was not done in 31 cases and so MPR data was not available. In total there were 1018 patients with MPR data.

In the final analysis group, the mean age was 60.9 +/-13 years. 702 (67%) were male, 298 (28%) had diabetes mellitus, 630 (60%) hypertension, 510 (49%) dyslipidaemia, 318 (30%) previous revascularisation, 360 (34%) smoking history, 63 (6%) previous stroke or TIA, 141 (13%) AF, 108 (10%) current or previous history of cancer. The mean EDV across all patients was 157+/- 52ml, LV mass 119 +/- 38g, mean EF for these patients was 60 +/- 13%, 309 (30%) patients had subendocardial, infarct pattern LGE and 133 (13%) had non-infarct pattern LGE. See Table 4 for a summary of patient baseline data and CMR data. Across all the patients, the mean stress MBF was 2.06+/-0.71 ml/g/min and MPR was 2.48+/-0.82. The median follow up was 605 (interquartile range 464-814) days.

*Predictors of MACE*

There were 42 (4.0%) deaths and 183 MACE events in 174 (16.6%) patients. The MACE events were 28 (2.7%) non-fatal myocardial infarction, 10 (0.95%) strokes, 18 (1.7%) heart failure admissions and 127 (12.1%) late revascularisations.

The mean MBF of patients that died was 1.70+/-0.65 ml/g/min vs 2.08 ml/g/min +/- 0.71 (P=0.001) in patients that survived. The mean MPR was 1.97 +/- 0.74 in the group that died and 2.50 +/- 0.81 in the group that survived (P<0.001). Similarly, the mean stress MBF in the total events (death or MACE) group was 1.62+/-0.56 ml/g/min vs 2.15 +/- 0.71 ml/g/min in the event-free group (P<0.001) and the mean MPR was 2.04 +/- 0.76 vs 2.57 +/- 0.80 respectively (P<0.001).

Patients that had a MACE were commonly male (78.2% vs 64.7%, P=0.001), older (65.9 +/- 10.2 vs 59.9 +/- 13.1 years, P<0.0001), had more prior revascularisations (40.8% vs 28.3%, P=0.002), were more commonly diabetic (42.0% vs 25.7%, P<0.0001), hypertensive (75.3% vs 57.0%, P<0.0001), dyslipidaemic (62.6% vs 45.8%, P<0.0001), were more likely to have had a previous stroke or TIA (9.8% vs 5.3%, P=0.034), were more likely to be smokers (42.5% vs 32.7%, P=0.014), had similar rates of AF (12.6% vs 13.6%, P=0.808), and similar rates of cancer (13.8% vs 9.6%, P=0.102). In terms of CMR parameters, there was similar LVEDV in patients who died or had MACE and in those that didn't (161.8 +/- 57.0ml vs 155.9 +/- 51.3ml, P=0.174), higher LV mass (129.0 +/- 41.9g vs 117.1 +/- 37.4g, P=0.0002) and lower LVEF (56.9 +/- 15.6% vs 60.8 +/- 12.8%, P=0.002). They had more infarct pattern LGE (54.0% vs 24.6%, P<0.0001) and similar non-infarct pattern LGE (10.3% vs 13.1%, P=0.382). See Table 5. For a breakdown of perfusion data and MACE for each field strength and site see Table 6 and Table 7.

To elucidate the factors contributing to death and MACE, cox hazard regression analysis was performed. Even after accounting for other risk factors, stress MBF and MPR were associated with events. Higher MBF and MPR was associated with a lower incidence of events. On multivariate Cox regression analysis, age, stress MBF or MPR, EF and history of cancer were

significantly associated with death. Age, a history of dyslipidaemia and stress MBF or MPR were associated with death or MACE. For each 1ml/g/min reduction in stress MBF, the adjusted hazard ratio (HR) for death was 1.93 (95% CI 1.08-3.48, P=0.028) and for MACE was 2.14 (95% CI 1.58-2.90, P<0.0001). For each 1-unit reduction in MPR, the adjusted HR for death was 2.45 (95% CI 1.42-4.24, P=0.001) and for MACE was 1.74 (95% CI 1.36-2.22, P<0.0001). See Table 8. The effect of MBF and MPR on outcome was investigated with a standardized hazard model and using Harrel's C-index. The standardized hazard model compared the effect of a 1 standard deviation (SD) decrease in MBF and MPR on outcome. The effect size was larger for MPR than stress MBF for death (standardized HR 2.08 vs 1.56 respectively) but not for total MACE (standardized HR 1.59 vs 1.79). Similarly, Harrell's C-index suggests that the predictive ability is better for MPR (C-index=0.69 (95% CI: 0.61-0.77) than for MBF (C-index=0.63 (95% CI: 0.54-0.73) when predicting death, but both variables have similar predictive ability for the total MACE (0.68 (0.64-0.73) MBF vs. 0.68 (0.64-0.72) MPR). A sensitivity analysis using Firth's penalised model did not show bias caused by low event rates.

Kaplan Meier survival estimate curves for MBF and MPR were calculated for death (Figure 22) and MACE (Figure 23).

Patients were analysed by median stress MBF / MPR. The median stress MBF was 1.99 ml/g/min and the median MPR 2.40. Those with MBF in the lowest 50$^{th}$ percentile had higher rates of death MACE compared to the highest 50$^{th}$ percentile. Death and MACE was 5.3% and 26.1% respectively if the stress MBF was below the median and 2.7% and 7.0% respectively if perfusion was above the median. Death and MACE was 6.3% and 24.6% respectively if the MPR was below the median and 2.0% and 8.6% respectively if perfusion was above the median. There were 266 patients (25.4%) with a perfusion defect on clinical review of the standard perfusion images. In patients with perfusion defects, deaths were not significantly different

from those with uniform perfusion (14 (5.3%) vs 28 (3.6%), P=0.276), but MACE was higher (103 (39%) vs 71 (9.1%), P<0.0001).

In the group of patients with no perfusion defects on clinical review, an additional multivariate Cox regression analysis was done. Death was associated with age, EF, history of cancer, history of hypertension and MPR but not stress MBF. MACE was associated with age, history of cancer and both stress MBF and MPR. The adjusted HR for a 1-unit decrease in MPR was similar to the entire cohort: 2.22 for death (95% CI 1.16-4.23, P=0.015) and 1.65 for MACE (95% CI 1.14-2.38, P=0.008). The HR for each 1ml/g/min decrease in stress MBF was 2.28 (95% CI 1.43-3.66) for MACE (P=0.001).

When patients with previous CAD, history of MI or LGE were excluded, another Cox hazard regression analysis was performed for death and MACE. Death was associated with age, history of cancer, dyslipidaemia and MPR. MACE was associated with age, a history of cancer and both stress MBF and MPR. For death, the adjusted HR for a 1-unit decrease in MPR was 2.49 (95% CI 1.01-6.13, P=0.049). For MACE the adjusted HR for a 1-unit decrease in MPR was 2.38 (95% CI 1.30-3.77, P=0.003) and for a 1ml/g/min decrease in stress MBF was 2.15 (95% CI 1.20-3.83, P=0.010).

Figure 21. Flow chart demonstrating the outcome study process. There were 1049 patients included in the analysis. 143 patients met the exclusion criteria, there were reconstruction errors in perfusion maps in 15 cases and there were 45 cases of inadequate stress (no splenic switch off). 104 patients were lost to follow up. There were 183 MACE events in 174 patients including 42 deaths.

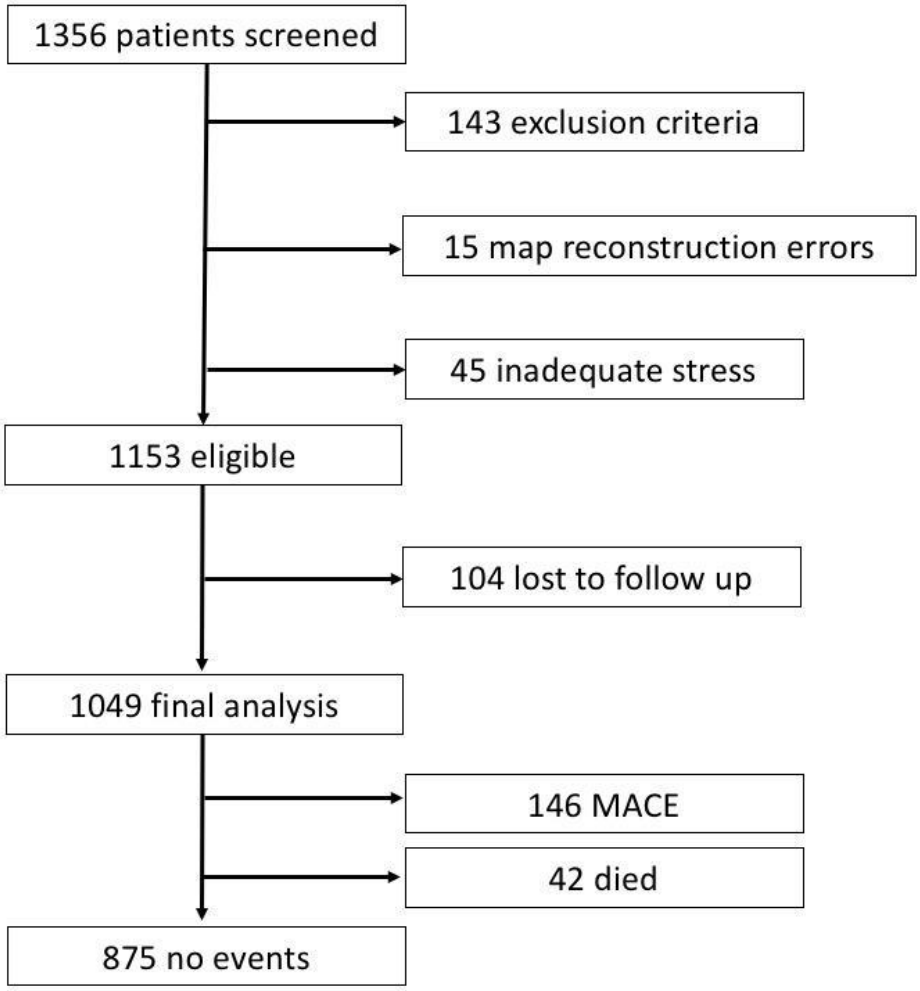

Table 4. Baseline characteristics of the patient population studied including patient demographics, CMR data and outcomes.

| | N = 1049 |
|---|---|
| *Demographics* | |
| Age (years) | 60.9 +/- 13 |
| Sex n (% male) | 702 (70) |
| *Co-morbidities* | |
| Hypertension, n (%) | 630 (60.1) |
| Dyslipidemia, n (%) | 510 (48.6) |
| Diabetes Mellitus, n (%) | 298 (28.4) |
| Previous PCI / CABG, n (%) | 319 (30.4) |
| AF, n (%) | 141 (13.4) |
| Stroke / TIA, n (%) | 63 (6.0) |
| Smoking history, n (%) | 360 (34.3) |
| Cancer, n (%) | 108 (10.3) |
| *CMR parameters* | |
| LVEDV, ml | 157 +/- 52.2 |
| LV mass, g | 119 +/- 38.4 |
| EF, % | 60.+/- 13.4 |
| Infarct pattern LGE, n (%) | 309 (29.5) |
| Non-infarct pattern LGE, n (%) | 133 (12.7) |
| Stress MBF (ml/g/min) | 2.06 +/- 0.71 |
| MPR | 2.48 +/- 0.82 |
| *Outcome* | |
| Death, n (%) | 42 (4.0) |
| MACE, n (%) | 174 (16.6) |
| Myocardial infarction, n (%) | 28 (2.7) |
| Stroke, n (%) | 10 (0.95) |
| Heart failure admission n, (%) | 18 (1.7) |
| Late revascularisation, n (%) | 127 (12.1) |

Table 5. Patient characteristics of those that had a MACE event and those that did not.

| | MACE<br>N=174 | No MACE<br>N=875 | Significance<br>(p-value) |
|---|---|---|---|
| *Demographics* | | | |
| Age (years) | 65.88 +/- 10.21 | 59.88 +/- 13.14 | **<0.0001** |
| Sex n (% male) | 136 (78.2) | 566 (64.7) | **0.001** |
| *Co-morbidities* | | | |
| Hypertension, n (%) | 131(75.3) | 499 (57.0) | **<0.0001** |
| Dyslipidemia, n (%) | 109 (62.6) | 401 (45.8) | **<0.0001** |
| Diabetes Mellitus, n (%) | 73 (42.0) | 225 (25.7) | **<0.0001** |
| Previous PCI / CABG, n (%) | 71 (40.8) | 248 (28.3) | **0.002** |
| AF, n (%) | 22 (12.6) | 119 (13.6) | 0.808 |
| Stroke / TIA, n (%) | 17 (9.8) | 46 (5.3) | **0.034** |
| Smoking history, n (%) | 74 (42.5) | 286 (32.7) | **0.014** |
| Cancer, n (%) | 24 (13.8) | 84 (9.6) | 0.102 |
| *CMR parameters* | | | |
| LVEDV, ml | 161.80 +/- 56.98 | 155.86 +/- 51.26 | 0.174 |
| LV mass, g | 129.01 +/- 41.93 | 117.05 +/- 37.40 | **0.0002** |
| EF, % | 56.88 +/- 15.58 | 60.83 +/- 12.78 | **0.002** |
| Infarct pattern LGE, n (%) | 94 (54.0) | 215 (24.6) | **<0.0001** |
| Non-infarct pattern LGE, n (%) | 18 (10.3) | 115 (13.1) | 0.382 |
| Stress MBF (ml/g/min) | 1.62 +/- 0.56 | 2.15 +/- 0.71 | **<0.0001** |
| MPR | 2.04 +/- 0.76 | 2.57 +/- 0.80 | **<0.0001** |

Table 6. Perfusion and MACE events by field strength (Tesla, T).

| | 1.5T (n=679) | 3.0T (n=370) | Significance (P value) |
|---|---|---|---|
| Stress MBF (ml/g/min) | 2.07 | 2.06 | 0.807 |
| MPR | 2.49 | 2.47 | 0.801 |
| Death, n (%) | 25 (3.7) | 17 (4.6) | 0.511 |
| MACE, n (%) | 116 (17.1) | 58 (15.7) | 0.603 |

Table 7. Comparison of MACE events by field strength and site.

| | MACE (n=174) | No MACE (n=875) | Significance (P value) |
|---|---|---|---|
| Stress MBF 1.5T (ml/g/min) | 1.61 | 2.16 | **<0.0001** |
| MPR 1.5T | 1.94 | 2.60 | **<0.0001** |
| Stress MBF 3.0T (ml/g/min) | 1.64 | 2.13 | **<0.0001** |
| MPR 3.0T | 2.24 | 2.52 | 0.020 |
| BHC MBF (ml/g/min) | 1.58 | 2.11 | **<0.0001** |
| BHC MPR | 2.06 | 2.54 | **<0.0001** |
| RFH MBF (ml/g/min) | 1.76 | 2.41 | **<0.0001** |
| RFH MPR | 1.97 | 2.72 | **<0.0001** |

Table 8. Cox proportional hazard models for a 1ml/g/min decrease in stress MBF and 1 unit decrease in MPR. * The models are adjusted for age, sex, left ventricular (LV) end diastolic volume, LV mass, LV ejection fraction, late gadolinium enhancement, previous revascularisation, diabetes, hypertension, dyslipidaemia, stroke history, atrial fibrillation and cancer. Stress MBF and MPR were independently associated with death and major adverse cardiovascular events (MACE) even after adjustment for the other risk factors. Abbreviations hazard ratio (HR).

| Predictor | | | Death | Death and MACE |
|---|---|---|---|---|
| Stress MBF (ml/g/min) | Unadjusted | HR (95% CI)<br>P value | 2.28 (1.39-3.75)<br>P=0.001 | 3.02 (2.34-3.89)<br>P<0.0001 |
| | Adjusted* | HR (95% CI)<br>P value | 1.93 (1.08-3.48)<br>P=0.028 | 2.14 (1.58-2.90)<br>P<0.0001 |
| MPR | Unadjusted | HR (95% CI)<br>P value | 2.72 (1.70-4.39)<br>P<0.0001 | 2.40 (1.91-3.01)<br>P<0.0001 |
| | Adjusted* | HR (95% CI)<br>P value | 2.45 (1.42-4.24)<br>P=0.001 | 1.74 (1.36-2.22)<br>P<0.0001 |

Figure 22. Kaplan Meier survival estimate curves for stress MBF and MPR. Stress MBF (A and B) and MPR (C and D). In red are the survival curves for the highest 50$^{th}$ percentile and in blue lines the lowest 50$^{th}$ percentile of patients. B and D are magnified graphs of A and B respectively and demonstrate the curve separation. Rates of death are higher with impaired perfusion. Patients in the highest 50$^{th}$ percentile have higher rates of death than the patients in the lowest 50$^{th}$ percentile of MBF and MPR (P=0.032 and P=0.01 respectively).

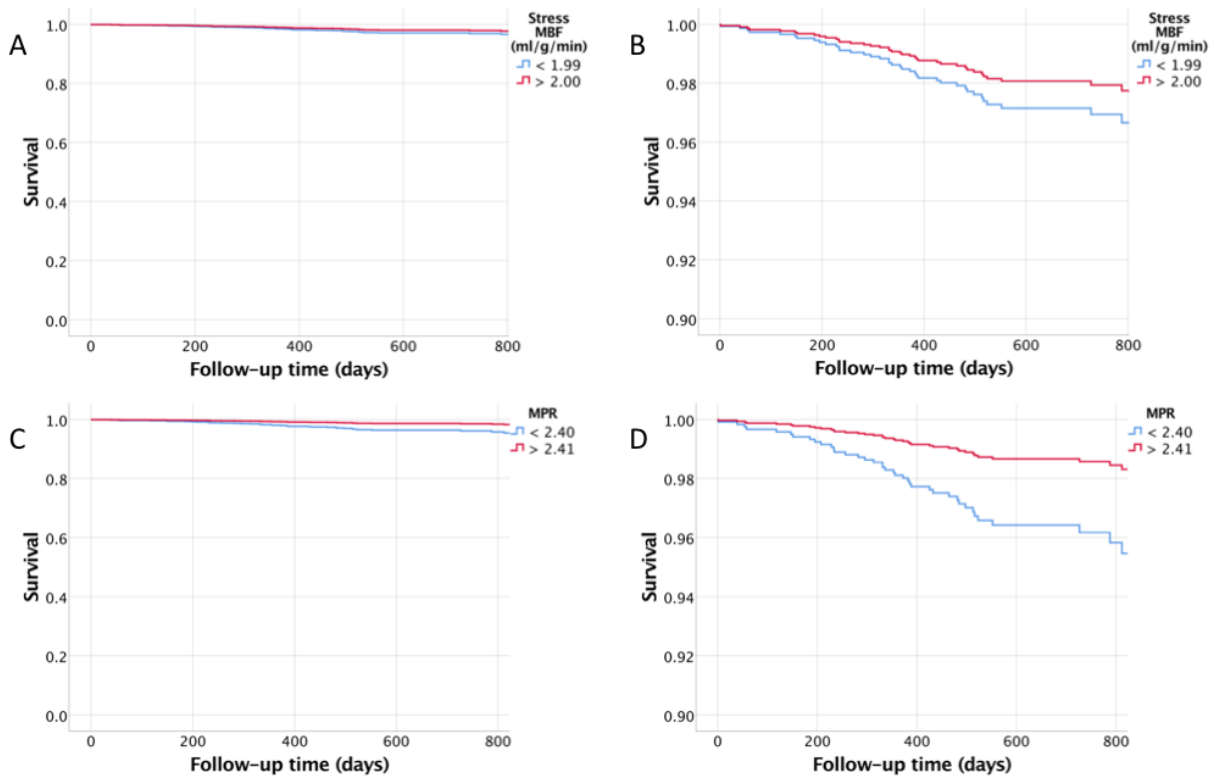


| | | Time (days) | | | | |
|---|---|---|---|---|---|---|
| | | 0 | 200 | 400 | 600 | 800 |
| Number at risk | MBF <1.99 | 525 | 518 | 459 | 264 | 135 |
| | MBF >2.00 | 524 | 521 | 460 | 269 | 143 |
| | MPR <2.40 | 510 | 501 | 443 | 252 | 130 |
| | MPR >2.40 | 508 | 507 | 448 | 265 | 138 |

Figure 23. Kaplan Meier survival estimate curves for MACE for stress MBF and MPR. Stress MBF (A) and MPR (B). In red are the survival curves for the highest 50$^{th}$ percentile and in blue the lowest 50$^{th}$ percentile of patients. Patients in the lowest 50$^{th}$ percentile of MBF and MPR had higher rates of death (P<0.001 for both).

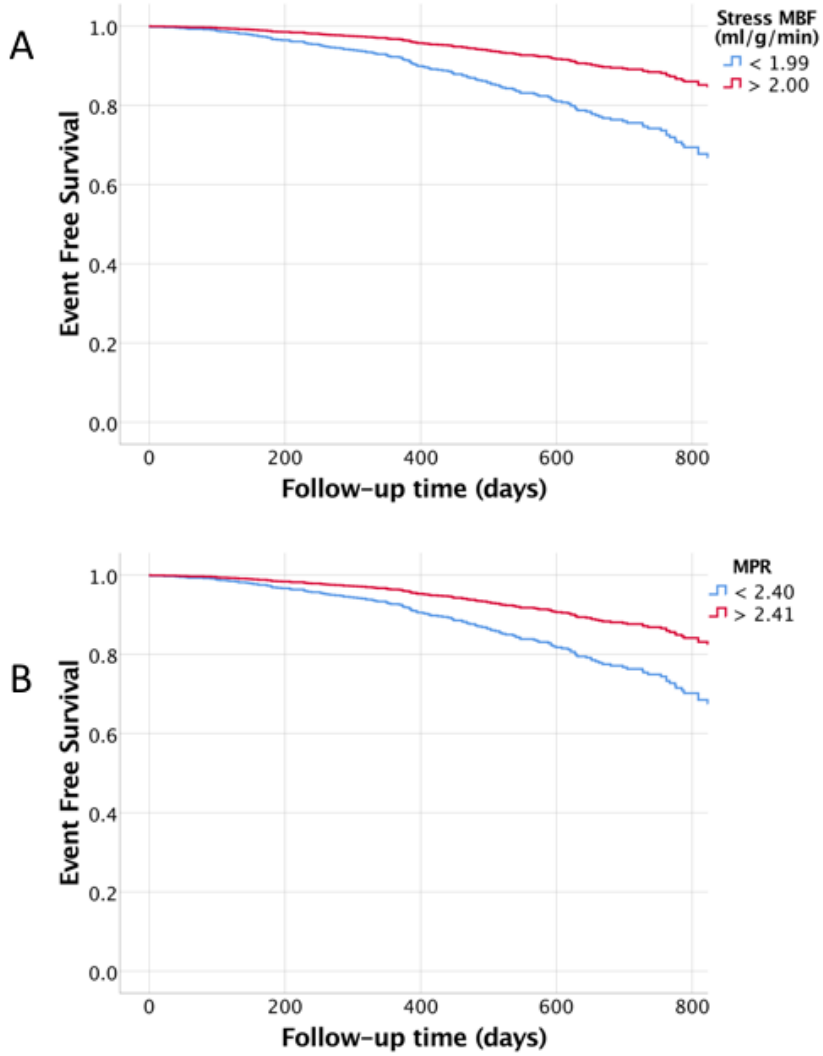


| | | Time (days) | | | | |
|---|---|---|---|---|---|---|
| | | **0** | **200** | **400** | **600** | **800** |
| **Number at risk** | **MBF <1.99** | 525 | 478 | 337 | 179 | 61 |
| | **MBF >2.00** | 524 | 501 | 373 | 179 | 63 |
| | **MPR <2.40** | 510 | 466 | 331 | 161 | 57 |
| | **MPR >2.40** | 508 | 484 | 361 | 182 | 59 |

## 5.5 Discussion

In this multicentre study of 1049 patients we have shown that, over a median 605 day follow up period, stress MBF and MPR are associated with death and MACE. This is the largest quantitative perfusion CMR outcome study that has been conducted and we have shown that it is possible to quantify perfusion automatically and inline at scale using CMR with clinically meaningful results.

Stress MBF and MPR are associated with outcomes over and above other cardiovascular risk factors. Using an artificial intelligence approach, the technique can be applied at scale to large datasets with instantaneous results. We have shown that a 1 SD increase in stress MBF (0.71ml/g/min) or MPR (0.82) is associated with a reduced risk of death by 36% and 52% and MACE by 54% and 37%, even after adjusting for other risk factors. The technique is appealing from a clinical perspective but also in research both as an endpoint in clinical studies and in therapeutics to see whether there are medical therapies that can improve perfusion and potentially improve outcomes.

This study confirms the prognostic relevance of myocardial perfusion, which has previously been shown in PET studies (94–96,182). Herzog et al recruited 256 patients and followed them up for a median 5.4 years (94). They found that even in patients with “normal” perfusion (i.e. no perfusion defects), an abnormal MPR (<2) was associated with worse outcomes. The survival curves converged after 3 years suggesting a warranty period of normal PET perfusion. Murthy et al 2011 followed up 2783 patients for a median 1.4 years (95). They measured the extent of a perfusion defect with a visual estimate and quantitative perfusion. Patients in the lowest tertile of coronary flow reserve (CFR, equivalent to MPR) (<1.5) had a 5.6 times increased risk of cardiac death compared to the highest tertile. Quantification allowed the re-classification of intermediate risk patients on visual estimation to high risk. They found peak stress MBF was a less powerful predictor than CFR. Taqueti et al 2014 followed up 329

patients for a median 3.1 years (182). When they compared CFR to angiographic score, CFR associated with outcome independently of angiographic coronary stenoses. Patel et al 2019 followed up 12594 patients for a median of 3.2 years to identify all-cause mortality, adjusted for the interaction between early revascularisation and CFR (96). Patients had a survival benefit based on early revascularisation regardless of type of revascularisation or level of ischemia.

Perfusion mapping has been previously directly compared to rubidium PET in patients with stable CAD with CMR and PET studies on the same day (150). In this study Engblom et al found that the absolute MBF correlated well between the techniques on a global (r=0.92) and regional (r=0.83) basis (150). Kotecha et al compared perfusion mapping with invasive coronary physiology with FFR and IMR (186). Myocardium perfused by coronary stenoses with a positive FFR had reduced perfusion than myocardium perfused by FFR negative arteries. When the IMR was high (suggestive of microvascular dysfunction) and FFR normal, the perfusion was intermediate. It has also been shown that the perfusion mapping is a relatively robust technique with a similar repeatability to the published PET data in healthy volunteers (170). With our study demonstrating the prognostic performance of perfusion mapping this is a further validation of the technique.

There has only been one previous quantitative perfusion outcome CMR study, a single centre study using a dual bolus, single sequence approach to quantification. In that study, Sammut et al found impaired myocardial perfusion reserve to contain prognostic information in a 395 patient cohort followed up for a median 460 days (187). They used a set threshold (1.5) of MPR for ischaemia in each segment and determined the number of ischaemic segments. That study considered only a composite MACE endpoint and there was no data on stress MBF. In our study we used a pixel-wise quantitative model which potentially allows a more reliable estimate of ischaemic burden rather than a segmental model. Furthermore, the Sammut group used the

dual bolus technique which, although highly accurate, has limitations in the integration into routine clinical care as it requires centre expertise in carrying out the study in a robust manner and labour intensive post processing. In order for quantitative CMR perfusion to be used routinely, it requires an automated process.

The pixel-wise perfusion mapping approach with full automation of analysis using AI has made a large-scale multicentre study feasible. The size of the study has allowed us to explore the prognostic significance of perfusion adjusted for other conventional risk factors of MACE and mortality. Automated map output and MBF analysis is now comparable to the PET technique. Additionally, in this study, we have shown that even in patients without perfusion defects on clinical review, perfusion contains similar prognostic information. This finding supports the potential use of outputting MBF and MPR in the clinical setting to allow for risk stratification of patients, even when there is no perfusion defect seen.

Whether stress MBF or MPR is more predictive of outcome has been debated extensively. Our study contributes to this debate, although with the relatively small number of deaths in the study, the finding that MPR is more predictive of death than stress MBF should not be overstated. However, the result is consistent with the PET literature in which MPR has been found to be superior for death than stress MBF. In one study, Gupta et al followed up 4029 patients for a median of 5.6 years and found MPR to be more predictive of cardiovascular death than MBF (188). If both the MPR and MBF were abnormal, patients had the worst outcomes. If MPR and MBF were normal, the patients had the best outcomes. If the MBF was impaired but MPR normal, patients had a low event rate but if the MPR was impaired and MBF was abnormal the event rate was intermediate. It is possible that the ability of the myocardium to vasodilate in response to stress is more important than the absolute peak MBF and that would explain these findings. Other explanations would include the cancelling out of biases / systematic errors in the stress and rest perfusion in the MPR which improves the accuracy. A

PET specific confounder is the use of the rubidium tracer. The extraction fraction of rubidium is lower than the gold standard $^{15}$O-water which potentially reduces the accuracy of the measurement of peak stress MBF.

It is not surprising that patients with impaired myocardial perfusion have worse outcomes. The explanation for the impaired perfusion is likely multifactorial and due to both pathology of the epicardial coronary arteries and the myocardial microvasculature. When an expert observer reviews a perfusion image, they compare the relative signal intensity in one part of the myocardium to another. This relies on the assumption that at least one segment of the myocardium is supplied by a "normal" epicardial vessel and has "normal" microvascular function and can therefore be a reference for the other myocardial segments. It is possible that either the microvasculature is globally impaired or that there is abnormal epicardial flow in all of the coronary arteries and this would not be appreciated on clinical read but could potentially be adversely prognostic for patients. For example, it has been shown that coronary arteries which are diffusely disease can have impaired vasodilatation and a continuous fall in pressure along the course of the artery resulting in ischaemia but no distinct stenosis (189). Microvascular dysfunction in the absence of coronary artery disease can also cause perfusion abnormalities (186,190). Although MBF and MPR are independently associated with outcome above conventional risk factors, there is likely some interplay and we observed that patients with lower MBF and MPR had more traditional cardiovascular risk factors, suggesting they may also be associated with impaired perfusion. It is possible that myocardial perfusion is additionally a surrogate marker for general vascular health and this explains the association with the MACE events observed.

We found no significant differences between stress MBF and MPR at 1.5 vs 3 Tesla. The RFH cohort had slightly higher MBF compared to the BHC cohort (2.27 vs 2.03 ml/g/min, $p<0.01$) with similar MPR (2.57 vs 2.47, $p=0.17$).

*Limitations*

There is a potential for bias in the study with the relatively low number of events and large number of variables entered into the models. However, we additionally performed a sensitivity analysis to check for biases and similar results were observed making this less likely. As this study is observational in nature, the associations observed do not definitively indicate causation. In our study we adjusted for several potential confounders / cardiovascular risk factors. Despite this it is still possible that unmeasured confounders influenced the results. In this study we used the electronic patient record to determine MACE events. It is therefore possible that some events were missed. This limitation is however also found in the previous perfusion outcome studies. We used all-cause mortality rather than cardiovascular death in our study. That was because the NHS spine is readily searchable for mortality data, compared to the Office for National Statistics. Furthermore, cause of death can be influenced by mis-classification bias. There was a relatively large number of patients who were lost to follow up (for which we could obtain no follow up data). I do not have the characteristics of this group of patients, and this is a limitation.

In our study we found that despite the robust nature of the technique, there were still errors in 1.1% of perfusion maps. Sources of error include motion correction failure, miss-identification of the LV blood pool and ECG miss-triggering. Although this resulted in the exclusion of patients from our study, in real clinical practice, there are quality control measures for each of these problems. First of all there are blood pool identification images outputted, AIF graphs, heart rate ECG trigger graphs on the scanner as well as the perfusion map outputs. This allows the reporting clinician to interrogate the raw data from which the maps are created and have confidence in the perfusion maps outputted.

## 5.6 Conclusion

We have shown in the largest quantitative perfusion CMR study to date (and the first multi-centre) that myocardial perfusion (MPR and MBF) is associated with death and MACE independent of other risk factors. The automated nature of the technique, and the use of artificial intelligence in the analysis, allow for large-scale use of quantitative perfusion in the clinical and research setting. Going forward the study provides the foundation for randomised interventional studies to see whether modifying MBF and MPR is possible and whether this impacts upon patient outcome.

# 6. Results 3 - Perfusion in non-obstructive coronary disease

6.1 Summary

Myocardial perfusion depends on the blood flow down the epicardial coronary arteries and the microvasculature. In order to understand the microvascular component of MBF, I explored MBF influences at stress and rest in patients with unobstructed epicardial coronary arteries. Further understanding of the microvasculature could help optimise epicardial coronary artery disease detection and potentially serve as an independent diagnostic and therapeutic target. Reference ranges are also needed for quantitative perfusion in clinical practice.

In this study 242 participants with unobstructed epicardial coronary arteries and no myocardial scar (mean +/- standard deviation age 56.0 +/- 12.8 years) from 5 European centres underwent perfusion mapping at stress and rest. The factors influencing MBF were determined using univariate and multivariate linear regression.

Mean rest perfusion was 0.91+/-0.24 ml/g/min. Factors independently associated with rest MBF were sex and the use of beta blockers. Rest perfusion was higher in females and lower in patients on beta blockers. Stress MBF was 2.53+/-0.82ml/g/min. Factors independently associated with reduced stress MBF were increasing age, diabetes, increasing left ventricular mass and the use of beta blockers. Stress MBF falls 10% over 19 years and diabetes drops the MBF by the equivalent of being 27 years older. Similarly, the presence of LVH would be the equivalent of ageing by 20 years.

These data may help develop reference ranges in quantitative perfusion for the detection of epicardial coronary artery disease, input to improve other modelling techniques (for example CT FFR), and advance perfusion mapping as a technique to measure microvascular function.

## 6.2 Introduction

Myocardial perfusion depends on the epicardial flow down the coronary arteries and the microvasculature. Historically the predominant focus is on epicardial disease, but the prevalence of this is falling and many patients who undergo invasive angiography do not have obstructive coronary artery disease to explain their symptoms (31). The major adverse cardiovascular event rates (MACE) in these patients with chest pain but non-obstructive coronary artery disease is higher than the general population (191) refocusing attention on the coronary microcirculation.

Microvascular dysfunction not only confounds techniques targeting epicardial disease detection (such as PET, perfusion mapping or FFR based approaches), but is a diagnosis and therapeutic target in its own right. Regulating perfusion through endothelial dependent and independent mechanisms, (192,193) the microvasculature can be assessed with quantitative perfusion techniques (194). Microvascular dysfunction can be measured invasively at coronary angiography with the index of microcirculatory resistance (IMR), or non-invasively with perfusion imaging. Previous studies have shown that microvascular dysfunction can alter flow as much as epicardial stenoses (186). If not recognized, this could potentially lead to an increase in downstream testing. Regardless of cause, reduction in myocardial blood flow is a useful biomarker associated with prognosis and may be a therapeutic target. It is important for clinicians to understand factors that influence perfusion and any insights into the biology of the microcirculation that perfusion mapping can provide. Also, as MBF is affected by both the microvasculature and epicardial compartments, the accurate diagnosis of epicardial coronary disease from quantitative perfusion techniques requires knowledge of the impact of the microvasculature on MBF. Accordingly, in this multi-centre study we sought to establish factors associated with myocardial blood flow using perfusion mapping in symptomatic patients in whom epicardial coronary disease had been excluded.

## 6.3 Methods

### Population

Patients referred for perfusion CMR at five centres: Barts Heart Centre (BHC), United Kingdom (UK); St Luca Hospital Milan, Italy (Milan); University of Leeds, UK (Leeds); Harefield Hospital, UK (HH); Royal Free Hospital, UK (RFH) between May 2016 and December 2019 were recruited. Institutional approval was obtained for data sharing and all data was anonymised. All patients had undergone contemporaneous invasive or computed tomography coronary angiography (CTCA), without interval coronary event or intervention within 6 months. Patients with coronary artery disease (diameter stenosis on coronary angiography >50%), previous coronary revascularisation or cardiomyopathy (hypertrophic, arrhythmogenic, dilated, amyloid) were excluded. In addition, patients with previous infarction / scar (ischaemic or non-ischaemic aetiology) seen with late gadolinium enhancement were excluded. Patient demographic data, clinical history and medication were documented from the medical notes. Also included in the cohort were 27 healthy volunteers who were prospectively recruited and only underwent CMR. These were individuals with no risk factors for coronary artery disease and were taking no medication.

### CMR protocol

For full details see the methods chapter. In brief, CMR scans were performed at 1.5 (Aera) and 3 Tesla (Prisma, Siemens Healthcare, Erlangen, Germany) using a standard clinical protocol (48). Stress and rest perfusion mapping was performed as described previously for 3 LV short axis slices.

### CMR analysis

MBF was calculated automatically inline using an artificial intelligence based approach in which the endocardial and epicardial borders are automatically traced on the perfusion maps

during scanning, outputting global (and regional) MBF across the three slices for both stress and rest (195) – Figure 24.

Coronary angiography

Invasive coronary angiography was performed according to standard protocols. Severity of stenoses were graded by an expert interventional cardiologist. For the CTCA scans, coronary lesion severity was graded by an expert observer according to the Society of Cardiovascular Computed Tomography (SCCT) guidelines (196). Patients were included if all vessels were visually unobstructed (<50%) and / or a negative pressure wire study was negative (Fractional flow reserve FFR >0.80).

Statistics

Comparison between numerical variables was performed using independent t-test; chi-square test for categorical variables. Variables were assessed for collinearity with a variance inflation factor threshold <3 chosen. Univariate linear regression analysis was used to describe the associations between demographics, co-morbidity and CMR parameters and stress and rest MBF. A stepwise multivariate model identified independent associations with each of these parameters. Only statistically significant univariate associations were included in the multivariate models. A p value of <0.05 was considered statistically significant. From the multivariate model, an equation relating these variables to stress MBF was derived using the beta coefficients.

Figure 24. An example of perfusion map analysis. Contours were drawn automatically using an artificial intelligence analysis approach. Displayed is a mid-ventricular slice at rest (A) and stress (B). The global MBF was recorded. MPR was calculated as the ratio of stress MBF and rest MBF.

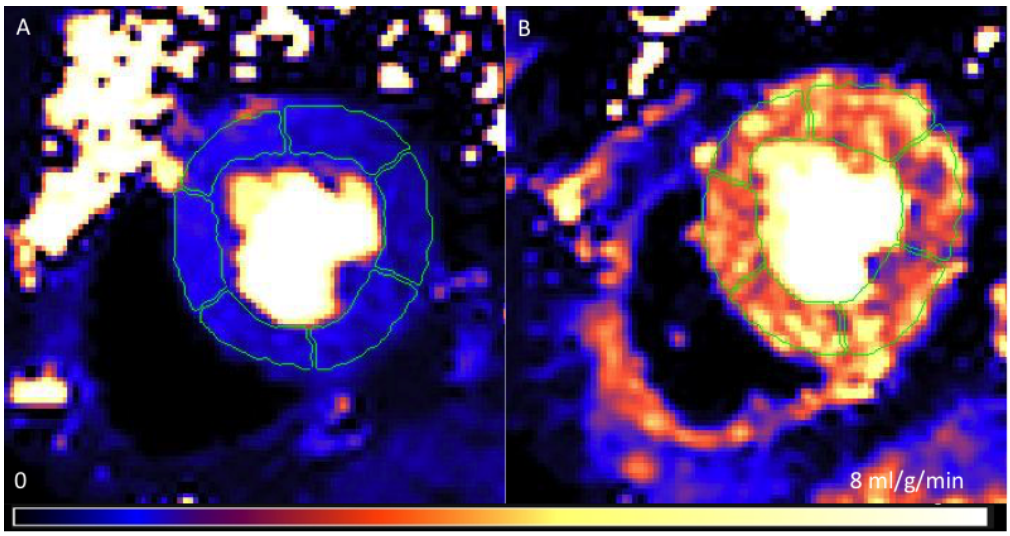


Figure 25. Flow chart demonstrating the study process. 242 patients were included in the final analysis. Initial univariate and then multivariate linear regression models were created. LGE = late gadolinium enhancement.

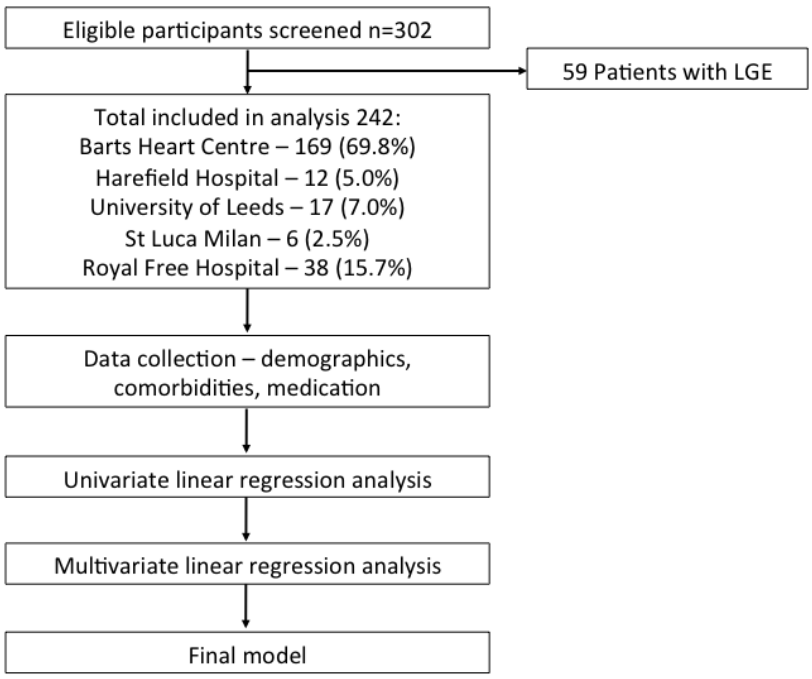

6.4 Results

302 eligible participants were screened across the 5 sites including 27 healthy volunteers (mean age +/- sd, 38 +/- 11.8 years). 59 were excluded due to positive late enhancement imaging. Therefore 242 (including the volunteers) were included, 169 from BHC, 12 from HH, 17 from Leeds, 6 from Milan and 38 from RFH, 133 patients had undergone invasive coronary angiography and 82 CTCA (Figure 25) The median time between CMR and angiography was 42 days (IQR 7 to 107 days). The mean age was 56.0 +/- 12.8 years, 114 were male (47.1%). See Table 9 for a full summary of the cohort.

The mean stress MBF was 2.53 +/- 0.82 ml/g/min and rest MBF 0.91 +/-0.24 ml/g/min. Compared to females, males were a similar age and had a similar proportion of co-morbidities and medication (Table 10). Males had similar EF and LVEDVi but higher LVMi than females. Stress MBF was higher in females than males (2.63 +/- 0.83 vs 2.42 +/- 0.81 ml/g/min, p=0.049). Rest MBF was also higher in females (0.83 +/- 0.24 vs 0.97 +/- 0.22 ml/g/min, p<0.001).

A univariate analysis was performed to explore which factors are associated with stress MBF. Demographics, co-morbidities and CMR parameters were assessed (Table 11). There was no significant collinearity of variables. Stress MBF was associated with increasing age, diabetes, hypertension, dyslipidaemia and LV mass indexed for BSA. Reduced stress MBF was also associated with the use of beta-blockers, ACE-inhibitor / ARB, antiplatelet agents, statins, diuretics, calcium channel blockers and oral hypoglycaemic agents on univariate analysis. These factors were then inputted into a multivariate linear regression analysis in a stepwise method and the factors associated with reduced perfusion were increasing age, diabetes, use of beta-blockers and increased LVMi (Figure 26). The overall $R^2$ was 0.236 (Table 12). From this model, the following equation for the estimation of stress MBF can be achieved:

Stress MBF = 2.66–0.015(age-60)–0.013(LVMi-57)-0.405(presence of diabetes) – 0.365(use of beta blocker)

A similar analysis was performed for rest perfusion. In the univariate analysis female sex, LVEDVi, LVMi and beta blocker use were the factors associated with perfusion (Table 13). In the stepwise multivariate linear regression, female sex was associated with increased perfusion and beta blocker use was associated with reduced perfusion (Figure 26, Table 14).

Table 9. Summary of the cohort data. Data are represented as mean +/- standard deviation for continuous variable or number and percentages for discrete variables.

| | **Overall cohort N=242 (%)** |
|---|---|
| Age (years) | 56.0 +/-12.8 |
| ***Co-morbidity*** | |
| Diabetes | 49 (20.2) |
| Hypertension | 114 (47.1) |
| Dyslipidaemia | 91 (37.6) |
| Smoker | 56 (23.1) |
| ***Medication*** | |
| Beta blocker | 108 (44.6) |
| ACEi/ARB | 85 (35.1) |
| Antiplatelet | 111 (45.9) |
| Statin | 123 (50.8) |
| Diuretic | 25 (10.3) |
| Nitrate | 16 (6.6) |
| Calcium channel blocker | 54 (22.3) |
| Oral hypoglycaemic agent | 32 (13.2) |
| Insulin | 4 (1.7) |
| ***CMR parameter*** | |
| LVEDVi (ml/m2) | 74.78 +/- 18.56 |
| LVMi (g/m2) | 56.04 +/- 13.94 |
| EF (%) | 65.20 +/- 8.72 |
| Stress MBF | 2.53 +/- 0.82 |
| Rest MBF | 0.91 +/- 0.24 |

Table 10. Summary of co-morbidity, medication and CMR data by sex. Data are represented as mean +/- standard deviations for continuous variable or number and percentages for discrete variables.

| | **Male N=114 (47.1%)** | **Female N=128 (52.9%)** | **P** |
|---|---|---|---|
| Age (years) | 54.3 +/- 12.3 | 57.6 +/- 13.0 | **0.044** |
| ***Co-morbidity*** | | | |
| Diabetes | 27 (23.7) | 22 (17.2) | 0.209 |
| Hypertension | 55 (48.2) | 59 (46.1) | 0.738 |
| Dyslipidaemia | 48 (42.1) | 43 (33.6) | 0.172 |
| Smoker | 32 (28.1) | 24 (18.8) | 0.086 |
| ***Medication*** | | | |
| Beta blocker | 51 (44.7) | 57 (44.5) | 0.974 |
| ACEi/ARB | 44 (38.6) | 41 (32.0) | 0.286 |
| Antiplatelet | 58 (50.9) | 53 (41.4) | 0.140 |
| Statin | 59 (51.8) | 64 (50.0) | 0.785 |
| Diuretic | 8 (7.0) | 17 (13.3) | 0.110 |
| Nitrate | 5 (4.4) | 11 (8.6) | 0.189 |
| CCB | 21 (18.4) | 33 (25.8) | 0.170 |
| OHA | 18 (15.8) | 14 (10.9) | 0.266 |
| Insulin | 2 (1.8) | 2 (1.6) | 0.907 |
| ***CMR parameter*** | | | |
| LVEDVi (ml/m2) | 75.0 +/- 18.1 | 70.9 +/- 15.7 | 0.063 |
| LV mass-I (g/m2) | 59.1 +/- 12.4 | 49.9 +/- 10.3 | **<0.001** |
| EF (%) | 65.2 +/- 7.96 | 65.2 +/- 9.37 | 0.975 |
| Stress MBF | 2.42 +/- 0.81 | 2.63 +/- 0.83 | **0.049** |
| Rest MBF | 0.83 +/- 0.24 | 0.97 +/- 0.22 | **<0.001** |

Table 11. Univariate regression analysis for the dependent variable stress MBF.

| | **Beta** | **P** | **LCI** | **UCI** |
|---|---|---|---|---|
| **Age (years)** | -0.02 | **<0.001** | -0.028 | -0.013 |
| **Sex (m vs f)** | -0.208 | **0.049** | -0.416 | -0.001 |
| **Diabetes** | -0.540 | **<0.001** | -0.791 | -0.289 |
| **HTN** | -0.364 | **0.001** | -0.568 | -0.160 |
| **Chol** | -0.286 | **0.009** | -0.499 | -0.074 |
| **Smoker** | -0.015 | 0.908 | -0.262 | 0.233 |
| **LVEDVi (ml/m²)** | 0.001 | 0.785 | -0.005 | 0.007 |
| **LVMi (g/m²)** | -0.012 | **0.006** | -0.020 | -0.003 |
| **LVEF (%)** | 0.001 | 0.890 | -0.011 | 0.013 |
| **B blocker** | -0.563 | **<0.001** | -0.761 | -0.366 |
| **ACE/ARB** | -0.341 | **0.002** | -0.556 | -0.127 |
| **Antiplatelet** | -0.217 | **0.041** | -0.425 | -0.009 |
| **Statin** | -0.377 | **<0.001** | -0.580 | -0.173 |
| **Diuretic** | -0.476 | 0.060 | -0.814 | 0.138 |
| **Nitrate** | 0.049 | 0.820 | -0.372 | 0.469 |
| **CCB** | -0.336 | **0.008** | -0.583 | -0.088 |
| **OHA** | -0.417 | **0.007** | -0.721 | -0.113 |
| **Insulin** | -0.466 | 0.263 | -1.283 | 0.352 |

Table 12. Stepwise multiple linear regression analysis for stress myocardial blood flow. R for the model is 0.486, $R^2 = 0.236$.

| | Unstandardized Coefficients | | Standardized Coefficients | | 95.0% Confidence Interval for B | |
|---|---|---|---|---|---|---|
| | Beta | Standard Error | Beta | P | Lower Bound | Upper Bound |
| (Constant) | 4.305 | 0.312 | | <0.001 | 3.691 | 4.919 |
| Age (years) | -0.015 | 0.004 | -0.238 | **<0.001** | -0.023 | -0.007 |
| Beta Blocker | -0.365 | 0.100 | -0.224 | **<0.001** | -0.562 | -0.168 |
| Diabetes | -0.405 | 0.118 | -0.199 | **0.001** | -0.638 | -0.172 |
| LVMi ($g/m^2$) | -0.013 | 0.004 | -0.192 | **0.001** | -0.020 | -0.005 |

Table 13. Univariate regression analysis for the dependent variable rest MBF.

| | **Beta** | **P** | **LCI** | **UCI** |
|---|---|---|---|---|
| **Age (years)** | 0.001 | 0.343 | -0.001 | 0.003 |
| **Sex (m vs f)** | -0.161 | **<0.001** | -0.216 | -0.107 |
| **Diabetes** | -0.030 | 0.424 | -0.105 | 0.044 |
| **HTN** | 0.028 | 0.336 | -0.029 | 0.086 |
| **Chol** | -0.055 | 0.064 | -0.114 | 0.003 |
| **Smoker** | -0.019 | 0.574 | -0.086 | 0.048 |
| **LVEDVi (ml/m²)** | -0.002 | **0.017** | -0.003 | 0.000 |
| **LVMi (g/m²)** | -0.004 | **<0.001** | -0.006 | -0.002 |
| **LVEF (%)** | 0.002 | 0.138 | -0.001 | 0.006 |
| **B blocker** | -0.064 | **0.031** | -0.121 | -0.006 |
| **ACE/ARB** | -0.033 | 0.270 | -0.092 | 0.026 |
| **Antiplatelet** | 0.028 | 0.345 | -0.030 | 0.086 |
| **Statin** | -0.012 | 0.690 | -0.070 | 0.046 |
| **Diuretic** | 0.026 | 0.566 | -0.063 | 0.114 |
| **Nitrate** | 0.068 | 0.286 | -0.057 | 0.192 |
| **CCB** | 0.003 | 0.930 | -0.064 | 0.070 |
| **OHA** | -0.027 | 0.545 | -0.116 | 0.061 |
| **Insulin** | 0.019 | 0.870 | -0.206 | 0.243 |

Table 14. Stepwise multiple linear regression analysis for rest myocardial blood flow. R for the model is 0.329, $R^2 = 0.108$

| | Unstandardized Coefficients | | Standardized Coefficients | | 95.0% Confidence Interval for B | |
|---|---|---|---|---|---|---|
| | B | Standard Error | Beta | P | Lower Bound | Upper Bound |
| (Constant) | 1.007 | 0.024 | | <0.001 | 0.959 | 1.055 |
| Sex (m vs f) | -0.141 | 0.030 | -0.293 | **<0.001** | -0.199 | -0.083 |
| Beta Blocker | -0.073 | 0.030 | -0.151 | **0.014** | -0.132 | -0.015 |

Figure 26. Summary of the determinants of myocardial perfusion after adjusting for confounders. Stress perfusion falls with age, diabetes mellitus, beta blocker use and increasing LV mass. Rest perfusion is higher in females and reduced with beta blocker use.

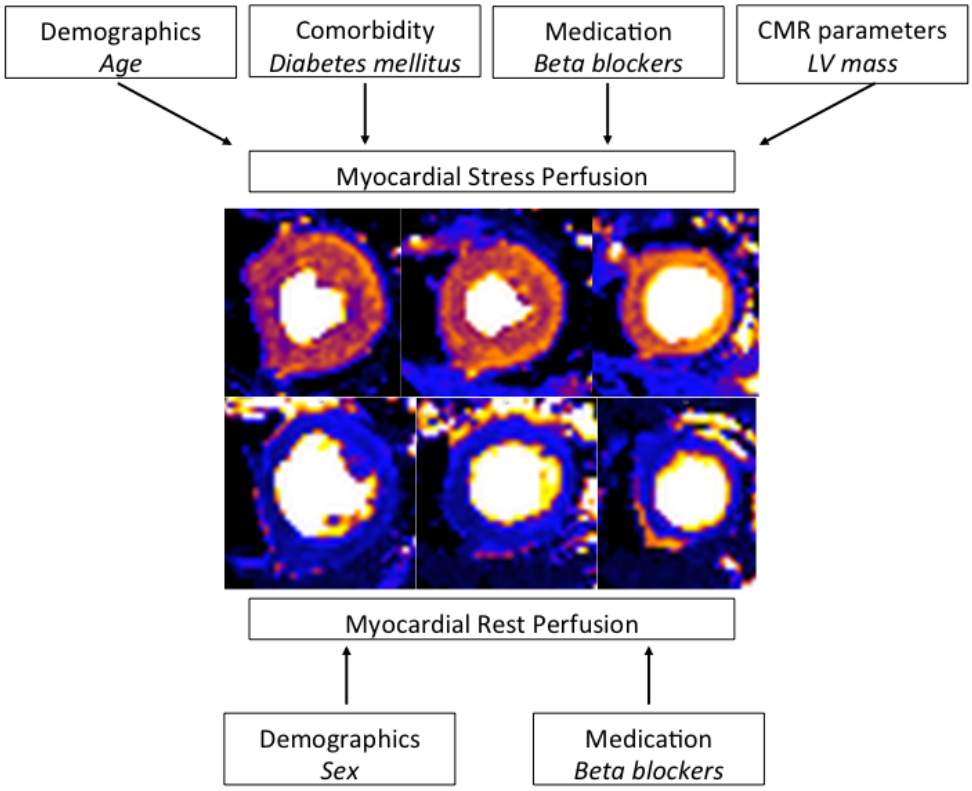

## 6.5 Discussion

Using quantitative perfusion mapping in five centres across Europe in 242 patients with chest pain but no obstructive coronary artery disease or myocardial scar, these data show that myocardial perfusion is variable and determined by a combination of patient demographic, pathological and medication factors. We have found rest flow is higher in females, and lower in those taking beta blockers.

Stress MBF falls with increasing age, diabetes, beta blocker use and increasing LV mass. Examples of estimated stress MBF for a 35-year-old with an indexed LV mass 55g/m$^2$ and no co-morbidities or medication would be 3.07 ml/g/min. For a similar 70-year-old it would be 2.54 ml/g/min (18% lower) and 2.14ml/g/min if also diabetic (30% lower). Therefore, stress MBF falls with increasing age (a 10% fall over 18 years or 5-6% fall for each decade) and is lower in diabetes (equivalent to being 27 year older), in those with higher LV mass (2 SD increase in LV mass - LVH - would be equivalent to being 20 years older) and in patients taking beta-blockers (equivalent to being 24 years older). The overall effect is large: for example, a 70-year-old diabetic would have 30% lower stress MBF than a 35-year-old non-diabetic; add LVH and beta blockers and MBF is less than half that of the 35-year-old.

Stress MBF is associated with factors that may impair the ability to vasodilate. Our data shows that ageing and diabetes are associated with reduced maximal myocardial hyperaemia despite the presence of unobstructed coronary arteries. Plausible explanations for this include disease of the cardiac microvasculature (179), autonomic dysfunction (88), reduced vasodilatation and impairment in the regulation of coronary flow (197) or blunted adenosine sensitivity. The MESA study (198) also found that age was the factor most strongly associated with stress perfusion and perfusion reserve. Invasive studies too have found patients with abnormal microvascular function are typically older and this is perhaps mediated by both endothelial-dependent (vasodilators such as acetylcholine, substance P) and independent mechanisms (the

ability of smooth muscle to relax) (199). Microcirculatory dysfunction in diabetes has been observed in mostly small PET and invasive studies (200,201). Mechanisms include hypertrophic remodelling of the small arteries (202), reduced capillary density (203) and the oxidative stress caused by hyperglycaemia (204).

We did not find an independent association of stress MBF or rest MBF with hypertension, smoking and dyslipidaemia. Hypertension, familial hypercholesterolemia and smoking have previously been shown to be associated with reduced perfusion reserve (205–208). These studies are typically small and have a highly selected patient cohort. Due to the wide range of ages in our study and the strength of association with age, other factors with a smaller contribution to perfusion may be masked. In MESA (198) hypertension and cholesterol were associated with MPR if age and sex were excluded. The population in MESA was asymptomatic individuals and as such had no angiographic confirmation of absence of epicardial coronary disease. Our results add to the literature by suggesting that ageing has the biggest impact on perfusion- and is a process that can be accelerated by additional contributory factors such as co-morbidity.

The impact of beta blockers and other medication on myocardial perfusion is controversial with a number of small contradictory studies. Here, beta-blocker use was associated with reduced stress perfusion. In SPECT imaging beta blockers have been shown to reduce the extent of perfusion defects (64). The current guidelines do not recommend that beta blockers are omitted prior to CMR and this is not something done routinely (48). What is not clear from our study is whether the beta blocker effect is causal or a surrogate for other unmeasured risk factors. It may be that patients taking beta blockers are more likely to have microvascular dysfunction or that beta blockers directly affect stress (and rest) MBF. Prospective studies of scanning patients with and without prior omission of beta blockers would be useful.

These data have several implications. If myocardial blood flow values are to be used clinically to diagnose epicardial coronary artery disease, there may need to be reference ranges that account for age, sex and co-morbidity. Our data suggest that the threshold for declaring a study positive for epicardial coronary artery disease would be different for different groups for example, in a similar way to CT calcium scores having age defined reference ranges. This would prevent potential false positive perfusion CMR and unnecessary invasive investigations whilst at the same time, using quantitative perfusion, help to better classify patients as having likely microvascular dysfunction.

Although a distinction should be made between the measurement of myocardial versus coronary blood flow, our findings highlight the potential limitations associated with both invasive FFR estimation as well as the use of advanced computational modelling methods such as Computed Tomography FFR ($CT^{FFR}$), in terms of the physiological assumptions incorporated in both techniques. A fundamental principle for both modalities is that pressure differences across stenotic vessels (directly measured or simulated) can be used to derive an estimate of coronary flow impairment. Achieving maximal vasodilatation is a key component of invasive FFR assessment, and a necessary step for achieving a near-linear relationship between pressure and flow within the coronaries. Similarly, computational modelling methods are based on the input of boundary conditions such as microvascular resistance and its response to adenosine-mediated vasodilation (209). If there is elevated microvascular resistance there is a drop in the pressure gradient and an increase in FFR (210). It is possible that incorporating more patient-related variables (such as age, diabetes, LV mass) into the assessment of a coronary stenosis would further improve the technique.

From a clinical biomarker perspective, impaired myocardial perfusion may be targetable with therapy and would be an interesting endpoint in clinical trials. Whilst impaired perfusion is

associated with poorer outcomes, it is unknown whether intensive management of these individuals will improve outcomes.

In the absence of epicardial coronary disease, our findings likely reflect pathophysiology of the myocardial microvascular compartment – the data is substantially based on subjects referred for chest pain for cardiac investigation. The observed associations of resting MBF with female sex are consistent with the PET literature (211,212). One PET study has implied that rest MBF is higher in patients with microvascular disease (182) than those without. However in that study microvascular disease was defined non-invasively as a coronary flow reserve <2 (there was no invasive IMR assessment). We did not make the same comparison in our study as we sought to discover what patient factors contribute to rest MBF rather than define which patients had microvascular disease. Also it is likely that microvascular disease is a continuum and using a cut-off value for flow reserve is somewhat arbitrary.

In our study we do not have invasive data in the form of IMR to determine whether the impact of these factors on myocardial perfusion is down to microvascular disease. Other factors could contribute such as residual caffeine (despite patients abstaining for 24 hours), reduced response to adenosine or adenosine receptor down regulation with ageing or co-morbidity. However the focus of this study was not to diagnose microvascular disease but to determine the factors that contribute to myocardial perfusion in patients without obstructive epicardial disease. This is required to avoid false positives and to perhaps determine age specific normal ranges for quantitative perfusion. Additionally PET and CMR studies have shown there is important prognostic information in myocardial perfusion without invasive data to show this is down to microvascular disease (94,213).

*Limitations*

This is a non-randomised, observational study and so there are inherent limitations in the study design. However our patient sample is representative of the population seen in clinical

practice in the UK and Europe. No sample size calculation was undertaken before the study and as such the findings are hypothesis generating.

## 6.6 Conclusions

In the absence of obstructive epicardial coronary disease, stress MBF falls with age, diabetes, increased LV mass and beta blockers; rest perfusion is associated sex and beta blocker use. These changes are large and diabetes and LVH are associated with perfusion reductions equivalent to over 2 decades of chronological ageing. These data may help develop reference ranges and input to other modelling techniques (e.g. CT FFR). Further work is needed to see whether these changes occur in volunteers (not individuals referred for CMR), whether they are modifiable and whether MBF measurement can be used as a surrogate endpoint in trials of microvascular disease therapy.

# 7. Results 4 - Perfusion mapping in Fabry disease

The following publication is based on this thesis chapter: “Quantitative Myocardial Perfusion in Fabry Disease”.

**Knott KD,** Augusto JB, Nordin S, Kozor R, Camaioni C, Xue H, Hughes RK, Manisty C, Brown LAE, Kellman P, Ramaswami U, Hughes D, Plein S, Moon JC.

Quantitative Myocardial Perfusion in Fabry Disease. Circ Cardiovasc Imaging. 2019 Jul;12(7):e008872. doi: 10.1161/CIRCIMAGING.119.008872.

## 7.1 Summary

In this study, I investigated myocardial perfusion in cardiomyopathy, with Fabry disease (FD) the chosen disease model.

Fabry disease (FD) is a slowly progressive multisystem X-linked lysosomal storage disease in which sphingolipids are deposited in tissues in the body including the myocardium. Cardiac involvement in FD is associated with adverse outcomes through arrhythmias and heart failure. There has been much interest in myocardial phenotype development in order to improve treatment and decide the optimum timing for treatment.

Using CMR, we have increased our understanding of the myocardial phenotype development and several processes have been elucidated. These include glycophospholipid storage, LVH, inflammation and fibrosis. Multiparametric CMR has been used to more precisely quantify these disease processes. As well as hypertrophy and fibrosis (seen with late gadolinium enhancement on CMR), glycophospholipid storage can be measured using T1 mapping and oedema and inflammation measured using T2 mapping. Microvascular dysfunction may also play a role in the pathogenesis of the cardiac FD. A full, multiparametric assessment of FD including microvascular dysfunction has not previously been performed. As CMR does not use ionising radiation, studying early myocardial FD is also more acceptable than nuclear imaging modalities. In this prospective, observational study we set out to investigate the relationship between microvascular dysfunction and glycophospholipid storage, hypertrophy, fibrosis and oedema in patients with FD.

I recruited 44 FD patients (mean 49 years, 43% male, 24 (55%) with LVH) and 27 healthy controls to undergo multiparametric CMR including adenosine stress perfusion mapping. Myocardial blood flow (MBF) was measured and its associations with other processes investigated.

I found that compared to patients with no LVH (LVH-) FD, those with LVH (LVH+) FD had higher LV ejection fraction (73% vs 68%), more LGE (85% vs 15%) and a lower stress MBF (1.76 vs 2.36ml/g/min). The reduction in stress MBF was more pronounced in the subendocardium than subepicardium. LVH-FD had lower stress MBF than controls (2.36 vs 3.00ml/g/min, p=0.002). Across all FD, LGE and low native T1 were independently associated with reduced stress MBF. On a segmental basis stress MBF was independently associated with wall thickness, T2, ECV and LGE.

In conclusion, this study has shown that FD patients have reduced perfusion compared to controls, the subendocardium is particularly affected and there are greater reductions in perfusion associated with LVH, glycophospholipd storage, inflammation and scar. Perfusion is reduced even when the patient does not have LVH. This finding suggests that microvascular dysfunction may be an early disease feature and could contribute to the progression from storage to fibrosis (and hence heart failure and arrhythmia). Because it may relate to endothelial rather than myocyte storage, it may be more readily treatable and is a candidate to be used as a surrogate endpoint in therapeutic trials of enzyme replacement and more novel therapies.

For this chapter I utilised the ethics as explained previously, recruited the patients and performed the majority of the CMR scans. I then analysed the scans, performed statistical analysis and wrote the chapter.

## 7.2 Introduction

Fabry disease (FD) is an X-linked lysosomal storage disease caused by mutations in the gene encoding the α-galactosidase A enzyme (GLA). As a result sphingolipids cannot be broken down and instead accumulate in the body's tissues, predominately the heart, skin, kidneys and brain (133). The effects on the myocardium are gradual with sphingolipids typically accumulating over years and decades but ultimately cause LVH, arrhythmias, heart failure and death (214,215). These cardiac complications are the main drivers of adverse outcomes in FD. There has been much interest in therapy for FD with a view to restore activity of the GLA enzyme. This was up until recently solely enzyme replacement therapy (ERT) which was administered as an infusion. There are now oral options with the newer oral chaperone therapies (OCT). By restoring enzymatic activity these treatments aim to reduce sphingolipid deposition in the myocardium and other organs and thus prevent these adverse events (216–218). The best time to initiate therapy is not definitively known and so elucidating the disease processes in FD is desirable in order to improve patient outcomes. Multiparametric cardiovascular magnetic resonance (CMR) has been used to characterise several of these processes within the cardiac FD phenotype development. It appears there is an initial sphingolipid storage phase in which sphingolipids accumulate in the myocardium and this can be detected as low myocardial T1 using T1 mapping (219). Following this there is triggered LVH with focal and then more widespread inflammation leading to myocardial fibrosis (135). Inflammation and fibrosis typically start in the basal inferolateral wall and can be detected on CMR with LGE (220,221). Oedema has been visualised using T2 mapping (high T2) and believed to signify inflammation and myocyte death and is associated with elevated troponin in the bloodstream (134). There may also be sex differences in the phenotype. As the condition is X-linked, males often present early and have more pronounced LV hypertrophy. The combination of myocardial fibrosis and sphingolipid storage often results in pseudo-

normalisation in myocardial T1 (135). In summary it seems the disease processes are sphingolipid storage, hypertrophy, inflammation and fibrosis and are consistent with other organ involvement in FD. In addition to myocyte storage, FD also causes endothelial storage and microvascular dysfunction (222,223) but this has not been well characterised in the heart. Microvascular dysfunction can be assessed using non-invasive imaging and PET has been the gold standard for quantitative myocardial blood flow assessment (224). PET has limitations including the relatively low spatial resolution, reducing the accuracy of regional myocardial perfusion assessment, it also uses ionising radiation which limits the repeated, serial assessment of patients and the acceptability of performing PET early in the disease course. Furthermore PET does not give the same multiparametric assessment that you get from CMR such as T1 and T2 as discussed above (18,47). In this way we can directly compare regional flow differences with regional changes in T1 or T2 which is not possible with other imaging modalities. Additionally, the superior spatial resolution allows the assessment of endocardial and epicardial myocardial blood flow. CMR perfusion mapping, being fast and free from ionising radiation, has potential in a wide range of circumstances including serial assessment and assessment in early disease. In hypertrophic cardiomyopathy (HCM), microvascular dysfunction has been noted, and found to increase with LVH and LGE and may even occur early, before hypertrophy (131,225). Also, impaired myocardial perfusion on non-invasive imaging in HCM is associated with adverse outcomes (132). In FD, there have been a few PET studies on myocardial perfusion where perfusion was relatively reduced (226) and not improved by ERT (136,227). The studies to date have had a small number of patients and have not explored the relationship of MBF to the other myocardial pathological processes in FD – sphingolipid storage, LV hypertrophy, inflammation and fibrosis.

In this study we recruited FD patients and control subjects for multiparametric CMR including myocardial perfusion mapping to further explore the relationship of myocardial perfusion with

other myocardial abnormalities in FD. We hypothesised that microvascular dysfunction is common and occurs early in FD and would be associated with markers of disease severity including sphingolipid storage, fibrosis and oedema.

## 7.3 Methods

44 patients with FD and 27 healthy control subjects were recruited. FD patients and controls underwent multiparametric CMR. The patient's cardiovascular history, symptoms and FD treatment status were assessed with a questionnaire at the time of CMR. The healthy control cohort had no cardiac symptoms or co-morbidities and were not taking any cardiac medications as mentioned previously.

*CMR scans*

All CMR scans were performed at 1.5 Tesla as described in the methods chapter. The protocol included long and short axis cine imaging, native T1 mapping (MOLLI), T2 mapping, stress and rest perfusion, late gadolinium enhancement (LGE) and post contrast T1 mapping (see Methods chapter). The native and post contrast T1 maps were used to derive the synthetic extracellular volume fraction (ECV) using the method described by Triebel et al (165). The same basal, mid and apical short axis slice locations were used for T1, T2 and ECV mapping. Perfusion images were acquired for basal mid and apical LV short-axis slices. The slice locations were matched as best as possible to the T1 and T2 maps. Splenic switch off was confirmed for all subjects to confirm adequate stress (66).

*CMR analysis*

The CMR data was analysed using CVI42, as previously described (see Methods chapter). The endo- and epicardial contours were manually drawn and the right ventricular (RV) insertion points identified for each of the parametric maps. The endo and epicardial contours were then offset by 10% and an AHA segment model (49) was created for each parameter (e.g. T1, T2, stress and rest MBF, ECV). Polar maps for 16 AHA myocardial segments (minus the apical cap) were generated as well as the global mean value, which was the mean of the parameter averaged across all myocardial segments. In order to investigate transmural perfusion gradients, the endocardial and epicardial stress MBF was determined by adjusting the contour

offsets in turn in CVI42 to 50% of the myocardium. LV volume analysis was performed by contouring the endocardium and epicardium of each LV short axis slice in diastole and systole as previously described. Papillary muscles were excluded from the LV volume and included as LV mass. The maximal diastolic wall thickness was measured using a dedicated module of CVI42. LV hypertrophy was defined as a maximum wall thickness greater than 12mm (228). LGE was assessed for each myocardial segment using a dedicated CVI42 module. A region of interest was manually drawn in visually normal myocardium and pixels with a signal intensity 5-standard deviations above that of the normal myocardium were automatically identified as LGE (229). Whether or not there was LGE present was noted for each segment and globally.

*Statistical analysis*

ANOVA or Kruskal-Wallis analysis (for parametric and non-parametric variables respectively) was used to compare FD patients who had LVH with those who did not have LVH. A chi-square test was used to compare categorical variables. Pairwise comparisons between groups were performed using a Bonferroni adjustment.

The factors that may contribute to stress MBF were assessed with a simple linear regression analysis. After this initial analysis, a multiple linear regression analysis was performed including the variables associated with stress MBF from the simple regression analysis. A "per patient" analysis was performed, inputting age, sex, treatment status, indexed EDV, indexed LV mass, LVEF, mean T1, T2, ECV, the presence of LGE and LVH. Also a "per segment" analysis was performed in which the effect of each CMR variable on stress MBF was considered on an AHA segment basis. LV wall thickness, native T1, T2, ECV and percentage of LGE per segment were treated as continuous variables. A mixed effects linear regression controlled for subject dependency.

## 7.4 Results

44 patients of which 19 were male (43%) and with a mean age 49 years were recruited. 30 patients (68%) were being treated for FD with either ERT (21 patients) or OCT (9 patients). 24 patients (55%) had LVH and 23 patients (52%) had myocardial late gadolinium enhancement. Patients had higher LV mass indexed for body surface area (90.6 vs 52.3g/$m^2$, p<0.001), a higher ejection fraction (70% vs 65%, p=0.007), lower septal native T1 (959 vs 1015ms, p<0.001) and higher septal T2 (49.3 vs 47.5ms, p=0.025 (Table 15) compared to the controls. The healthy control group were a similar age to the LVH negative FD patients (38.1 vs 42.3 years, p=0.264). Patients with LVH were older (54.6 vs 42.3 years, p=0.006) and more likely to be male (62.5 vs 20%, p=0.003) than the LVH negative FD group. They also had a higher EF (72.8 vs 66.7%, p=0.03) and a higher indexed LV mass (117.4 vs 58.43g/$m^2$, p<0.001) (Table 16). Compared to the control group, a greater proportion of LVH negative FD patients were female. There were no other significant differences between the groups (Table 16). Of the LVH negative patients, 7 (35%) had low septal T1. The patients on ERT had more advanced cardiac FD than those on no therapy. They had a higher LV mass (115 vs 60 g/m2), lower native T1 (933 vs 1000ms), and a higher proportion of patients had LGE (77% vs 21%). All patients on ERT had been receiving therapy for >1 year. The OCT group was composed of patients who had previously been on ERT long-term and patients who had recently started on FD therapy. The shortest duration of therapy in this group was 6 months. They had a more advanced cardiac phenotype than patients with no therapy but less advanced than those on ERT. The mean LV mass was 77g/m2, mean T1 959ms, and LGE in 38% of patients.

The cardiovascular risk factor profile was similar in the LVH positive and LVH negative FD patients groups. Only atrial fibrillation (AF) was statistically higher in the patients with LVH - 5 (21%) vs 0 patients (0%) in the LVH negative group, p=0.02. 4 (17%) LVH positive patients were hypertensive vs 3 LVH negative patients (15%), p=0.88 , 4 (17%) vs 1 patient (5%) had

hyperlipidaemia, p=0.21, 3 (13%) vs 1 patient (5%), p=0.40 had renal impairment, 1 (4%) vs 2 patients (10%), p=0.46 had a previous stroke respectively for LVH positive and LVH negative FD patients. Across the entire FD group, a minority had symptoms. 8 (33%) LVH positive and 4 (20%) LVH negative patients had palpitations. 6 (25%) LVH positive patients and 1 (5%) of LVH negative patients were breathless. 4 (17%) LVH positive patients and 2 (10%) LVH negative patients had chest pain. 30/44 patients were New York Heart Association functional class I (68%), 12 patients were class II (27%) and 2 (5%) patients had mobility limited by musculoskeletal problems.

The overall, mean stress MBF across all segments was lower in FD patients than controls (2.04 vs 3.00 ml/g/min, p<0.001). Rest MBF was the same (0.85 vs 0.86, p=0.85 for patients vs controls respectively). Stress MBF was lower in patients with LVH (1.76 vs 2.36 ml/g/min, p=0.005) than in those with no LVH. However, stress MBF was also lower in LVH negative FD compared to controls (2.36 vs 3.00ml/g/min, p=0.002, Figure 27 and Figure 28). Patients with chest pain and / or breathlessness had a lower stress MBF than those patients with no symptoms (1.68 vs 2.11ml/g/min, p=0.039) indicating possible microvascular disease causing those symptoms.

Endocardial perfusion was lower than epicardial perfusion in FD patients (1.84 vs 2.13 ml/g/min, p=0.022) but not in the healthy controls (2.85 vs 3.10 ml/g/min, p=0.271). This was only significant in those patients with LVH (1.50 vs 1.88 ml/g/min, p=0.013) but not in LVH negative patients (2.25 vs 2.44 ml/g/min, p=0.2078) (Figure 29).

A linear regression analysis was used to see which of the patient demographic (age, sex), treatment (ERT/OCT), and CMR parameters (indexed EDV, EF, indexed LV mass, presence of LGE, LVH, native T1, T2 and ECV) were associated with stress MBF in FD. Age, native T1, T2, ECV, LGE and LVH were associated with stress MBF and therefore put into the multivariate

model. In the multivariate model, the factors independently associated with perfusion were the presence of LGE and low T1 ($R^2$ for the model 0.572, $p<0.001$, Table 17).

A second multivariate model was performed to predict regional stress MBF in FD. In total 704 segments were included in a multivariate model which included segment wall thickness, native T1, T2, ECV and LGE. The model controlled for within subject dependency. Myocardial wall thickness was associated with reduced stress MBF (Figure 30). The other factors independently associated with low stress MBF were high T2, high ECV and the presence of LGE (Table 18).

Table 15. Characteristics of patients with Fabry disease and controls. Data are presented as mean +/- standard deviation unless stated. Abbreviations: BSA – body surface area, ERT – enzyme replacement therapy, LVEDVi – Left ventricular end diastolic volume indexed for BSA, LVESVi – left ventricular end systolic volume indexed for BSA, LVEF – left ventricular ejection fraction, LGE – late gadolinium enhancement, MBF – myocardial blood flow.

| | **Fabry Disease n=44** | **Controls n=27** | **P value** |
|---|---|---|---|
| **Age (years)** | 49.0+/-13.5 | 38.1+/-11.8 | **0.001** |
| **Male, n (%)** | 19 (43.2) | 14 (51.8) | 0.484 |
| **Height (cm)** | 170.3+/-10.5 | 173.2+/-10.3 | 0.265 |
| **Weight (kg)** | 72.2+/-13.1 | 77.2+/-14.7 | 0.137 |
| **BSA** | 1.8+/-0.20 | 1.9+/-0.21 | 0.061 |
| **ERT/OCT, n (%)** | 30 (68.2) | 0 (0) | **<0.001** |
| **LVEDVi (ml/m²)** | 81.9+/-18.9 | 78.1+/-14.3 | 0.367 |
| **LVESVi (ml/m²)** | 26.0+/-12.5 | 26.8+/-6.3 | 0.757 |
| **LVEF (%)** | 70.1+/-9.6 | 65.5+/-4.2 | **0.007** |
| **LV mass indexed (g/m²)** | 90.6+/-41.0 | 52.3+/-9.3 | **<0.001** |
| **LVH, n (%)** | 24 (54.5) | 0 (0) | **<0.001** |
| **LGE, n (%)** | 23 (52.3) | 0 (0) | **<0.001** |
| **Septal T1 (ms)** | 959.1+/-60.6 | 1015.2+/-32.0 | **<0.001** |
| **Septal T2 (ms)** | 49.3+/-3.3 | 47.5+/-2.4 | **0.024** |
| **Septal ECV (%)** | 25.7+/-2.4 | 24.3+/-2.6 | **0.025** |
| **Stress MBF (ml/g/min)** | 2.04+/-0.56 | 3.00+/-0.76 | **<0.001** |
| **Rest MBF (ml/g/min)** | 0.85+/-0.26 | 0.86+/-0.26 | 0.848 |

Table 16. Demographic, treatment and CMR data for Fabry disease (FD) patients and controls. FD patients have been divided into patients with left ventricular hypertrophy (LVH+) and with no hypertrophy (LVH-). Values are presented as mean +/- standard deviation unless stated. The P value for trend has been calculated using ANOVA or Kruskal-Wallis for parametric and non-parametric variables, respectively, and chi-square for categorical variables. Pairwise comparisons between groups were performed using a Bonferroni adjustment. * p<0.05 Vs FD LVH-, † p<0.05 vs Controls.

| | **FD LVH+ (n=24)** | **FD LVH- (n=20)** | **Controls (n=27)** | **P value for trend** |
|---|---|---|---|---|
| **Age, years** | 54.6+/-10.9*,† | 42.3+/-13.4 | 38.1+/-11.8 | **<0.001** |
| **Male, n (%)** | 15 (62.5)* | 4 (20) | 14 (51.8) | **0.015** |
| **BSA** | 1.85+/-0.21 | 1.83+/-0.19 | 1.93+/-0.21 | 0.166 |
| **ERT/OCT, n (%)** | 23 (96)* | 7 (35) | N/A | **<0.001** |
| **LVEDVi (ml/m²)** | 83.1+/-24.0 | 80.3+/-10.3 | 78.1+/-14.3 | 0.380 |
| **LVESVi (ml/m²)** | 25.7+/-15.4 | 26.4+/-8.1 | 26.8+/-6.3 | 0.201 |
| **LVEF (%)** | 72.8+/-9.5*,† | 66.7+/-8.8 | 65.5+/-4.2 | **0.001** |
| **LV mass indexed (g/m²)** | 117.4+/-37.2*,† | 58.4+/-11.3 | 52.3+/-9.3 | **<0.001** |
| **LGE, n (%)** | 20 (83.3)* | 3 (15) | 0 | **<0.001** |
| **Septal T1 (ms)** | 936.5+/-60.7† | 985.0+/-50.1 | 1015.2+/-32.0 | **<0.001** |
| **Septal T2 (ms)** | 50.4+/-3.8† | 47.8+/-1.7 | 47.5+/-2.4 | **0.009** |
| **Septal ECV (%)** | 25.9+/-2.6 | 25.5+/-2.1 | 24.3+/-2.6 | 0.072 |
| **Stress MBF (ml/g/min)** | 1.76+/-0.49*,† | 2.36+/-0.44 | 3.00+/-0.76* | **<0.001** |
| **Rest MBF (ml/g/min)** | 0.77+/-0.16 | 0.93+/-0.33 | 0.86+/-0.26 | 0.188 |

Table 17. A multiple linear regression model for factors influencing the global mean stress myocardial blood flow (MBF). Independent associations with stress MBF were T1 time (low T1 associated with impaired flow) and late gadolinium enhancement (LGE). Age, T1, T2 and extracellular volume fraction (ECV) were continuous variables; LGE and left ventricular hypertrophy were categorical variables. The $R^2$ for the model was 0.572, $p<0.001$.

| | Beta | Standard error | 95% CI Lower Bound | 95% CI Upper Bound | P value |
|---|---|---|---|---|---|
| **Constant** | 1.239 | 1.458 | -1.731 | 4.210 | 0.402 |
| **Age (years)** | -0.009 | 0.007 | -0.022 | 0.005 | 0.190 |
| **LVH** | 0.089 | 0.205 | -0.986 | 0.105 | 0.668 |
| **T1** | 0.003 | 0.001 | 0.000 | 0.006 | **0.040** |
| **T2** | -0.013 | 0.025 | -0.066 | 0.028 | 0.426 |
| **LGE** | -0.546 | 0.220 | -0.986 | -0.105 | **0.017** |
| **ECV** | -0.031 | 0.029 | -0.081 | 0.033 | 0.394 |

Table 18. Mixed effects linear regression model for factors influencing segmental (regional) stress myocardial blood flow (MBF). The model controlled for within subject dependency. Segmental wall thickness, native T1, T2, ECV and late gadolinium enhancement (the percentage of LGE in each AHA segment) were included in the model. All variables were continuous variables. The factors independently associated with stress MBF were wall thickness, T2, ECV and LGE.

| | Beta | Standard error | 95% CI Lower Bound | 95% CI Upper Bound | P value |
|---|---|---|---|---|---|
| **Intercept** | 2.630 | 0.526 | 1.597 | 3.662 | <0.001 |
| **Wall thickness (mm)** | -0.031 | 0.006 | -0.043 | -0.020 | **<0.001** |
| **T1 (ms)** | -0.000 | 0.000 | -0.001 | 0.001 | 0.662 |
| **T2 (ms)** | -0.013 | 0.005 | -0.023 | -0.003 | **0.009** |
| **ECV (%)** | 0.021 | 0.005 | 0.010 | 0.031 | **<0.001** |
| **LGE (%)** | -0.005 | 0.002 | -0.043 | -0.020 | **0.002** |

Figure 27. Multiparametric CMR assessment in the Fabry disease study. The images show a healthy volunteer (A), FD patient with no left ventricular hypertrophy (B) and FD patient with LVH (C). From left to right the images for each patient / volunteer are diastolic steady state free precession cine images, native T1 maps, T2 maps, stress MBF maps, LGE all at a similar slice location. In (A), healthy control, all of the images are normal – no LVH, normal T1, normal T2, normal stress MBF, no LGE. In (B) there is no LVH, low T1 (indicating sphingolipid storage), normal T2, no LGE (B). In (C) there is severe LVH, sphingolipid storage (including T1 pseudonormalisation where there is fibrosis), high T2 in LGE areas and extensive LGE. The figure demonstrates the fall in with increasing disease severity and this is most pronounced in the endocardium.

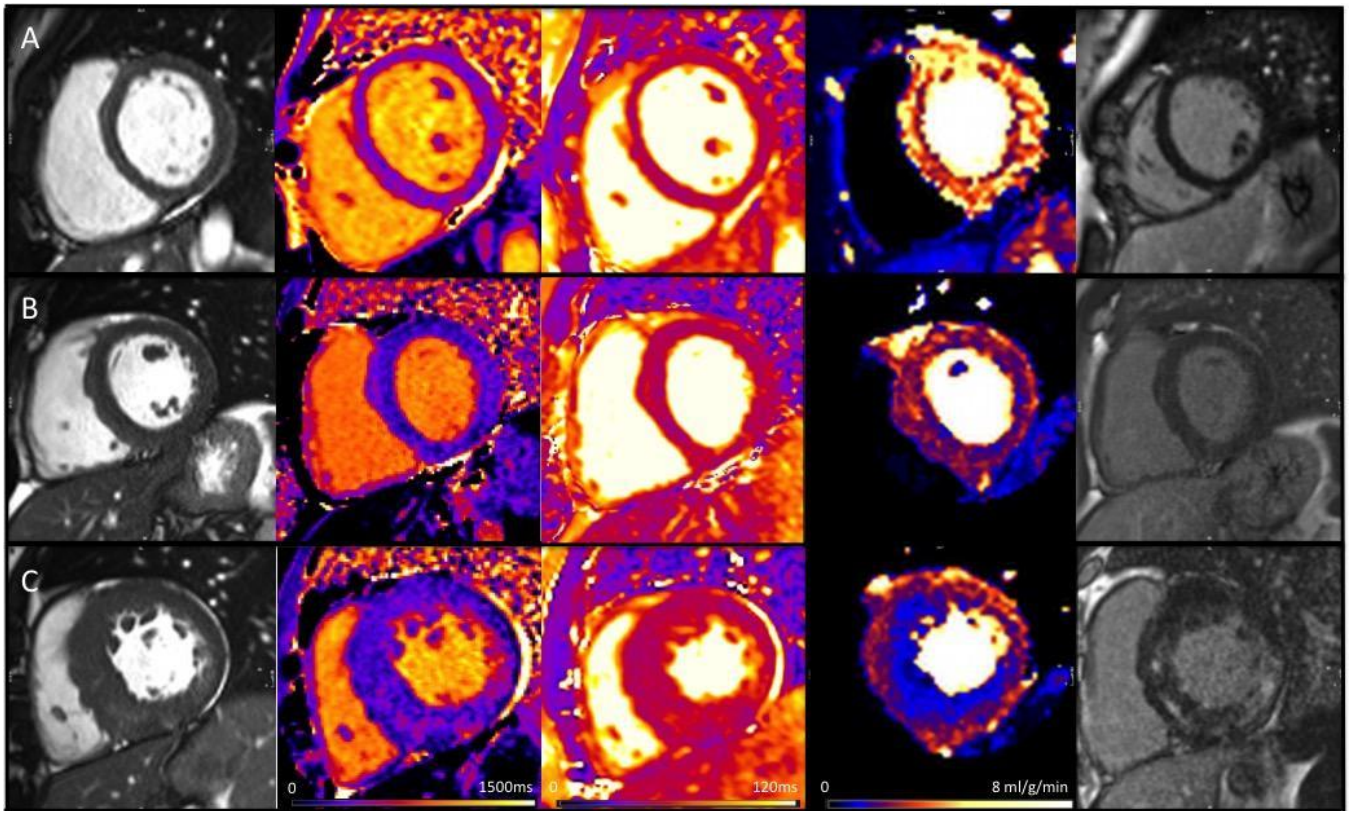

Figure 28. Box and whisker plots for stress MBF in FD and controls. The boxes show the median (line within the box) and interquartile ranges (IQR, upper and lower end of the box) for MBF. The tips of the whiskers demonstrate the values 1.5 x the IQR. Outliers (beyond the whiskers, >1.5x the IQR) are displayed as circles. Patients without FD have higher MBF than FD patients. This is the case even for patients who did not have (LVH, p=0.002). FD patients with LVH have lower stress MBF than those patients who did not have LVH (p=0.005).

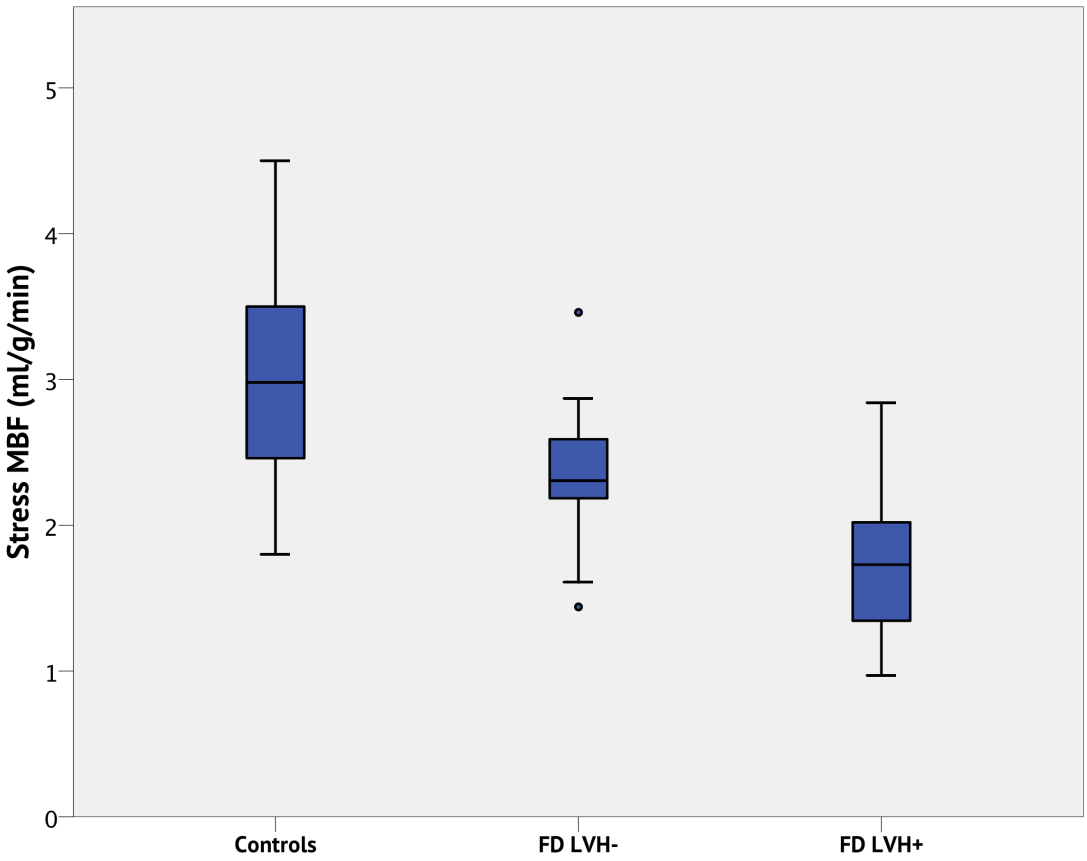

Figure 29. Stress MBF in controls and patients with FD. The endocardial (orange) and epicardial (blue) MBF is demonstrated. The box shows the median and interquartile ranges (IQR) for MBF. The whiskers represent 1.5 x the IQR. Outliers (>1.5x the IQR) are indicated by the circles. There is an epicardial to endocardial perfusion gradient in FD patients with left ventricular hypertrophy (LVH+, p=0.013) but not in patients without LVH (p=0.208) or healthy controls (p=0.271).

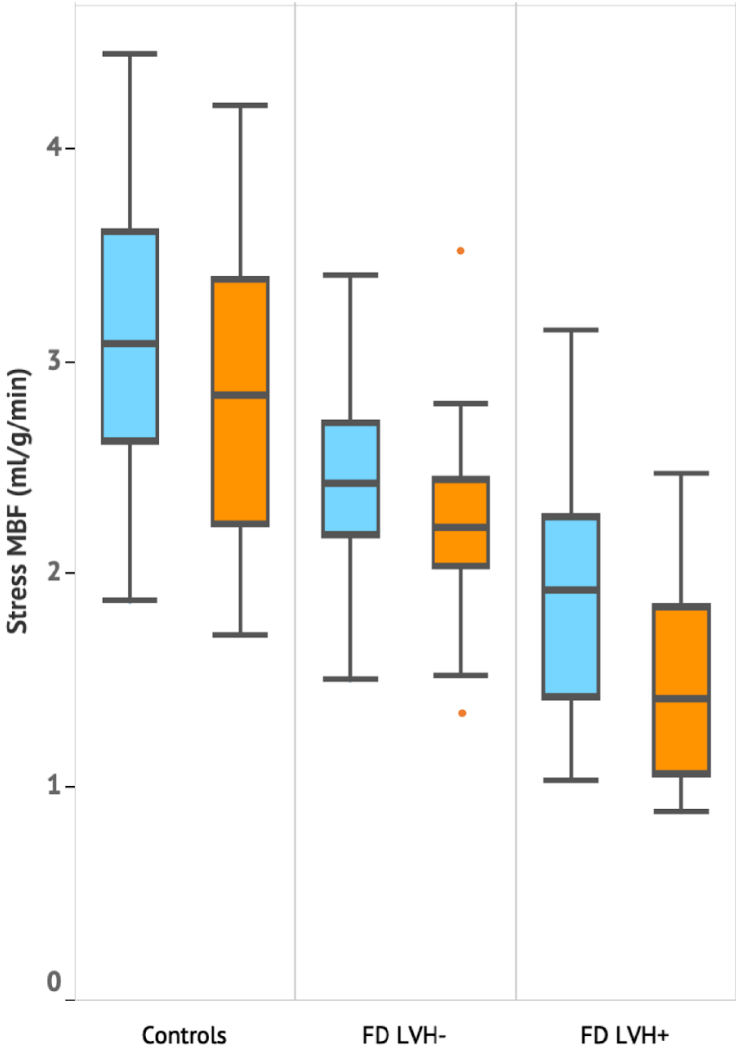

Figure 30. A segmental analysis of stress MBF and segmental wall thickness in FD. The boxes display the median and IQR for MBF. The whiskers show 1.5 x the IQR. Outliers 1.5-3x the IQR are indicated by the circles. As wall thickness increases, the stress myocardial blood flow (MBF) falls ($p<0.001$).

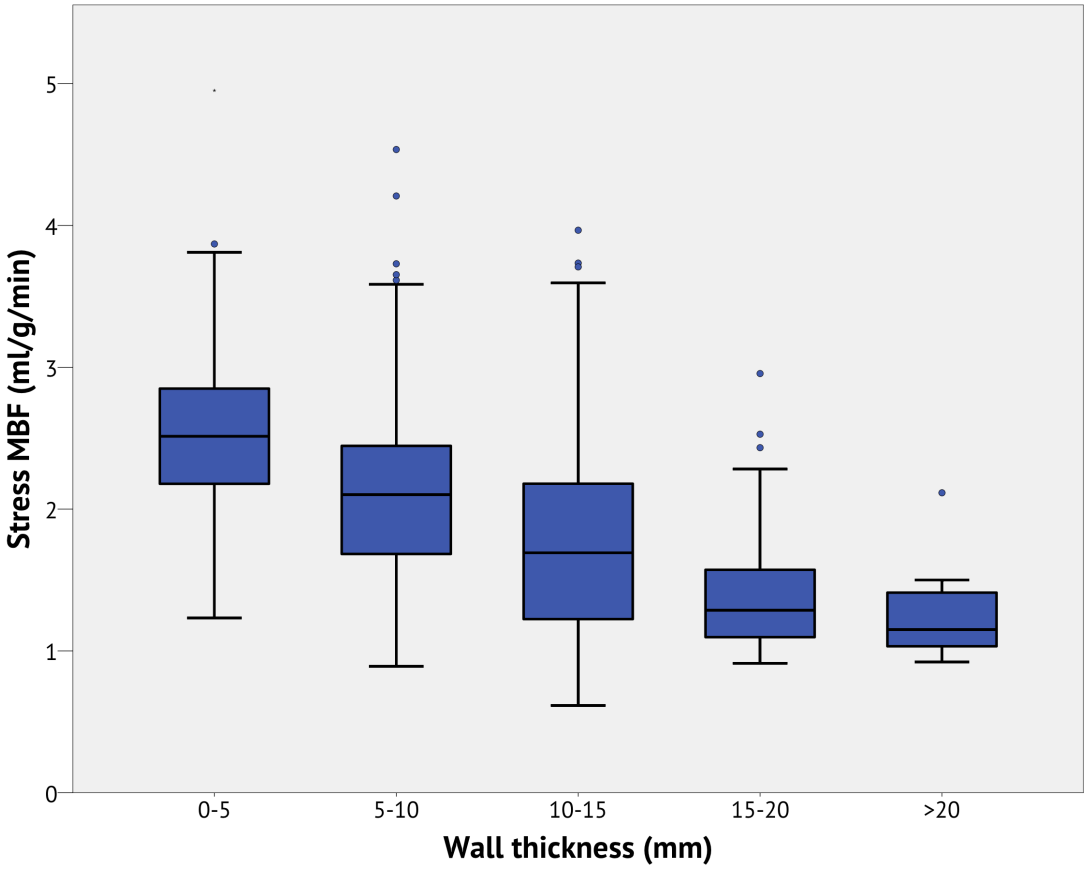

## 7.5 Discussion

In this study we have shown that patients with Fabry disease have lower stress myocardial blood flow than age matched healthy controls. This is even the case if the FD patients have normal LV wall thickness. As the severity of the FD increases, perfusion worsens and this is shown by the association with LVH, oedema / inflammation (high T2) and fibrosis (high ECV and the presence and extent of LGE).

The results presented here are the first in which a multiparametric CMR assessment of patients with FD has been performed including myocardial perfusion. There have been some PET based perfusion studies but as PET does not permit multiparametric assessment these studies were unable to assess perfusion in the context of other myocardial disease processes in FD. Our study is also larger than previous FD perfusion studies in any modality and the first to directly compare LVH negative FD patients with healthy controls. These results presented here are consistent with the PET literature that showed impaired perfusion in FD patients (136,227). These previous PET studies attempted to assess the effect of treatment with ERT on perfusion. One study showed no improvement in perfusion with ERT, but the other study found a correlation between pre-treatment relative wall thickness and post-treatment changes in flow reserve. From this, the group suggested that patients treated with ERT early, might benefit with improvements in perfusion. The multiparametric nature of CMR allows further future exploration of this suggestion as the disease stages of FD are more readily investigated from storage to hypertrophy to inflammation and fibrosis (134,219,220).

The myocardial perfusion appears to be affected early in the disease course (i.e. before the onset of LVH) of FD and is subsequently associated with severity of disease. However the exact timing of perfusion in the disease course requires further investigation. For example the relation of perfusion to sphingolipid storage could be investigated in cohorts of LVH negative patients with normal and low myocardial native T1. There was not the statistical power to do

this in the current study. The T1 lowering effect of sphingolipid deposition is due to myocyte storage. It is possible that there is endothelial storage too and if this was the case perfusion abnormalities could occur before or at the same time of myocyte storage and could be the earliest abnormality detected by CMR in FD. Alternatively, perhaps there is a threshold effect whereby a certain amount of storage is required to be detected as a low T1 on a CMR scan and that changes in MBF are more sensitive with perfusion mapping. In the podocytes of the kidneys sphingolipids appear to clear faster than other cells in response to ERT (230). Perhaps in a similar way, endothelial cells in the heart may also clear sphingolipids faster and so early treatment with ERT may be useful in preventing microvascular dysfunction. Based on our results, perfusion could prove to be a surrogate endpoint in drug studies and may provide insights into drivers of hypertrophy and inflammation and fibrosis in FD.

There have also been histological studies in FD, which have looked at the microvasculature of the myocardium. In one study, Chimenti et al compared endomyocardial biopsies of symptomatic FD patients who had chest pain to a group of FD patients with no symptoms (231). They noted several pathological findings with the biopsies. The endothelial cells were swollen and proliferating due to sphingolipid storage and the lumens of the arterioles were narrowed due to hypertrophy and hyperplasia of the smooth muscle cells and increased fibrosis within the intimal and medial layers. They found that the pathological patterns were more often associated with perivascular myocardial fibrosis surrounding the most affected vessels and that the degree of luminal stenosis was lower in patients without symptoms. Our study is in agreement with these histological validations. Using CMR we have shown the relation of impairment of myocardial perfusion to LVH, sphingolipid deposition (low T1) and fibrosis (high ECV and LGE). As few studies have considered microvascular dysfunction in FD (or hypertrophic cardiomyopathy), there has been minimal evidence into its treatment. With perfusion mapping this is now possible. As well as ERT and OCT other medications may have

an impact on myocardial perfusion. In a hypertensive LVH model, it has been suggested that the combination of angiotensin-converting enzyme (ACE) inhibitors and thiazide diuretics improve microvascular function. This has been demonstrated in animal (rat) models and small human studies but the effect in FD is unknown (232,233).

As previously mentioned, another advantage of CMR compared to PET is the ability to analyse transmyocardial perfusion gradients due to the higher spatial resolution. We have found that the subendocardium is particularly vulnerable to impaired perfusion in FD. The subendocardium is in general susceptible to ischaemia and even in healthy animal models it seems that stress MBF in the subendocardium is relatively reduced compared to the subepicardium. Furthermore, this transmyocardial gradient is more pronounced in heart failure models due to chronic subendocardial fibrosis (234). It is possible that a similar mechanism is responsible for the myocardial perfusion gradients seen in the FD patients with LVH in our study and that chronic fibrosis that preferentially affects the sub-endocardium is responsible for the more pronounced perfusion reductions in these patients.

The ECV in Fabry patients (across the entire cohort) was higher than in controls. Although not specifically investigated (and with no histological confirmation), this is likely due to diffuse and focal fibrosis in the Fabry patients, particularly in those with LVH and would be partially reflected by LGE in some of these patients.

*Limitations*

As this is an observational study there are associated limitations. We suggest that the impairment in perfusion that we have observed is due to microvascular dysfunction (rather than, for example, impaired response to adenosine in these patients) but without a histological correlation this cannot be confirmed. Similar limitations exist with the other CMR tissue characterisation parameters that we assume to reflect sphingolipid storage, inflammation and

fibrosis. As a sample size calculation was not performed prior to the study, the findings are hypothesis generating and require further validation in larger studies.

## 7.6 Conclusion

Myocardial perfusion in Fabry disease is impaired compared to healthy controls, even before the onset of left ventricular hypertrophy. The perfusion impairment is associated with sphingolipid storage and myocardial fibrosis and on a regional basis with oedema and hypertrophy. It appears that microvascular dysfunction is affected early in the disease course and furthermore, perfusion mapping can be used clinically as an end-point in clinical trials including outcome studies.

# 8. Discussion and Conclusions

**Background**

The goal of this thesis was to investigate perfusion mapping in order to build a body of evidence to facilitate the introduction of quantitative perfusion cardiovascular magnetic resonance into clinical practice in a similar way that T1 and T2 mapping have now become routine techniques. The approach taken was to investigate patients with suspected coronary artery disease prior to coronary angiography, determine whether quantitative myocardial perfusion was prognostic, explore factors that may contribute to perfusion in order to begin to develop reference ranges and to investigate patients with cardiomyopathy, using Fabry Disease as the exemplar disease.

**Key findings, limitations and clinical implications**

*Quantitative perfusion mapping in coronary artery disease (CAD).* In this study I demonstrated that quantitative perfusion calculated using perfusion mapping was accurate for the detection of CAD using 3D quantitative coronary angiography as the truth standard. The technique was particularly useful in excluding CAD with a high negative predictive value and sensitivity on both a "per-vessel" and "per-patient" basis. The specificity and positive predictive value were also good. Practically, with a suitable colour look-up table, this enables the clinician to easily review the perfusion maps, and if the maps are uniformly yellow (in our look-up table), they can have confidence that the likelihood of coronary artery disease is low. I found that stress MBF was more accurate for the detection of CAD than MPR. This study was the largest

quantitative perfusion CMR study that prospectively recruited patients and looked at diagnostic accuracy. The main limitation of the study was the three-dimensional quantitative coronary angiography gold standard, rather than a functional gold standard. The 3D QCA is however a better method than visual assessment of coronary angiography. Subsequently, our collaborators at the Royal Free have validated the technique against fractional flow reserve with similar results. Similarly overall atheroma was not quantified and only focal stenoses were considered. Another limitation is the relatively small sample size and that no sample size calculation was carried out prior to the study. Although the largest such study at the time and provides good evidence for perfusion mapping, the 50 patient study of patients from a diverse area of London, the results should only cautiously be extrapolated to other settings and other patient groups and requires larger studies for validation. Overall, this study provides validation of perfusion mapping in diagnosing coronary artery disease and, in particular, ruling out CAD in patients with entirely normal quantitative perfusion. Clinically this provides evidence for using perfusion maps as a rule out technique for CAD. Further work is required going forward to validate with larger, multi-centre cohorts the accuracy of perfusion mapping both as a rule out and rule in technique for diagnosing CAD.

*The prognostic significance of quantitative perfusion mapping.* This was a study in which patients referred for CMR studies at Barts Heart Centre and the Royal Free Hospital were recruited. In total there were 1049 patients included in the study with a median follow up of 605 days (IQR 464-814 days). The perfusion maps were analysed for the first time with an artificial intelligence LV segmentation approach to improve accuracy and reliability and eliminate bias. After adjusting for co-morbidities, both stress MBF and MPR were associated with death and MACE. A 1ml/g/min decrease in MBF was associated with an adjusted hazard ratio for MACE of 2.14. A 1-unit decrease in MPR was associated with an adjusted hazard ratio

for MACE of 1.74. Similar results were seen even if there were no perfusion defects on clinical read and if patients with previous CAD were excluded. This study was the first multicentre perfusion outcome study using any imaging modality and the largest quantitative perfusion outcome study using CMR. The observational nature of the study is a limitation and associations do not necessarily imply causation. Also, there is a potential for bias as there were a large number of covariates and relatively few outcomes. However, a sensitivity analysis was additionally performed to check for this and stress MBF and MPR remained prognostic. Finally, a small number of events may have been missed as the electronic record was relied upon to get this data. In summary, this study showed that quantitative perfusion mapping encodes prognostic information. MBF and MPR could be used as additional clinical parameters to stratify patients and target those at highest risk. Also, perfusion could be used as an endpoint in clinical trials, to see if prognosis can be improved by targeting myocardial perfusion. Whether MPR or MBF is the more useful marker is debatable. We attempted to answer this question by comparing the predictive performance of these parameters. Our results suggest that MPR may be the stronger predictor in respect to mortality but not combined MACE outcomes. The reason for this is unclear and requires further work and understanding. It is possible that the ability to vasodilate in response to stress is more important than the absolute MBF. For example, patients who are already vasodilated at rest due to epicardial disease or microvascular dysfunction would have a blunted vasodilatory response to stress and would have a reduced ability to increase their MBF compared to healthy comparators. Another explanation could be that the minor differences in the calculated MBF with different field strengths, different hospital sites and different patient populations are corrected for with the MPR. It is also conceivable that MPR would be more comparable across different imaging modalities for example with PET than the absolute MBF as there are many factors involved in the calculation of MBF. However, the number of deaths in our study was relatively few and so

the comparison between stress MBF and MPR should not be over-stressed. Also, in contrast, I found that stress MBF was more accurate for the detection of coronary artery disease than MPR in the perfusion mapping CAD chapter. Further work and longer term follow up is required to fully answer these questions. The results of the recent ISCHEMIA trial have questioned the role of ischaemia in the prognosis of patients with stable coronary artery disease. However, that study focused on medical vs revascularisation for patients with coronary artery disease and significant ischaemia on functional imaging. There was no difference in outcome if the patient was managed medically or revascularised with PCI or CABG. The ISCHEMIA study did not use quantitative perfusion and it is possible that the severity of ischaemia would have been re-classified if fully quantitative perfusion was used. Secondly, ischaemia is often due to a combination of epicardial and microvascular dysfunction. Although the epicardial stenosis was treated, there was no specific treatment for the microvasculature. Thirdly, only a small percentage of patients in the study had a perfusion CMR as the ischaemia test. Finally medical therapy is very good for the treatment of stable CAD and the additional benefit of coronary intervention is unclear. In summary, whilst our study (and others) has shown the prognostic value of ischaemia, others have not shown this can be modified with revascularisation. Studies focusing on improving absolute MBF with medical therapy or coronary intervention could be considered in the future.

*Perfusion in patients with unobstructed coronary arteries.* Perfusion is influenced by the epicardial coronary arteries and the microvasculature. I therefore sought to determine what factors would influence perfusion in patients with unobstructed coronary arteries and no myocardial scar in order to begin to understand what is “normal” for patients with cardiac co-morbidities. I showed that rest myocardial blood flow was higher in females and lower with the use of beta blockers. The stress perfusion was reduced with increasing age, diabetes,

increasing left ventricular mass and the use of beta blockers. This was a retrospective analysis of patients referred for clinical perfusion scans and so has limitations. However it does give an insight into factors that influence microvascular perfusion. Further work is required to develop patient specific reference ranges and explore whether patient factors could be used to improve the modelling of techniques that simulate epicardial coronary flow such as CT FFR. Larger studies would be required to validate our findings as sample size calculations were not performed.

*Quantitative perfusion mapping in Fabry disease.* In this study I prospectively recruited patients with Fabry disease for a perfusion scan with quantitative perfusion mapping. This was to investigate the utility of quantitative perfusion in patients with cardiomyopathy and determine at what stage perfusion was affected in the natural history of Fabry disease. This study showed that perfusion is impaired in Fabry disease and that the process seems to occur early in the disease course. Fabry patients with no left ventricular hypertrophy had reduced perfusion compared to an age-matched control cohort. Furthermore, perfusion was increasingly impaired with increasing disease severity. Markers of disease severity include native T1, T2, LVH and late gadolinium enhancement. With increasing abnormalities in these known disease markers, perfusion was increasingly impaired. The subendocardium was particularly vulnerable to impaired perfusion. This was the first quantitative perfusion CMR study in Fabry disease and the first to investigate perfusion as part of a full, multiparametric assessment. There have only been minimal Fabry studies across all modalities and these have generally involved PET perfusion. Therefore, it was also the largest perfusion study in Fabry across all modalities. There are however limitations with the study. Firstly, whilst we assume the impaired perfusion reflects microvascular dysfunction in Fabry patients, another explanation could be impaired response to adenosine. Also we did not perform myocardial biopsies on

these patients. Although it is assumed that the parametric mapping reflects disease stages such as myocyte sphingolipid and inflammation this has not been proven in our study. This lack of histology limitation is common to the majority of Fabry studies. Sample size calculations were not performed and so the findings are hypothesis generating. In summary this study showed that perfusion is impaired in Fabry disease, particularly in the subendocardium and worsens with increasing disease severity. Perfusion mapping has been shown to provide disease insights in cardiomyopathy and perfusion could be used as an outcome in interventional drug studies. As CMR does not use ionising radiation it is a more suitable technique for serial repeated scans than PET. For example, after a period of treatment the CMR could be repeated to see the effect of the drug on perfusion and other parameters. Although we have seen that perfusion is impaired prior to the development of LVH with the numbers in our study, we did not have the statistical power to detect whether perfusion falls even earlier in the disease course. For example whether it falls before the sphingolipid storage phase, whether these disease phases are independent or if there is inter-play between them. This will require further work. Additionally, in PET studies in patients with hypertrophic cardiomyopathy, perfusion has been shown to be related to patient prognosis. Whether quantitative perfusion CMR conveys prognostic information remains unknown in Fabry disease. It seems logical that, as impaired perfusion is associated with other factors markers of disease severity, then it would have adverse prognostic implications. However, whether this is an independent risk factor is unclear. This is another area that warrants further investigation. Patients with high risk of sudden cardiac death in Fabry disease are treated with an implantable cardioverter defibrillator (ICD). The decision algorithm is less strong than for HCM but ICDs are more commonly implanted in patients with ventricular arrhythmias and / or extensive scarring. It is possible that perfusion is an additional biomarker that could better stratify patients at risk of sudden cardiac death in Fabry disease.

**Ongoing and future work / collaborations**

Following these initial validations, work has been taken forward on a number of fronts at UCL / Barts Heart Centre to further investigate myocardial perfusion in heart disease.

1. Predictors of functional recovery from surgical revascularisation of poor ventricles. This BHF funded study by Dr Andreas Seraphim is ongoing and involves multiparametric CMR before and after bypass surgery in patients with impaired LV function. I contributed to the grant application and have remained involved with the study. One of the parameters being investigated is the MBF, to see whether a change in MBF is related to change in LV function. The work builds upon the quantitative perfusion data in CAD presented in this thesis and has resulted in publications in JACC and Frontiers in Cardiovascular Medicine.
2. The extended spectrum of apical hypertrophic cardiomyopathy. In this BHF funded study by Dr Rebecca Hughes is investigating patients with apical hypertrophic cardiomyopathy and athletes with hypertrophy with perfusion mapping CMR to gain insights into the disease processes. I have also contributed to the grant application and ongoing work in the area. The work builds on the cardiomyopathy perfusion work presented in this thesis.

**Conclusion**

In this thesis I have presented data that show quantitative perfusion is accurate for the detection of coronary artery disease. Peak vasodilator stress MBF seems more accurate than MPR and the high negative predictive value and sensitivity make quantitative perfusion with perfusion mapping a good test to rule out angiographically significant coronary disease. Myocardial perfusion is associated with patient outcome, with major adverse cardiovascular

events increasing with worsening perfusion. This is the case even after adjusting for conventional risk factors. Myocardial perfusion in patients without obstructive coronary artery disease is influenced by multiple patient factors including age, diabetes, LVH and the use of beta blockers. Myocardial perfusion is also abnormal in Fabry disease. It seems to fall relatively early in the disease course, before the onset of left ventricular hypertrophy. The endocardium is particularly susceptible to impaired perfusion, and perfusion progressively worsens with disease severity.

Quantitative perfusion has previously been outside the realm of clinical practice but with the evidence presented here I have shown that it is feasible to perform absolute quantification in the clinical routine. The information provided by quantitative perfusion is useful in patients with coronary artery disease and cardiomyopathy.

# 9. Academic outputs

## 9.1 Study funding

- British Heart Foundation Clinical Research Training Fellowship awarded 2017 – award number FS/17/34/32901.

Other BHF grant applications awarded that I have contributed to:

- Predictors of functional recovery from surgical revascularisation of poor ventricles. Dr Andreas Seraphim.
- The extended spectrum of apical hypertrophic cardiomyopathy. Dr Rebecca Hughes.

## 9.2 Publications

***First author original research publications:***

33. **Knott KD**, Seraphim A, Augusto JB, Xue H, Chacko L, Aung N, Petersen SE, Cooper JA, Manisty C, Bhuva AN, Kotecha T, Bourantas CV, Davies RH, Brown LAE, Plein S, Fontana M, Kellman P, Moon JC. The Prognostic Significance of Quantitative Myocardial Perfusion: An Artificial Intelligence Based Approach Using Perfusion Mapping. ***Circulation*.** 2020. https://doi.org/10.1161/CIRCULATIONAHA.119.044666.

32. **Knott KD**, Camaioni C, Augusto JB, Seraphim S, Rosmini S, Ricci F, Boubertakh R, Xue H, Hughes R, Captur G, Lopes LR, Brown LAE, Manisty C, Petersen SE, Plein S, Kellman P, Mohiddin SA, Moon JC. Inline perfusion mapping provides insights into the disease mechanism in hypertrophic cardiomyopathy. ***Heart*** Published Online First: 10 December 2019. doi: 10.1136/heartjnl-2019-315848. **Joint first author.**

31. **Knott KD,** Augusto JB, Nordin S, Kozor R, Camaioni C, Xue H, Hughes RK, Manisty C, Brown LAE, Kellman P, Ramaswami U, Hughes D, Plein S, Moon JC. Quantitative. Myocardial Perfusion in Fabry Disease. ***Circ Cardiovasc Imaging***. 2019 Jul;12(7):e008872. doi: 10.1161/CIRCIMAGING.119.008872. Epub 2019 Jul 4.

30. **Knott KD,** Camaioni C, Ramasamy A, Augusto JA, Bhuva AN, Xue H, Manisty C, Hughes RK, Brown LAE, Amersey R, Bourantas C, Kellman P, Plein S, Moon JC. Quantitative myocardial perfusion in coronary artery disease: A perfusion mapping study. ***J Magn Reson Imaging.*** 2019 Jan 25. doi: 10.1002/jmri.26668.

***First author review articles:***

29. **Knott KD,** Fernandes JL, Moon JC. Automated Quantitative Stress Perfusion in a Clinical Routine. ***Magn Reson Imaging Clin N Am.*** 2019 Aug;27(3):507-520. doi: 10.1016/j.mric.2019.04.003. Epub 2019 May 13. Review.

28. Seraphim A, **Knott KD,** Augusto J, Bhuva AN, Manisty C, Moon JC. Quantitative cardiac MRI. ***J Magn Reson Imaging***. 2019 May 20. doi: 10.1002/jmri.26789. Review. **Joint first author.**

***Co-author publications:***

27. Seraphim A, Dowsing B, Rathod KS, Shiwani H, Patel K, **Knott KD,** Zaman S, Johns I, Razvi Y, Patel R, Xue H, Jones DA, Fontana M, Cole G, Uppal R, Davies R, Moon JC, Kellman P, Manisty C. Quantitative Myocardial Perfusion Predicts Outcomes in Patients With Prior Surgical Revascularization. ***J Am Coll Cardiol. 2022*** Mar 29;79(12):1141-1151. doi: 10.1016/j.jacc.2021.12.037. Original research

26. Menacho KD, Ramirez S, Perez A, Dragonetti L, Perez de Arenaza D, Katekaru D, Illatopa V, Munive S, Rodriguez B, Shimabukuro A, Cupe K, Bansal R, Bhargava V, Rodriguez I, Seraphim A, **Knott K,** Abdel-Gadir A, Guerrero S, Lazo M, Uscamaita D, Rivero M, Amaya N, Sharma S, Peix A, Treibel T, Manisty C, Mohiddin S, Litt H, Han Y, Fernandes J, Jacob R, Westwood M, Ntusi N, Herrey A, Walker JM, Moon J. Improving cardiovascular magnetic resonance access in low- and middle-income countries for cardiomyopathy assessment: rapid cardiovascular magnetic resonance. ***Eur Heart J. 2022*** Feb 9:ehac035. doi: 10.1093/eurheartj/ehac035. Original research

25. Alfarih, M., Augusto, J.B., **Knott, K.D.** et al. Saturation-pulse prepared heart-rate independent inversion-recovery (SAPPHIRE) biventricular T1 mapping: inter-field strength, head-to-head comparison of diastolic, systolic and dark-blood measurements. ***BMC Med Imaging 22, 122 (2022).*** https://doi.org/10.1186/s12880-022-00843-0. Original research

24. Seraphim A, **Knott KD**, Augusto JB, Menacho K, Tyebally S, Dowsing B, Bhattacharyya S, Menezes LJ, Jones DA, Uppal R, Moon JC, Manisty C. Non-invasive Ischaemia Testing in Patients With Prior Coronary Artery Bypass Graft Surgery: Technical Challenges, Limitations, and Future Directions. ***Front Cardiovasc Med. 2021*** Dec 23;8:795195. doi: 10.3389/fcvm.2021.795195. PMID: 35004905. Original research

23. Thornton GD, Shetye A, Knight DS, **Knott K,** Artico J, Kurdi H, Yousef S, Antonakaki D, Razvi Y, Chacko L, Brown J, Patel R, Vimalesvaran K, Seraphim A, Davies R, Xue H, Kotecha T, Bell R, Manisty C, Cole GD, Moon JC, Kellman P, Fontana M, Treibel TA. Myocardial Perfusion Imaging After Severe COVID-19 Infection Demonstrates Regional Ischemia Rather Than Global Blood Flow Reduction. ***Front Cardiovasc Med. 2021*** Dec 7;8:764599. doi: 10.3389/fcvm.2021.764599. Original research

22. Rosmini S, Seraphim A, **Knott K,** Brown JT, Knight DS, Zaman S, Cole G, Sado D, Captur G, Gomes AC, Zemrak F, Treibel TA, Cash L, Culotta V, O'Mahony C, Kellman P, Moon JC, Manisty C. Non-invasive characterization of pleural and pericardial effusions using T1 mapping by magnetic resonance imaging. ***Eur Heart J Cardiovasc Imaging.*** 2021 Jul 30:jeab128. doi: 10.1093/ehjci/jeab128. Epub ahead of print. PMID: 34331054. Original research

21. Hughes RK, Camaioni C, Augusto JB, **Knott K,** Quinn E, Captur G, Seraphim A, Joy G, Syrris P, Elliott PM, Mohiddin S, Kellman P, Xue H, Lopes LR, Moon JC. Myocardial Perfusion Defects in Hypertrophic Cardiomyopathy Mutation Carriers. ***J Am Heart Assoc.*** 2021 Jul 26:e020227. doi: 10.1161/JAHA.120.020227. Epub ahead of print. PMID: 34310159. Original research

20. Seraphim A, **Knott KD,** Menacho K, Augusto JB, Davies R, Pierce I, Joy G, Bhuva AN, Xue H, Treibel TA, Cooper JA, Petersen SE, Fontana M, Hughes AD, Moon JC, Manisty C, Kellman P. Prognostic Value of Pulmonary Transit Time and Pulmonary Blood Volume Estimation Using Myocardial Perfusion CMR. ***JACC Cardiovasc Imaging***. 2021 May 12:S1936-878X(21)00344-2. doi: 10.1016/j.jcmg.2021.03.029. Original research.

19. Seraphim A, **Knott KD,** Beirne AM, Augusto JB, Menacho K, Artico J, Joy G, Hughes R, Bhuva AN, Torii R, Xue H, Treibel TA, Davies R, Moon JC, Jones DA, Kellman P, Manisty C. Use of quantitative cardiovascular magnetic resonance myocardial perfusion mapping for characterization of ischemia in patients with left internal mammary coronary artery bypass grafts. ***J Cardiovasc Magn Reson.*** 2021 Jun 17;23(1):82. doi: 10.1186/s12968-021-00763-y. PMID: 34134696. Original research.

18. Augusto JB, Davies RH, Bhuva AN, **Knott KD,** Seraphim A, Alfarih M, Lau C, Hughes RK, Lopes LR, Shiwani H, Treibel TA, Gerber BL, Hamilton-Craig C, Ntusi NAB, Pontone G, Desai MY, Greenwood JP, Swoboda PP, Captur G, Cavalcante J, Bucciarelli-Ducci C, Petersen SE, Schelbert E, Manisty C, Moon JC. Diagnosis and risk stratification in hypertrophic cardiomyopathy using machine learning wall thickness measurement: a comparison with human test-retest performance. ***Lancet Digit Health.*** 2021 Jan;3(1):e20-e28. doi: 10.1016/S2589-7500(20)30267-3. Original research.

17. Brown LAE, Saunderson CED, Das A, Craven T, Levelt E, **Knott KD,** Dall'Armellina E, Xue H, Moon JC, Greenwood JP, Kellman P, Swoboda PP, Plein S. A comparison of standard and high dose adenosine protocols in routine vasodilator stress cardiovascular magnetic resonance: dosage affects hyperaemic myocardial blood flow in patients with severe left ventricular systolic impairment. ***J Cardiovasc Magn Reson.*** 2021 Mar 18;23(1):37. doi: 10.1186/s12968-021-00714-7. Original research.

16. Bhuva AN, Treibel TA, Seraphim A, Scully P, **Knott KD,** Augusto JB, Torlasco C, Menacho K, Lau C, Patel K, Moon JC, Kellman P, Manisty CH. Measurement of T1 Mapping in Patients With Cardiac Devices: Off-Resonance Error Extends Beyond Visual Artifact but Can Be Quantified and Corrected. ***Front Cardiovasc Med.*** 2021 Jan 29;8:631366. doi:10.3389/fcvm.2021.631366. Original research.

15. Xue H, Davies RH, Brown LAE, **Knott KD,** Kotecha T, Fontana M, Plein S, Moon JC, Kellman P. Automated Inline Analysis of Myocardial Perfusion MRI with Deep Learning. ***Radiol Artif Intell***. 2020 Oct 21;2(6):e200009. doi: 10.1148/ryai.2020200009. PMID: 33330849. Original research.

14. Kotecha T, Monteagudo JM, Martinez-Naharro A, Chacko L, Brown J, Knight D, **Knott KD**, Hawkins P, Moon JC, Plein S, Xue H, Kellman P, Lockie T, Patel N, Rakhit R, Fontana M. Quantitative cardiovascular magnetic resonance myocardial perfusion mapping to assess hyperaemic response to adenosine stress. ***Eur Heart J Cardiovasc Imaging.*** 2020 Nov 14:jeaa252. doi: 10.1093/ehjci/jeaa252. PMID: 33188683. Original research.

13. Kotecha T, Chacko L, Chehab O, O'Reilly N, Martinez-Naharro A, Lazari J, **Knott KD,** Brown J, Knight D, Muthurangu V, Hawkins P, Plein S, Moon JC, Xue H, Kellman P, Rakhit R, Patel N, Fontana M. Assessment of Multivessel Coronary Artery Disease Using Cardiovascular Magnetic Resonance Pixelwise Quantitative Perfusion Mapping. ***JACC Cardiovasc Imaging***. 2020 Sep 30:S1936-878X(20)30649-5. doi: 10.1016/j.jcmg.2020.06.041. Original research.

12. Torlasco C, D'Silva A, Bhuva AN, Faini A, Augusto JB, **Knott KD,** Benedetti G, Jones S, Van Zalen J, Scully P, Lobascio I, Parati G, Lloyd G, Hughes AD, Manisty CH, Sharma S, Moon JC. Age matters: differences in exercise-induced cardiovascular remodelling in young and middle aged healthy sedentary individuals. ***Eur J Prev Cardiol.*** 2020. doi:10.1177/2047487320926305. Original research.

11. Augusto JB, Johner N, Shah D, Nordin S, **Knott KD,** Rosmini S, Lau C, Alfarih M, Hughes R, Seraphim A, Vijapurapu R, Bhuva A, Lin L, Ojrzynska N, Geberhiwot T, Captur G, Ramaswami U, Steeds R, Kozor R, Hughes D, Moon JC, Namdar M. The Myocardial Phenotype of Fabry Disease Pre-Hypertrophy and Pre-Detectable Storage Early cardiac involvement in Fabry disease. Accepted ***European Heart Journal – Cardiovascular Imaging***. Original research.

10. Xue H, Tseng E, **Knott KD**, Kotecha T, Brown L, Plein S, Fontana M, Moon JC, Kellman P. Automated detection of left ventricle in arterial input function images for inline perfusion mapping using deep learning: A study of 15,000 patients. ***Magn Reson Med.*** 2020 Nov;84(5):2788-2800. PMID: 32378776. Original research.

9. Westwood M, **Knott KD.** Stress CMR and Combination Testing in the World of Multimodality Imaging. ***JACC Cardiovasc Imaging.*** 2020 Mar 13. pii: S1936-878X(20)30157-1. doi: 10.1016/j.jcmg.2020.02.002. Editorial.

8. Augusto JB, Nordin S, Vijapurapu R, Baig S, Bulluck H, Castelletti S, Alfarih M, **Knott K,** Captur G, Kotecha T, Ramaswami U, Tchan M, Geberhiwot T, Fontana M, Steeds RP, Hughes D, Kozor R, Moon JC. Myocardial Edema, Myocyte Injury, and Disease Severity in Fabry Disease. ***Circ Cardiovasc Imaging.*** 2020 Mar;13(3):e010171. doi: 10.1161/CIRCIMAGING.119.010171. Epub 2020 Mar 2. Original research.

7. Hughes RK, **Knott KD,** Malcolmson J, Augusto JB, Mohiddin SA, Kellman P, Moon JC, and Captur G. Apical Hypertrophic Cardiomyopathy: The Variant Less Known. ***J Am Heart Assoc.*** 2020 Mar 3;9(5):e015294. doi: 10.1161/JAHA.119.015294. Epub 2020 Feb 28. Review article.

6. Nordin S, Kozor R, Vijapurapu R, Augusto JB, **Knott KD**, Captur G, Treibel TA, Ramaswami U, Tchan M, Geberhiwot T, Steeds RP, Hughes DA, Moon JC. Myocardial Storage, Inflammation, and Cardiac Phenotype in Fabry Disease After One Year of Enzyme Replacement Therapy. ***Circulation: Cardiovascular Imaging***. 2019;12:e009430. Original research.

5. Hughes RK, **Knott KD**, Malcolmson J, Augusto JB, Kellman P, Moon JC, Captur G. Advanced Imaging Insights in Apical Hypertrophic Cardiomyopathy. ***JACC: Cardiovascular Imaging***, 2019. https://doi.org/10.1016/j.jcmg.2019.09.010. Review article

4. Bhuva AN, Bai W, Lau C, Davies RH, Ye Y, Bulluck H, McAlindon E, Culotta V, Swoboda PP, Captur G, Treibel TA, Augusto JB, **Knott KD,** Seraphim A, Cole GD, Petersen SE, Edwards NC, Greenwood JP, Bucciarelli-Ducci C, Hughes AD, Rueckert D, Moon JC, Manisty CH, 2019. A Multicenter, Scan-Rescan, Human and Machine Learning CMR Study to Test Generalizability and Precision in Imaging Biomarker Analysis. ***Circulation: Cardiovascular Imaging*** 12, e009214. Original research.

3. Bhuva, AN, D'Silva A, Torlasco C, Nadarajan N, Jones S, Boubertakh R, Van Zalen J, Scully P, **Knott K,** Benedetti G, Augusto JB, Bastiaenen R, Lloyd G, Sharma S, Moon JC, Parker KH, Manisty CH, Hughes AD, 2019. Non-invasive assessment of ventriculo-arterial coupling using aortic wave intensity analysis combining central blood pressure and phase-contrast cardiovascular magnetic resonance. ***European Heart Journal - Cardiovascular Imaging***. https://doi.org/10.1093/ehjci/jez227. Original research.

2. Bollache E, **Knott KD,** Jarvis K, Boubertakh R, Dolan RS, Camaioni C, Collins L, Scully P, Rabin S, Treibel T, Carr JC, van Ooij P, Collins JD, Geiger J, Moon JC, Barker AJ, Petersen SE, Markl M, 2019. Two-minute k-t accelerated aortic 4D flow MRI: Dual-center study of feasibility and impact on velocity and wall shear stress quantification. ***Radiol Cardiothorac Imaging*** 1, e180008. https://doi.org/10.1148/ryct.2019180008. Original research

1. Brown LAE, Onciul SC, Broadbent DA, Johnson K, Fent GJ, Foley JRJ, Garg P, Chew PG, **Knott K,** Dall'Armellina E, Swoboda PP, Xue H, Greenwood JP, Moon JC, Kellman P, Plein S. Fully automated, inline quantification of myocardial blood flow with cardiovascular magnetic resonance: repeatability of measurements in healthy subjects. ***J Cardiovasc Magn Reson.*** 2018 Jul 9;20(1):48. doi: 10.1186/s12968-018-0462-y. Original research.

### 9.3 Presentations

First author presentations during the studentship only:

9. The Prognostic Significance of Quantitative Myocardial Perfusion Mapping. **Knott KD,** Seraphim A, Augusto JB, Xue H, Chacko L, Aung N, Petersen SE, Cooper JA, Brown LAE, Manisty C, Plein S, Fontana M, Kellman P, Moon JC. **An oral presentation at SCMR 2020, Orlando, USA**.

8. Quantitative perfusion mapping in Fabry disease. **Knott KD,** Augusto JB, Nordin S, Kozor R, Camaioni C, Xue H, Hughes RK, Manisty C, Brown LAE, Ramaswami U, Hughes D, Kellman P, Plein S, Moon JC. **An oral presentation at EuroCMR 2019,** Venice, Italy.

7. Using systolic SAPPHIRE to optimize T1 mapping for thin-walled hearts and arrhythmia. **Knott KD,** Alfarih M, Augusto JB, Boubertakh R, Chaturverdi N, Hughes AD, Moon JC, Weingartner S, Captur G. **A poster presentation at EuroCMR 2019.**

6. Myocardial perfusion falls early and tracks disease severity in Fabry disease. **Knott KD,** Augusto JB, Nordin S, Camaioni C, Kellman P, Kozor R, Manisty C, Xue H, Brown LAE, Ramaswami U, Hughes D, Plein S, Moon JC. **A poster presentation at SCMR 2019, Seattle USA.**

5. Optimising T1 mapping for thin-walled hearts – a systolic approach using SAPPHIRE adds value. **Knott KD,** Alfarih M, Augusto JB, Boubertakh R, Chaturverdi N, Hughes AD, Moon JC, Weingartner S, Captur G. **A poster presentation at SCMR 2019, Seattle USA.**

4. Myocardial perfusion is influenced by age, gender, diabetes, myocardial fibrosis and the use of beta-blockers: a perfusion mapping study. **Knott KD,** Camaioni C, Bhuva AN, Xue H, Manisty C, Brown LAE, Pugliese F, Bourantas C, Kellman P, Plein S, Moon JC. A poster presentation at the **British Society of Cardiovascular Magnetic Resonance**, Edinburgh, UK, May 2018.

3. Quantitative perfusion in patients at high risk of coronary artery disease. **Knott KD,** Camaioni C, Cash L, Bhuva AN, Brown LAE, Xue H, Manisty C, Bourantas C, Plein S, Kellman P, Moon JC. **An oral presentation at the SCMR/ISMRM workshop, International Conference, Barcelona, Spain, February 2018**

2. Myocardial perfusion reserve falls in diabetes and with increasing age – a perfusion mapping study. **Knott KD,** Camaioni C, Bhuva AN, Captur G, Xue H, Manisty C, Bourantas C, Plein S, Kellman P, Moon JC. A poster presentation at the **British Society of Cardiovascular Magnetic Resonance**, Manchester, UK, March 2017.

1. Myocardial perfusion mapping in a patient with apical hypertrophic cardiomyopathy. **Knott KD**, Bhuva AN, Scully P, Xue H, Manisty C, Kellman P, Herrey AS, Moon JC. An oral presentation at the **Society for Cardiovascular Magnetic Resonance International Conference, Washington USA,** February 2017.

### 9.4 Invited presentations and teaching

Rapid Cardiac Magnetic Resonance Project and Conference, Lima Peru, January 2019. Senior faculty – Prof James Moon, Dr Ron Jacob, Dr Malcolm Walker, Dr Katia Menacho. I gave talks on various CMR topics and assisted in the hands-on case reporting sessions.

MRI for Cardiac Device Patient Study Day, Barts Heart Centre, London, UK. Regular speaker on the course, lecture on the safety / guideline aspects of scanning a patient with a cardiac device. Senior faculty – Dr Charlotte Manisty, Dr Anish Bhuva, Dr John Baksi, Prof James Moon. Regular dates throughout 2018 and 2019.

University College London examining / teaching.

- Marked essays for the Cardiology MSc
- Examiner MSc clinical cardiology case presentations
- Second year medical student reflective essay examiner
- Second year medical student small group tutor

Course organiser / faculty on the “CMR Workshop on CMR Stress Imaging”. Organised the 2-day international workshop along with course director Prof Steffen Petersen. Gave a talk on the second day on quantitative CMR perfusion. 6 monthly courses from 2017-2019.

Co-organiser of the CMR radiographer improvement course, 2-day course at Barts Heart Centre. Participants travelled from throughout the UK (and Europe) to attend the course. Duties included formulating the programme, arranging the speakers, contacting sponsors, choosing an appropriate venue, giving a presentation on ECG interpretation and running an imaging post processing session.

Clinical trainer and faculty member British Cardiovascular Society 2018-2022. Training participants in sessions on CMR scanning and image post-processing.

### 9.5 Collaborations

- Dr Peter Kellman, Director of the Medical Signal and Image Processing Program at the National Heart Lung and Blood Institute, National Institutes of Health, Bethesda, Maryland, USA.
- Dr Hui Xue, Deputy Director of the Medical Signal and Image Processing Program at the National Heart Lung and Blood Institute, National Institutes of Health, Bethesda, Maryland, USA.
- Prof Steffen Petersen, Professor of Cardiovascular Medicine, Queen Mary University of London.
- Dr Marianna Fontana, Consultant Cardiologist Royal Free Hospital and Associate Professor University College London.
- Prof Sven Plein, Professor of Cardiology, University of Leeds.

## 10. Bibliography


1. Finegold JA, Asaria P, Francis DP. Mortality from ischaemic heart disease by country, region, and age: statistics from World Health Organisation and United Nations. Int J Cardiol. 2013 Sep 30;168(2):934–45.

2. Townsend N, Bhatnagar P, Wilkins, E, Wickramasinghe, K, Rayner, M. Cardiovascular disease statistics, 2015. British Heart Foundation: London.

3. Wilson L, Wilkins E, Wickramasinghe K, Bhatnagar P, Leal J, Luengo-Fernandez R, Burns R, Rayner M, Townsend N. European Cardiovascular Disease Statistics 2017. European Heart Network, Brussels. 2017;

4. British Heart Foundation. UK Factsheet, November 2018. 2018;

5. Whitlock RP, Sun JC, Fremes SE, Rubens FD, Teoh KH. Antithrombotic and thrombolytic therapy for valvular disease: Antithrombotic Therapy and Prevention of Thrombosis, 9th ed: American College of Chest Physicians Evidence-Based Clinical Practice Guidelines. Chest. 2012 Feb;141(2 Suppl):e576S-e600S.

6. Randomised trial of cholesterol lowering in 4444 patients with coronary heart disease: the Scandinavian Simvastatin Survival Study (4S). Lancet. 1994 Nov 19;344(8934):1383–9.

7. Sacks FM, Pfeffer MA, Moye LA, Rouleau JL, Rutherford JD, Cole TG, et al. The effect of pravastatin on coronary events after myocardial infarction in patients with average cholesterol levels. Cholesterol and Recurrent Events Trial investigators. N Engl J Med. 1996 Oct 3;335(14):1001–9.

8. Bavry AA, Kumbhani DJ, Rassi AN, Bhatt DL, Askari AT. Benefit of early invasive therapy in acute coronary syndromes: a meta-analysis of contemporary randomized clinical trials. J Am Coll Cardiol. 2006 Oct 3;48(7):1319–25.

9. O'Donoghue M, Boden WE, Braunwald E, Cannon CP, Clayton TC, de Winter RJ, et al. Early invasive vs conservative treatment strategies in women and men with unstable angina and non-ST-segment elevation myocardial infarction: a meta-analysis. JAMA. 2008 Jul 2;300(1):71–80.

10. Roffi M, Patrono C, Collet JP, Mueller C, Valgimigli M, Andreotti F, et al. 2015 ESC Guidelines for the management of acute coronary syndromes in patients presenting without persistent ST-segment elevationTask Force for the Management of Acute Coronary Syndromes in Patients Presenting without Persistent ST-Segment Elevation of the European Society of Cardiology (ESC). Eur Heart J. 2016 Jan 14;37(3):267–315.

11. Jernberg T, Johanson P, Held C, Svennblad B, Lindbäck J, Wallentin L, et al. Association between adoption of evidence-based treatment and survival for patients with ST-elevation myocardial infarction. JAMA. 2011 Apr 27;305(16):1677–84.

12. Knuuti J, Wijns W, Saraste A, Capodanno D, Barbato E, Funck-Brentano C, et al. 2019 ESC Guidelines for the diagnosis and management of chronic coronary syndromes: The Task

Force for the diagnosis and management of chronic coronary syndromes of the European Society of Cardiology (ESC). European Heart Journal [Internet]. 2019 Aug 31 [cited 2019 Oct 9]; Available from: https://doi.org/10.1093/eurheartj/ehz425

13. Tonino PAL, De Bruyne B, Pijls NHJ, Siebert U, Ikeno F, van `t Veer M, et al. Fractional Flow Reserve versus Angiography for Guiding Percutaneous Coronary Intervention. New England Journal of Medicine. 2009 Jan 15;360(3):213–24.

14. Pijls NHJ, Fearon WF, Tonino PAL, Siebert U, Ikeno F, Bornschein B, et al. Fractional flow reserve versus angiography for guiding percutaneous coronary intervention in patients with multivessel coronary artery disease: 2-year follow-up of the FAME (Fractional Flow Reserve Versus Angiography for Multivessel Evaluation) study. J Am Coll Cardiol. 2010 Jul 13;56(3):177–84.

15. De Bruyne B, Pijls NHJ, Kalesan B, Barbato E, Tonino PAL, Piroth Z, et al. Fractional Flow Reserve–Guided PCI versus Medical Therapy in Stable Coronary Disease. New England Journal of Medicine. 2012 Sep 13;367(11):991–1001.

16. Bech GJ, De Bruyne B, Bonnier HJ, Bartunek J, Wijns W, Peels K, et al. Long-term follow-up after deferral of percutaneous transluminal coronary angioplasty of intermediate stenosis on the basis of coronary pressure measurement. J Am Coll Cardiol. 1998 Mar 15;31(4):841–7.

17. Rieber J, Jung P, Schiele TM, Koenig A, Erhard I, Segmiller T, et al. Safety of FFR-based treatment strategies: the Munich experience. Z Kardiol. 2002;91 Suppl 3:115–9.

18. Einstein AJ. Radiation risk from coronary artery disease imaging: how do different diagnostic tests compare? Heart. 2008 Dec;94(12):1519–21.

19. Arora N, Matheny ME, Sepke C, Resnic FS. A propensity analysis of the risk of vascular complications after cardiac catheterization procedures with the use of vascular closure devices. Am Heart J. 2007 Apr;153(4):606–11.

20. Al-Lamee R, Thompson D, Dehbi HM, Sen S, Tang K, Davies J, et al. Percutaneous coronary intervention in stable angina (ORBITA): a double-blind, randomised controlled trial. Lancet. 2018 06;391(10115):31–40.

21. Vermeltfoort I a. C, Raijmakers PGHM, Odekerken D a. M, Kuijper AFM, Zwijnenburg A, Teule GJJ. Association between anxiety disorder and the extent of ischemia observed in cardiac syndrome X. J Nucl Cardiol. 2009 Jun;16(3):405–10.

22. Ford TJ, Stanley B, Good R, Rocchiccioli P, McEntegart M, Watkins S, et al. Stratified Medical Therapy Using Invasive Coronary Function Testing in Angina: The CorMicA Trial. J Am Coll Cardiol. 2018 11;72(23 Pt A):2841–55.

23. Fihn SD, Gardin JM, Abrams J, Berra K, Blankenship JC, Dallas AP, et al. 2012 ACCF/AHA/ACP/AATS/PCNA/SCAI/STS guideline for the diagnosis and management of patients with stable ischemic heart disease: a report of the American College of Cardiology Foundation/American Heart Association task force on practice guidelines, and the American College of Physicians, American Association for Thoracic Surgery, Preventive Cardiovascular Nurses Association, Society for Cardiovascular Angiography and

Interventions, and Society of Thoracic Surgeons. Circulation. 2012 Dec 18;126(25):e354-471.

24. National Institute for Health and Clinical Excellence (2016) Chest pain of recent onset: assessment and diagnosis. NICE guideline (CG95).

25. Fintel DJ, Links JM, Brinker JA, Frank TL, Parker M, Becker LC. Improved diagnostic performance of exercise thallium-201 single photon emission computed tomography over planar imaging in the diagnosis of coronary artery disease: a receiver operating characteristic analysis. J Am Coll Cardiol. 1989 Mar 1;13(3):600–12.

26. Greenwood JP, Maredia N, Younger JF, Brown JM, Nixon J, Everett CC, et al. Cardiovascular magnetic resonance and single-photon emission computed tomography for diagnosis of coronary heart disease (CE-MARC): a prospective trial. Lancet. 2012 Feb 4;379(9814):453–60.

27. Nakazato R, Berman DS, Dey D, Le Meunier L, Hayes SW, Fermin JS, et al. Automated quantitative Rb-82 3D PET/CT myocardial perfusion imaging: normal limits and correlation with invasive coronary angiography. J Nucl Cardiol. 2012 Apr;19(2):265–76.

28. Schwitter J, Wacker CM, Wilke N, Al-Saadi N, Sauer E, Huettle K, et al. MR-IMPACT II: Magnetic Resonance Imaging for Myocardial Perfusion Assessment in Coronary artery disease Trial: perfusion-cardiac magnetic resonance vs. single-photon emission computed tomography for the detection of coronary artery disease: a comparative multicentre, multivendor trial. Eur Heart J. 2013 Mar;34(10):775–81.

29. Loimaala A, Groundstroem K, Pasanen M, Oja P, Vuori I. Comparison of bicycle, heavy isometric, dipyridamole-atropine and dobutamine stress echocardiography for diagnosis of myocardial ischemia. Am J Cardiol. 1999 Dec 15;84(12):1396–400.

30. Shaw LJ, Berman DS, Maron DJ, Mancini GBJ, Hayes SW, Hartigan PM, et al. Optimal medical therapy with or without percutaneous coronary intervention to reduce ischemic burden: results from the Clinical Outcomes Utilizing Revascularization and Aggressive Drug Evaluation (COURAGE) trial nuclear substudy. Circulation. 2008 Mar 11;117(10):1283–91.

31. Patel MR, Peterson ED, Dai D, Brennan JM, Redberg RF, Anderson HV, et al. Low Diagnostic Yield of Elective Coronary Angiography. New England Journal of Medicine. 2010 Mar 11;362(10):886–95.

32. Safavi KC, Li SX, Dharmarajan K, Venkatesh AK, Strait KM, Lin H, et al. Hospital Variation in the Use of Noninvasive Cardiac Imaging and Its Association With Downstream Testing, Interventions, and Outcomes. JAMA Intern Med. 2014 Apr 1;174(4):546–53.

33. Atkinson DJ, Burstein D, Edelman RR. First-pass cardiac perfusion: evaluation with ultrafast MR imaging. Radiology. 1990 Mar;174(3 Pt 1):757–62.

34. Al-Saadi N, Nagel E, Gross M, Bornstedt A, Schnackenburg B, Klein C, et al. Noninvasive detection of myocardial ischemia from perfusion reserve based on cardiovascular magnetic resonance. Circulation. 2000 Mar 28;101(12):1379–83.

35. Hamon M, Fau G, Née G, Ehtisham J, Morello R, Hamon M. Meta-analysis of the diagnostic performance of stress perfusion cardiovascular magnetic resonance for detection of coronary artery disease. J Cardiovasc Magn Reson. 2010 May 19;12(1):29.

36. Rieber J, Huber A, Erhard I, Mueller S, Schweyer M, Koenig A, et al. Cardiac magnetic resonance perfusion imaging for the functional assessment of coronary artery disease: a comparison with coronary angiography and fractional flow reserve. European Heart Journal. 2006 Jun 1;27(12):1465–71.

37. Ebersberger U, Makowski MR, Schoepf UJ, Platz U, Schmidtler F, Rose J, et al. Magnetic resonance myocardial perfusion imaging at 3.0 Tesla for the identification of myocardial ischaemia: comparison with coronary catheter angiography and fractional flow reserve measurements. European Heart Journal - Cardiovascular Imaging. 2013 Dec 1;14(12):1174–80.

38. Nandalur KR, Dwamena BA, Choudhri AF, Nandalur MR, Carlos RC. Diagnostic performance of stress cardiac magnetic resonance imaging in the detection of coronary artery disease: a meta-analysis. J Am Coll Cardiol. 2007 Oct 2;50(14):1343–53.

39. Li M, Zhou T, Yang L feng, Peng Z hui, Ding J, Sun G. Diagnostic Accuracy of Myocardial Magnetic Resonance Perfusion to Diagnose Ischemic Stenosis With Fractional Flow Reserve as Reference: Systematic Review and Meta-Analysis. JACC: Cardiovascular Imaging. 2014 Nov;7(11):1098–105.

40. Ingkanisorn WP, Kwong RY, Bohme NS, Geller NL, Rhoads KL, Dyke CK, et al. Prognosis of negative adenosine stress magnetic resonance in patients presenting to an emergency department with chest pain. J Am Coll Cardiol. 2006 Apr 4;47(7):1427–32.

41. Jahnke C, Nagel E, Gebker R, Kokocinski T, Kelle S, Manka R, et al. Prognostic Value of Cardiac Magnetic Resonance Stress Tests Adenosine Stress Perfusion and Dobutamine Stress Wall Motion Imaging. Circulation. 2007 Apr 3;115(13):1769–76.

42. Greenwood JP, Herzog BA, Brown JM, Everett CC, Nixon J, Bijsterveld P, et al. Prognostic Value of Cardiovascular Magnetic Resonance and Single-Photon Emission Computed Tomography in Suspected Coronary Heart Disease: Long-Term Follow-up of a Prospective, Diagnostic Accuracy Cohort Study. Ann Intern Med. 2016 May 10;

43. Nagel E, Greenwood JP, McCann GP, Bettencourt N, Shah AM, Hussain ST, et al. Magnetic Resonance Perfusion or Fractional Flow Reserve in Coronary Disease. N Engl J Med. 2019 20;380(25):2418–28.

44. Kwong RY, Ge Y, Steel K, Bingham S, Abdullah S, Fujikura K, et al. Cardiac Magnetic Resonance Stress Perfusion Imaging for Evaluation of Patients With Chest Pain. J Am Coll Cardiol. 2019 Oct 8;74(14):1741–55.

45. Wahl A, Paetsch I, Roethemeyer S, Klein C, Fleck E, Nagel E. High-dose dobutamine-atropine stress cardiovascular MR imaging after coronary revascularization in patients with wall motion abnormalities at rest. Radiology. 2004 Oct;233(1):210–6.

46. Bodi V, Sanchis J, Nunez J, Mainar L, Lopez-Lereu MP, Monmeneu JV, et al. Prognostic value of a comprehensive cardiac magnetic resonance assessment soon after a first ST-segment elevation myocardial infarction. JACC Cardiovasc Imaging. 2009 Jul;2(7):835–42.

47. Bruder O, Wagner A, Lombardi M, Schwitter J, van Rossum A, Pilz G, et al. European Cardiovascular Magnetic Resonance (EuroCMR) registry--multi national results from 57 centers in 15 countries. J Cardiovasc Magn Reson. 2013;15:9.

48. Kramer CM, Barkhausen J, Flamm SD, Kim RJ, Nagel E, Society for Cardiovascular Magnetic Resonance Board of Trustees Task Force on Standardized Protocols. Standardized cardiovascular magnetic resonance (CMR) protocols 2013 update. J Cardiovasc Magn Reson. 2013 Oct 8;15:91.

49. Cerqueira MD, Weissman NJ, Dilsizian V, Jacobs AK, Kaul S, Laskey WK, et al. Standardized myocardial segmentation and nomenclature for tomographic imaging of the heart. A statement for healthcare professionals from the Cardiac Imaging Committee of the Council on Clinical Cardiology of the American Heart Association. Circulation. 2002 Jan 29;105(4):539–42.

50. Villa ADM, Corsinovi L, Ntalas I, Milidonis X, Scannell C, Di Giovine G, et al. Importance of operator training and rest perfusion on the diagnostic accuracy of stress perfusion cardiovascular magnetic resonance. J Cardiovasc Magn Reson. 2018 Nov 19;20(1):74.

51. Schwitter J, Nanz D, Kneifel S, Bertschinger K, Büchi M, Knüsel PR, et al. Assessment of myocardial perfusion in coronary artery disease by magnetic resonance: a comparison with positron emission tomography and coronary angiography. Circulation. 2001 May 8;103(18):2230–5.

52. Klem I, Heitner JF, Shah DJ, Sketch MH, Behar V, Weinsaft J, et al. Improved detection of coronary artery disease by stress perfusion cardiovascular magnetic resonance with the use of delayed enhancement infarction imaging. J Am Coll Cardiol. 2006 Apr 18;47(8):1630–8.

53. Wolff SD, Schwitter J, Coulden R, Friedrich MG, Bluemke DA, Biederman RW, et al. Myocardial first-pass perfusion magnetic resonance imaging: a multicenter dose-ranging study. Circulation. 2004 Aug 10;110(6):732–7.

54. Giang TH, Nanz D, Coulden R, Friedrich M, Graves M, Al-Saadi N, et al. Detection of coronary artery disease by magnetic resonance myocardial perfusion imaging with various contrast medium doses: first European multi-centre experience. Eur Heart J. 2004 Sep;25(18):1657–65.

55. Sakuma H, Suzawa N, Ichikawa Y, Makino K, Hirano T, Kitagawa K, et al. Diagnostic Accuracy of Stress First-Pass Contrast-Enhanced Myocardial Perfusion MRI Compared with Stress Myocardial Perfusion Scintigraphy. American Journal of Roentgenology. 2005 Jul 1;185(1):95–102.

56. Ishida N, Sakuma H, Motoyasu M, Okinaka T, Isaka N, Nakano T, et al. Noninfarcted myocardium: correlation between dynamic first-pass contrast-enhanced myocardial MR imaging and quantitative coronary angiography. Radiology. 2003 Oct;229(1):209–16.

57. Flotats A, Bengel FM, Knuuti J, Guludec DL, Marcassa C. CMR versus SPECT for diagnosis of coronary heart disease. The Lancet. 2012 Jun 9;379(9832):2145.

58. Underwood R, Harbinson M, Kelion A, Sabharwal N. CMR versus SPECT for diagnosis of coronary heart disease. The Lancet. 2012 Jun 9;379(9832):2146.

59. Mohiuddin SM, Ravage CK, Esterbrooks DJ, Lucas BD, Hilleman DE. The comparative safety and diagnostic accuracy of adenosine myocardial perfusion imaging in women versus men. Pharmacotherapy. 1996 Aug;16(4):646–51.

60. Schwitter J, Wacker CM, Rossum AC van, Lombardi M, Al-Saadi N, Ahlstrom H, et al. MR-IMPACT: comparison of perfusion-cardiac magnetic resonance with single-photon emission computed tomography for the detection of coronary artery disease in a multicentre, multivendor, randomized trial. European Heart Journal. 2008 Feb 1;29(4):480–9.

61. Plein S, Greenwood JP, Ridgway JP, Cranny G, Ball SG, Sivananthan MU. Assessment of non-ST-segment elevation acute coronary syndromes with cardiac magnetic resonance imaging. J Am Coll Cardiol. 2004 Dec 7;44(11):2173–81.

62. Cury RC, Cattani CAM, Gabure LAG, Racy DJ, de Gois JM, Siebert U, et al. Diagnostic performance of stress perfusion and delayed-enhancement MR imaging in patients with coronary artery disease. Radiology. 2006 Jul;240(1):39–45.

63. Mishra RK, Dorbala S, Logsetty G, Hassan A, Heinonen T, Schelbert HR, et al. Quantitative relation between hemodynamic changes during intravenous adenosine infusion and the magnitude of coronary hyperemia. Journal of the American College of Cardiology. 2005 Feb 15;45(4):553–8.

64. Reyes E, Stirrup J, Roughton M, D'Souza S, Underwood SR, Anagnostopoulos C. Attenuation of Adenosine-Induced Myocardial Perfusion Heterogeneity by Atenolol and Other Cardioselective β-Adrenoceptor Blockers: A Crossover Myocardial Perfusion Imaging Study. J Nucl Med. 2010 Jul 1;51(7):1036–43.

65. Sharir T, Rabinowitz B, Livschitz S, Moalem I, Baron J, Kaplinsky E, et al. Underestimation of Extent and Severity of Coronary Artery Disease by Dipyridamole Stress Thallium-201 Single-Photon Emission Computed Tomographic Myocardial Perfusion Imaging in Patients Taking Antianginal Drugs. Journal of the American College of Cardiology. 1998 Jun 1;31(7):1540–6.

66. Manisty C, Ripley DP, Herrey AS, Captur G, Wong TC, Petersen SE, et al. Splenic Switch-off: A Tool to Assess Stress Adequacy in Adenosine Perfusion Cardiac MR Imaging. Radiology. 2015 Sep;276(3):732–40.

67. Iskandrian AS, Heo J, Kong B, Lyons E. Effect of exercise level on the ability of thallium-201 tomographic imaging in detecting coronary artery disease: analysis of 461 patients. J Am Coll Cardiol. 1989 Nov 15;14(6):1477–86.

68. Maddahi J, Van Train K, Prigent F, Garcia EV, Friedman J, Ostrzega E, et al. Quantitative single photon emission computed thallium-201 tomography for detection and localization of coronary artery disease: optimization and prospective validation of a new technique. J Am Coll Cardiol. 1989 Dec;14(7):1689–99.

69. Grover-McKay M, Milne N, Atwood JE, Lyons KP. Comparison of thallium-201 single-photon emission computed tomographic scintigraphy with intravenous dipyridamole and arm exercise. Am Heart J. 1994 Jun;127(6):1516–20.

70. Nguyen T, Heo J, Ogilby JD, Iskandrian AS. Single photon emission computed tomography with thallium-201 during adenosine-induced coronary hyperemia: correlation with coronary arteriography, exercise thallium imaging and two-dimensional echocardiography. J Am Coll Cardiol. 1990 Nov;16(6):1375–83.

71. Marwick T, Willemart B, D'Hondt AM, Baudhuin T, Wijns W, Detry JM, et al. Selection of the optimal nonexercise stress for the evaluation of ischemic regional myocardial dysfunction and malperfusion. Comparison of dobutamine and adenosine using echocardiography and 99mTc-MIBI single photon emission computed tomography. Circulation. 1993 Feb;87(2):345–54.

72. Pennell DJ, Mavrogeni SI, Forbat SM, Karwatowski SP, Underwood SR. Adenosine combined with dynamic exercise for myocardial perfusion imaging. Journal of the American College of Cardiology. 1995 May 1;25(6):1300–9.

73. Kapur A, Latus KA, Davies G, Dhawan RT, Eastick S, Jarritt PH, et al. A comparison of three radionuclide myocardial perfusion tracers in clinical practice: the ROBUST study. Eur J Nucl Med Mol Imaging. 2002 Dec;29(12):1608–16.

74. Greenwood JP, Brown JM, Dickinson CJ, Ball SG, Plein S. CMR versus SPECT for diagnosis of coronary heart disease – Authors' reply. The Lancet. 2012 Jun 9;379(9832):2147–8.

75. Miller TD, Hodge DO, Christian TF, Milavetz JJ, Bailey KR, Gibbons RJ. Effects of adjustment for referral bias on the sensitivity and specificity of single photon emission computed tomography for the diagnosis of coronary artery disease. The American Journal of Medicine. 2002 Mar 1;112(4):290–7.

76. Verberne HJ, Acampa W, Anagnostopoulos C, Ballinger J, Bengel F, De Bondt P, et al. EANM procedural guidelines for radionuclide myocardial perfusion imaging with SPECT and SPECT/CT: 2015 revision. Eur J Nucl Med Mol Imaging. 2015;42(12):1929–40.

77. Senior R, Lahiri A. Enhanced detection of myocardial ischemia by stress dobutamine echocardiography utilizing the "biphasic" response of wall thickening during low and high dose dobutamine infusion. Journal of the American College of Cardiology. 1995 Jul 1;26(1):26–32.

78. Arnese M, Fioretti PM, Cornel JH, Postma-Tjoa J, Reijs AEM, Roelandt JRTC. Akinesis becoming dyskinesis during high-dose dobutamine stress echocardiography: A marker of myocardial ischemia or a mechanical phenomenon? The American Journal of Cardiology. 1994 May 1;73(12):896–9.

79. Armstrong WF, Pellikka PA, Ryan T, Crouse L, Zoghbi WA. Stress echocardiography: recommendations for performance and interpretation of stress echocardiography. Stress Echocardiography Task Force of the Nomenclature and Standards Committee of the American Society of Echocardiography. J Am Soc Echocardiogr. 1998 Jan;11(1):97–104.

80. Sicari R, Nihoyannopoulos P, Evangelista A, Kasprzak J, Lancellotti P, Poldermans D, et al. Stress Echocardiography Expert Consensus Statement—Executive SummaryEuropean Association of Echocardiography (EAE) (a registered branch of the ESC). Eur Heart J. 2009 Feb 1;30(3):278–89.

81. Marwick TH, Nemec JJ, Pashkow FJ, Stewart WJ, Salcedo EE. Accuracy and limitations of exercise echocardiography in a routine clinical setting. J Am Coll Cardiol. 1992 Jan;19(1):74–81.

82. Moir S, Haluska BA, Jenkins C, Fathi R, Marwick TH. Incremental benefit of myocardial contrast to combined dipyridamole-exercise stress echocardiography for the assessment of coronary artery disease. Circulation. 2004 Aug 31;110(9):1108–13.

83. Beleslin BD, Ostojic M, Stepanovic J, Djordjevic-Dikic A, Stojkovic S, Nedeljkovic M, et al. Stress echocardiography in the detection of myocardial ischemia. Head-to-head comparison of exercise, dobutamine, and dipyridamole tests. Circulation. 1994 Sep;90(3):1168–76.

84. Dagianti A, Penco M, Agati L, Sciomer S, Dagianti A, Rosanio S, et al. Stress echocardiography: Comparison of exercise, dipyridamole and dobutamine in detecting and predicting the extent of coronary artery disease. Journal of the American College of Cardiology. 1995 Jul 1;26(1):18–25.

85. Schröder K, Völler H, Dingerkus H, Münzberg H, Dissmann R, Linderer T, et al. Comparison of the diagnostic potential of four echocardiographic stress tests shortly after acute myocardial infarction: submaximal exercise, transesophageal atrial pacing, dipyridamole, and dobutamine-atropine. Am J Cardiol. 1996 May 1;77(11):909–14.

86. Armstrong WF, O'Donnell J, Ryan T, Feigenbaum H. Effect of prior myocardial infarction and extent and location of coronary disease on accuracy of exercise echocardiography. J Am Coll Cardiol. 1987 Sep;10(3):531–8.

87. Crouse LJ, Harbrecht JJ, Vacek JL, Rosamond TL, Kramer PH. Exercise echocardiography as a screening test for coronary artery disease and correlation with coronary arteriography. Am J Cardiol. 1991 Jun 1;67(15):1213–8.

88. Quiñones MA, Verani MS, Haichin RM, Mahmarian JJ, Suarez J, Zoghbi WA. Exercise echocardiography versus 201Tl single-photon emission computed tomography in evaluation of coronary artery disease. Analysis of 292 patients. Circulation. 1992 Mar;85(3):1026–31.

89. Perrone-Filardi P, Pace L, Prastaro M, Squame F, Betocchi S, Soricelli A, et al. Assessment of Myocardial Viability in Patients With Chronic Coronary Artery Disease: Rest–4-Hour–24-Hour 201Tl Tomography Versus Dobutamine Echocardiography. Circulation. 1996 Dec 1;94(11):2712–9.

90. Arnese M, Cornel JH, Salustri A, Maat APWM, Elhendy A, Reijs AEM, et al. Prediction of Improvement of Regional Left Ventricular Function After Surgical Revascularization: A Comparison of Low-Dose Dobutamine Echocardiography With 201Tl Single-Photon Emission Computed Tomography. Circulation. 1995 Jun 1;91(11):2748–52.

91. Tillisch J, Brunken R, Marshall R, Schwaiger M, Mandelkern M, Phelps M, et al. Reversibility of cardiac wall-motion abnormalities predicted by positron tomography. N Engl J Med. 1986 Apr 3;314(14):884–8.

92. Botsch H, Beringer K, Petersen J, Bauer B, Weidemann H. Single-photon emission tomography studies of rubidium-81 in the detection of ischaemic heart disease, using a stress-reinjection protocol. Eur J Nucl Med. 1994 May;21(5):407–14.

93. Bateman TM, Heller GV, McGhie AI, Friedman JD, Case JA, Bryngelson JR, et al. Diagnostic accuracy of rest/stress ECG-gated Rb-82 myocardial perfusion PET: comparison with ECG-gated Tc-99m sestamibi SPECT. J Nucl Cardiol. 2006 Feb;13(1):24–33.

94. Herzog BA, Husmann L, Valenta I, Gaemperli O, Siegrist PT, Tay FM, et al. Long-term prognostic value of 13N-ammonia myocardial perfusion positron emission tomography added value of coronary flow reserve. J Am Coll Cardiol. 2009 Jul 7;54(2):150–6.

95. Murthy VL, Naya M, Foster CR, Hainer J, Gaber M, Carli GD, et al. Improved Cardiac Risk Assessment With Noninvasive Measures of Coronary Flow ReserveClinical Perspective. Circulation. 2011 Nov 15;124(20):2215–24.

96. Patel KK, Spertus JA, Chan PS, Sperry BW, Al Badarin F, Kennedy KF, et al. Myocardial blood flow reserve assessed by positron emission tomography myocardial perfusion imaging identifies patients with a survival benefit from early revascularization. Eur Heart J. 2019 Jun 22;

97. Beyer T, Townsend DW, Brun T, Kinahan PE, Charron M, Roddy R, et al. A combined PET/CT scanner for clinical oncology. J Nucl Med. 2000 Aug;41(8):1369–79.

98. Sciagrà R. Quantitative cardiac positron emission tomography: the time is coming! Scientifica (Cairo). 2012;2012:948653.

99. Juarez-Orozco LE, Cruz-Mendoza JR, Guinto-Nishimura GY, Walls-Laguarda L, Casares-Echeverría LJ, Meave-Gonzalez A, et al. PET myocardial perfusion quantification: anatomy of a spreading functional technique. Clin Transl Imaging. 2018 Feb 1;6(1):47–60.

100. Kaufmann PA, Camici PG. Myocardial blood flow measurement by PET: technical aspects and clinical applications. J Nucl Med. 2005 Jan;46(1):75–88.

101. Monroy-Gonzalez AG, Juarez-Orozco LE, Han C, Vedder IR, García DV, Borra R, et al. Software reproducibility of myocardial blood flow and flow reserve quantification in ischemic heart disease: A 13N-ammonia PET study. J Nucl Cardiol. 2019 Mar 22;

102. Khorsand A, Graf S, Pirich C, Muzik O, Kletter K, Dudczak R, et al. Assessment of myocardial perfusion by dynamic N-13 ammonia PET imaging: comparison of 2 tracer kinetic models. J Nucl Cardiol. 2005 Aug;12(4):410–7.

103. Nesterov SV, Deshayes E, Sciagrà R, Settimo L, Declerck JM, Pan XB, et al. Quantification of Myocardial Blood Flow in Absolute Terms Using 82Rb PET Imaging: The RUBY-10 Study. JACC: Cardiovascular Imaging. 2014 Nov 1;7(11):1119–27.

104. Detrano R, Hsiai T, Wang S, Puentes G, Fallavollita J, Shields P, et al. Prognostic value of coronary calcification and angiographic stenoses in patients undergoing coronary angiography. J Am Coll Cardiol. 1996 Feb;27(2):285–90.

105. Keelan PC, Bielak LF, Ashai K, Jamjoum LS, Denktas AE, Rumberger JA, et al. Long-term prognostic value of coronary calcification detected by electron-beam computed tomography in patients undergoing coronary angiography. Circulation. 2001 Jul 24;104(4):412–7.

106. Shaw LJ, Raggi P, Schisterman E, Berman DS, Callister TQ. Prognostic value of cardiac risk factors and coronary artery calcium screening for all-cause mortality. Radiology. 2003 Sep;228(3):826–33.

107. van Waardhuizen CN, Langhout M, Ly F, Braun L, Genders TSS, Petersen SE, et al. Diagnostic performance and comparative cost-effectiveness of non-invasive imaging tests in patients presenting with chronic stable chest pain with suspected coronary artery disease: a systematic overview. Curr Cardiol Rep. 2014;16(10):537.

108. Waardhuizen V, N C, Khanji MY, Genders TSS, Ferket BS, Fleischmann KE, et al. Comparative cost-effectiveness of non-invasive imaging tests in patients presenting with chronic stable chest pain with suspected coronary artery disease: a systematic review. Eur Heart J Qual Care Clin Outcomes. 2016 Oct 1;2(4):245–60.

109. Montalescot G, Achenbach S, Andreotti F, Arden C, Budaj A, Bugiardini R, et al. 2013 ESC guidelines on the management of stable coronary artery disease. European Heart Journal. 2013 Oct 7;34(38):2949–3003.

110. Mowatt G, Cook JA, Hillis GS, Walker S, Fraser C, Jia X, et al. 64-Slice computed tomography angiography in the diagnosis and assessment of coronary artery disease: systematic review and meta-analysis. Heart. 2008 Nov 1;94(11):1386–93.

111. von Ballmoos MW, Haring B, Juillerat P, Alkadhi H. Meta-analysis: diagnostic performance of low-radiation-dose coronary computed tomography angiography. Ann Intern Med. 2011 Mar 15;154(6):413–20.

112. Vorre MM, Abdulla J. Diagnostic accuracy and radiation dose of CT coronary angiography in atrial fibrillation: systematic review and meta-analysis. Radiology. 2013 May;267(2):376–86.

113. Nørgaard BL, Leipsic J, Gaur S, Seneviratne S, Ko BS, Ito H, et al. Diagnostic performance of noninvasive fractional flow reserve derived from coronary computed tomography angiography in suspected coronary artery disease: the NXT trial (Analysis of Coronary Blood Flow Using CT Angiography: Next Steps). J Am Coll Cardiol. 2014 Apr 1;63(12):1145–55.

114. Neglia D, Rovai D, Caselli C, Pietila M, Teresinska A, Aguadé-Bruix S, et al. Detection of significant coronary artery disease by noninvasive anatomical and functional imaging. Circ Cardiovasc Imaging. 2015 Mar;8(3).

115. Douglas PS, Hoffmann U, Patel MR, Mark DB, Al-Khalidi HR, Cavanaugh B, et al. Outcomes of Anatomical versus Functional Testing for Coronary Artery Disease. New England Journal of Medicine. 2015 Apr 2;372(14):1291–300.

116. Colleran R, Douglas PS, Hadamitzky M, Gutberlet M, Lehmkuhl L, Foldyna B, et al. An FFRCT diagnostic strategy versus usual care in patients with suspected coronary artery disease planned for invasive coronary angiography at German sites: one-year results of a subgroup analysis of the PLATFORM (Prospective Longitudinal Trial of FFRCT: Outcome and Resource Impacts) study. Open Heart. 2017;4(1):e000526.

117. Lubbers M, Coenen A, Kofflard M, Bruning T, Kietselaer B, Galema T, et al. Comprehensive Cardiac CT With Myocardial Perfusion Imaging Versus Functional Testing in Suspected Coronary Artery Disease: The Multicenter, Randomized CRESCENT-II Trial. JACC Cardiovasc Imaging. 2018 Nov;11(11):1625–36.

118. Celeng C, Leiner T, Maurovich-Horvat P, Merkely B, de Jong P, Dankbaar JW, et al. Anatomical and Functional Computed Tomography for Diagnosing Hemodynamically Significant Coronary Artery Disease: A Meta-Analysis. JACC Cardiovasc Imaging. 2019 Jul;12(7 Pt 2):1316–25.

119. Ng ACT, Sitges M, Pham PN, Tran DT, Delgado V, Bertini M, et al. Incremental value of 2-dimensional speckle tracking strain imaging to wall motion analysis for detection of coronary artery disease in patients undergoing dobutamine stress echocardiography. Am Heart J. 2009 Nov;158(5):836–44.

120. Nekolla SG, Reder S, Saraste A, Higuchi T, Dzewas G, Preissel A, et al. Evaluation of the novel myocardial perfusion positron-emission tomography tracer 18F-BMS-747158-02: comparison to 13N-ammonia and validation with microspheres in a pig model. Circulation. 2009 May 5;119(17):2333–42.

121. SCOT-HEART Investigators, Newby DE, Adamson PD, Berry C, Boon NA, Dweck MR, et al. Coronary CT Angiography and 5-Year Risk of Myocardial Infarction. N Engl J Med. 2018 06;379(10):924–33.

122. Williams MC, Hunter A, Shah A, Assi V, Lewis S, Mangion K, et al. Symptoms and quality of life in patients with suspected angina undergoing CT coronary angiography: a randomised controlled trial. Heart. 2017 Jul 1;103(13):995.

123. Gould KL. PET perfusion imaging and nuclear cardiology. J Nucl Med. 1991 Apr;32(4):579–606.

124. Kajander SA, Joutsiniemi E, Saraste M, Pietilä M, Ukkonen H, Saraste A, et al. Clinical Value of Absolute Quantification of Myocardial Perfusion With 15O-Water in Coronary Artery Disease. Circ Cardiovasc Imaging. 2011 Nov 1;4(6):678–84.

125. Parkash R, deKemp RA, Ruddy TD, Kitsikis A, Hart R, Beauschene L, et al. Potential utility of rubidium 82 PET quantification in patients with 3-vessel coronary artery disease. Journal of Nuclear Cardiology. 2004 Jul;11(4):440–9.

126. Patel AR, Antkowiak PF, Nandalur KR, West AM, Salerno M, Arora V, et al. Assessment of advanced coronary artery disease: advantages of quantitative cardiac magnetic resonance perfusion analysis. J Am Coll Cardiol. 2010 Aug 10;56(7):561–9.

127. Neglia D, Michelassi C, Trivieri MG, Sambuceti G, Giorgetti A, Pratali L, et al. Prognostic role of myocardial blood flow impairment in idiopathic left ventricular dysfunction. Circulation. 2002 Jan 15;105(2):186–93.

128. Maron BJ, Wolfson JK, Epstein SE, Roberts WC. Intramural ("small vessel") coronary artery disease in hypertrophic cardiomyopathy. J Am Coll Cardiol. 1986 Sep;8(3):545–57.

129. Basso C, Thiene G, Corrado D, Buja G, Melacini P, Nava A. Hypertrophic cardiomyopathy and sudden death in the young: pathologic evidence of myocardial ischemia. Hum Pathol. 2000 Aug;31(8):988–98.

130. Dilsizian V, Bonow RO, Epstein SE, Fananapazir L. Myocardial ischemia detected by thallium scintigraphy is frequently related to cardiac arrest and syncope in young patients with hypertrophic cardiomyopathy. J Am Coll Cardiol. 1993 Sep;22(3):796–804.

131. Petersen SE, Jerosch-Herold M, Hudsmith LE, Robson MD, Francis JM, Doll HA, et al. Evidence for microvascular dysfunction in hypertrophic cardiomyopathy: new insights from multiparametric magnetic resonance imaging. Circulation. 2007 May 8;115(18):2418–25.

132. Cecchi F, Olivotto I, Gistri R, Lorenzoni R, Chiriatti G, Camici PG. Coronary microvascular dysfunction and prognosis in hypertrophic cardiomyopathy. N Engl J Med. 2003 Sep 11;349(11):1027–35.

133. Zarate YA, Hopkin RJ. Fabry's disease. Lancet. 2008 Oct 18;372(9647):1427–35.

134. Nordin S, Kozor R, Bulluck H, Castelletti S, Rosmini S, Abdel-Gadir A, et al. Cardiac Fabry Disease With Late Gadolinium Enhancement Is a Chronic Inflammatory Cardiomyopathy. J Am Coll Cardiol. 2016 11;68(15):1707–8.

135. Nordin S, Kozor R, Medina-Menacho K, Abdel-Gadir A, Baig S, Sado DM, et al. Proposed Stages of Myocardial Phenotype Development in Fabry Disease. JACC Cardiovasc Imaging. 2018 May 11;

136. Elliott PM, Kindler H, Shah JS, Sachdev B, Rimoldi OE, Thaman R, et al. Coronary microvascular dysfunction in male patients with Anderson-Fabry disease and the effect of treatment with alpha galactosidase A. Heart. 2006 Mar;92(3):357–60.

137. Christian TF, Rettmann DW, Aletras AH, Liao SL, Taylor JL, Balaban RS, et al. Absolute Myocardial Perfusion in Canines Measured by Using Dual-Bolus First-Pass MR Imaging. Radiology. 2004 Sep 1;232(3):677–84.

138. Klocke FJ, Simonetti OP, Judd RM, Kim RJ, Harris KR, Hedjbeli S, et al. Limits of detection of regional differences in vasodilated flow in viable myocardium by first-pass magnetic resonance perfusion imaging. Circulation. 2001 Nov 13;104(20):2412–6.

139. Mordini FE, Haddad T, Hsu LY, Kellman P, Lowrey TB, Aletras AH, et al. Diagnostic accuracy of stress perfusion CMR in comparison with quantitative coronary angiography: fully quantitative, semiquantitative, and qualitative assessment. JACC Cardiovasc Imaging. 2014 Jan;7(1):14–22.

140. Jerosch-Herold M, Wilke N, Stillman AE. Magnetic resonance quantification of the myocardial perfusion reserve with a Fermi function model for constrained deconvolution. Med Phys. 1998 Jan;25(1):73–84.

141. Neimatallah MA, Chenevert TL, Carlos RC, Londy FJ, Dong Q, Prince MR, et al. Subclavian MR arteriography: reduction of susceptibility artifact with short echo time and dilute gadopentetate dimeglumine. Radiology. 2000 Nov;217(2):581–6.

142. Christian TF, Aletras AH, Arai AE. Estimation of absolute myocardial blood flow during first-pass MR perfusion imaging using a dual-bolus injection technique: comparison to single-bolus injection method. J Magn Reson Imaging. 2008 Jun;27(6):1271–7.

143. Gatehouse PD, Elkington AG, Ablitt NA, Yang GZ, Pennell DJ, Firmin DN. Accurate assessment of the arterial input function during high-dose myocardial perfusion cardiovascular magnetic resonance. J Magn Reson Imaging. 2004 Jul;20(1):39–45.

144. Biglands JD, Magee DR, Sourbron SP, Plein S, Greenwood JP, Radjenovic A. Comparison of the Diagnostic Performance of Four Quantitative Myocardial Perfusion Estimation Methods Used in Cardiac MR Imaging: CE-MARC Substudy. Radiology. 2015 May;275(2):393–402.

145. Miller CA, Naish JH, Ainslie MP, Tonge C, Tout D, Arumugam P, et al. Voxel-wise quantification of myocardial blood flow with cardiovascular magnetic resonance: effect of variations in methodology and validation with positron emission tomography. Journal of Cardiovascular Magnetic Resonance. 2014 Jan 24;16(1):11.

146. van Dijk R, van Assen M, Vliegenthart R, de Bock GH, van der Harst P, Oudkerk M. Diagnostic performance of semi-quantitative and quantitative stress CMR perfusion analysis: a meta-analysis. J Cardiovasc Magn Reson. 2017 Nov 27;19(1):92.

147. Costa MA, Shoemaker S, Futamatsu H, Klassen C, Angiolillo DJ, Nguyen M, et al. Quantitative magnetic resonance perfusion imaging detects anatomic and physiologic coronary artery disease as measured by coronary angiography and fractional flow reserve. J Am Coll Cardiol. 2007 Aug 7;50(6):514–22.

148. Lockie T, Ishida M, Perera D, Chiribiri A, De Silva K, Kozerke S, et al. High-resolution magnetic resonance myocardial perfusion imaging at 3.0-Tesla to detect hemodynamically significant coronary stenoses as determined by fractional flow reserve. J Am Coll Cardiol. 2011 Jan 4;57(1):70–5.

149. Morton G, Chiribiri A, Ishida M, Hussain ST, Schuster A, Indermuehle A, et al. Quantification of Absolute Myocardial Perfusion in Patients With Coronary Artery Disease: Comparison Between Cardiovascular Magnetic Resonance and Positron Emission Tomography. Journal of the American College of Cardiology. 2012 Oct 16;60(16):1546–55.

150. Engblom H, Xue H, Akil S, Carlsson M, Hindorf C, Oddstig J, et al. Fully quantitative cardiovascular magnetic resonance myocardial perfusion ready for clinical use: a comparison between cardiovascular magnetic resonance imaging and positron emission tomography. Journal of Cardiovascular Magnetic Resonance. 2017 Oct 19;19:78.

151. Messroghli DR, Moon JC, Ferreira VM, Grosse-Wortmann L, He T, Kellman P, et al. Clinical recommendations for cardiovascular magnetic resonance mapping of T1, T2, T2* and extracellular volume: A consensus statement by the Society for Cardiovascular Magnetic Resonance (SCMR) endorsed by the European Association for Cardiovascular Imaging (EACVI). J Cardiovasc Magn Reson. 2017 Oct 9;19(1):75.

152. Kellman P, Hansen MS, Nielles-Vallespin S, Nickander J, Themudo R, Ugander M, et al. Myocardial perfusion cardiovascular magnetic resonance: optimized dual sequence and reconstruction for quantification. Journal of Cardiovascular Magnetic Resonance. 2017;19(1):43.

153. Hansen MS, Sørensen TS. Gadgetron: an open source framework for medical image reconstruction. Magn Reson Med. 2013 Jun;69(6):1768–76.

154. Chow K, Kellman P, Spottiswoode BS, Nielles-Vallespin S, Arai AE, Salerno M, et al. Saturation pulse design for quantitative myocardial T1 mapping. J Cardiovasc Magn Reson [Internet]. 2015 Oct 1 [cited 2016 Jun 23];17. Available from: http://www.ncbi.nlm.nih.gov/pmc/articles/PMC4589956/

155. Xue H, Hansen MS, Nielles-Vallespin S, Arai AE, Kellman P. Inline quantitative myocardial perfusion flow mapping. Journal of Cardiovascular Magnetic Resonance. 2016;18(1):1–3.

156. Breuer FA, Kellman P, Griswold MA, Jakob PM. Dynamic autocalibrated parallel imaging using temporal GRAPPA (TGRAPPA). Magn Reson Med. 2005 Apr 1;53(4):981–5.

157. Kellman P, Arai AE. Imaging sequences for first pass perfusion --a review. J Cardiovasc Magn Reson. 2007;9(3):525–37.

158. Kellman P, Epstein FH, McVeigh ER. Adaptive sensitivity encoding incorporating temporal filtering (TSENSE)†. Magn Reson Med. 2001 May 1;45(5):846–52.

159. Kellman P, McVeigh ER. Image Reconstruction in SNR Units: A General Method for SNR Measurement. Magn Reson Med. 2005 Dec;54(6):1439–47.

160. Nielles-Vallespin S, Kellman P, Hsu LY, Arai AE. FLASH proton density imaging for improved surface coil intensity correction in quantitative and semi-quantitative SSFP perfusion cardiovascular magnetic resonance. J Cardiovasc Magn Reson [Internet]. 2015 Feb 17 [cited 2016 Jun 23];17(1). Available from: http://www.ncbi.nlm.nih.gov/pmc/articles/PMC4331176/

161. Kellman P, Larson AC, Hsu LY, Chung YC, Simonetti OP, McVeigh ER, et al. Motion-Corrected Free-Breathing Delayed Enhancement Imaging of Myocardial Infarction. Magn Reson Med. 2005 Jan;53(1):194–200.

162. Ledesma-Carbayo MJ, Kellman P, Hsu LY, Arai AE, McVeigh ER. Motion corrected free-breathing delayed-enhancement imaging of myocardial infarction using nonrigid registration. J Magn Reson Imaging. 2007 Jul;26(1):184–90.

163. Xue H, Zuehlsdorff S, Kellman P, Arai A, Nielles-Vallespin S, Chefdhotel C, et al. Unsupervised inline analysis of cardiac perfusion MRI. Med Image Comput Comput Assist Interv. 2009;12(Pt 2):741–9.

164. Xue H, Shah S, Greiser A, Guetter C, Littmann A, Jolly MP, et al. Motion correction for myocardial T1 mapping using image registration with synthetic image estimation. Magn Reson Med. 2012 Jun;67(6):1644–55.

165. Treibel TA, Fontana M, Maestrini V, Castelletti S, Rosmini S, Simpson J, et al. Automatic Measurement of the Myocardial Interstitium: Synthetic Extracellular Volume Quantification Without Hematocrit Sampling. JACC Cardiovasc Imaging. 2016 Jan;9(1):54–63.

166. Xue H, Hansen MS, Nielles-Vallespin S, Arai AE, Kellman P. Correcting T2* effects in the myocardial perfusion arterial input function avoids overestimation of myocardial blood flow. Journal of Cardiovascular Magnetic Resonance. 2016;18(1):1–2.

167. Kellman P, Olivieri L, Grant E, Berul CI, O'Brien K, Ratnayaka K, et al. Dark blood Late Gadolinium Enhancement improves conspicuity of ablation lesions. Journal of Cardiovascular Magnetic Resonance. 2016;18(1):1–2.

168. Bassingthwaighte JB. Overview of the processes of delivery: flow, transmembrane transport, reaction, and retention. Circulation. 1985 Nov;72(5 0 2):IV39–46.

169. Bassingthwaighte JB, Sparks HV. INDICATOR DILUTION ESTIMATION OF CAPILLARY ENDOTHELIAL TRANSPORT. Annu Rev Physiol. 1986;48:321–34.

170. Brown LAE, Onciul SC, Broadbent DA, Johnson K, Fent GJ, Foley JRJ, et al. Fully automated, inline quantification of myocardial blood flow with cardiovascular magnetic resonance: repeatability of measurements in healthy subjects. J Cardiovasc Magn Reson. 2018 Jul 9;20(1):48.

171. Messroghli DR, Radjenovic A, Kozerke S, Higgins DM, Sivananthan MU, Ridgway JP. Modified Look-Locker inversion recovery (MOLLI) for high-resolution T1 mapping of the heart. Magn Reson Med. 2004 Jul;52(1):141–6.

172. Bassingthwaighte JB, Wang CY, Chan IS. Blood-tissue exchange via transport and transformation by capillary endothelial cells. Circ Res. 1989 Oct;65(4):997–1020.

173. Xue H, Tseng E, Knott KD, Kotecha T, Brown L, Plein S, et al. Automated detection of left ventricle in arterial input function images for inline perfusion mapping using deep learning: A study of 15,000 patients. Magn Reson Med. 2020 May 7;

174. Tu S, Xu L, Ligthart J, Xu B, Witberg K, Sun Z, et al. In vivo comparison of arterial lumen dimensions assessed by co-registered three-dimensional (3D) quantitative coronary angiography, intravascular ultrasound and optical coherence tomography. Int J Cardiovasc Imaging. 2012 Aug;28(6):1315–27.

175. DeLong ER, DeLong DM, Clarke-Pearson DL. Comparing the areas under two or more correlated receiver operating characteristic curves: a nonparametric approach. Biometrics. 1988 Sep;44(3):837–45.

176. Hsu LY, Groves DW, Aletras AH, Kellman P, Arai AE. A quantitative pixel-wise measurement of myocardial blood flow by contrast-enhanced first-pass CMR perfusion imaging: microsphere validation in dogs and feasibility study in humans. JACC Cardiovasc Imaging. 2012 Feb;5(2):154–66.

177. Kunze KP, Nekolla SG, Rischpler C, Zhang SH, Hayes C, Langwieser N, et al. Myocardial perfusion quantification using simultaneously acquired 13NH3-ammonia PET and dynamic contrast-enhanced MRI in patients at rest and stress. Magnetic Resonance in Medicine [Internet]. [cited 2018 May 7]; Available from: https://onlinelibrary.wiley.com/doi/abs/10.1002/mrm.27213

178. Gould KL, Johnson NP, Bateman TM, Beanlands RS, Bengel FM, Bober R, et al. Anatomic versus physiologic assessment of coronary artery disease. Role of coronary flow reserve, fractional flow reserve, and positron emission tomography imaging in revascularization decision-making. J Am Coll Cardiol. 2013 Oct 29;62(18):1639–53.

179. Di Carli MF, Janisse J, Grunberger G, Ager J. Role of chronic hyperglycemia in the pathogenesis of coronary microvascular dysfunction in diabetes. J Am Coll Cardiol. 2003 Apr 16;41(8):1387–93.

180. Naya M, Murthy VL, Foster CR, Gaber M, Klein J, Hainer J, et al. Prognostic Interplay of Coronary Artery Calcification and Underlying Vascular Dysfunction in Patients With Suspected Coronary Artery Disease. J Am Coll Cardiol. 2013 May 21;61(20):2098–106.

181. Pepine CJ, Anderson RD, Sharaf BL, Reis SE, Smith KM, Handberg EM, et al. Coronary microvascular reactivity to adenosine predicts adverse outcome in women evaluated for suspected ischemia results from the National Heart, Lung and Blood Institute WISE (Women's Ischemia Syndrome Evaluation) study. J Am Coll Cardiol. 2010 Jun 22;55(25):2825–32.

182. Taqueti VR, Solomon SD, Shah AM, Desai AS, Groarke JD, Osborne MT, et al. Coronary microvascular dysfunction and future risk of heart failure with preserved ejection fraction. Eur Heart J. 2018 Mar 7;39(10):840–9.

183. Bhuva Anish N., Bai Wenjia, Lau Clement, Davies Rhodri H., Ye Yang, Bulluck Heeraj, et al. A Multicenter, Scan-Rescan, Human and Machine Learning CMR Study to Test Generalizability and Precision in Imaging Biomarker Analysis. Circulation: Cardiovascular Imaging. 2019 Oct 1;12(10):e009214.

184. Xue, Hui, Davies, Rhodri H., Brown, Louise AE, Knott, Kristopher D., Kotecha, Tushar, Fontana, Marianna, et al. Automated Inline Analysis of Myocardial Perfusion MRI with Deep Learning. Available from: https://arxiv.org/abs/191100625 [December 2019].

185. FIRTH D. Bias reduction of maximum likelihood estimates. Biometrika. 1993 Mar 1;80(1):27–38.

186. Kotecha T, Martinez-Naharro A, Boldrini M, Knight D, Hawkins P, Kalra S, et al. Automated Pixel-Wise Quantitative Myocardial Perfusion Mapping by CMR to Detect Obstructive Coronary Artery Disease and Coronary Microvascular Dysfunction: Validation Against Invasive Coronary Physiology. JACC Cardiovasc Imaging. 2019 Feb 11;

187. Sammut EC, Villa ADM, Di Giovine G, Dancy L, Bosio F, Gibbs T, et al. Prognostic Value of Quantitative Stress Perfusion Cardiac Magnetic Resonance. JACC Cardiovasc Imaging. 2018 May;11(5):686–94.

188. Gupta A, Taqueti VR, van de Hoef TP, Bajaj NS, Bravo PE, Murthy VL, et al. Integrated Noninvasive Physiological Assessment of Coronary Circulatory Function and Impact on Cardiovascular Mortality in Patients With Stable Coronary Artery Disease. Circulation. 2017 Dec 12;136(24):2325–36.

189. De Bruyne B, Hersbach F, Pijls NH, Bartunek J, Bech JW, Heyndrickx GR, et al. Abnormal epicardial coronary resistance in patients with diffuse atherosclerosis but "Normal" coronary angiography. Circulation. 2001 Nov 13;104(20):2401–6.

190. Ahn SG, Suh J, Hung OY, Lee HS, Bouchi YH, Zeng W, et al. Discordance Between Fractional Flow Reserve and Coronary Flow Reserve: Insights From Intracoronary Imaging and Physiological Assessment. JACC Cardiovasc Interv. 2017 22;10(10):999–1007.

191. Jespersen L, Hvelplund A, Abildstrøm SZ, Pedersen F, Galatius S, Madsen JK, et al. Stable angina pectoris with no obstructive coronary artery disease is associated with increased risks of major adverse cardiovascular events. Eur Heart J. 2012 Mar;33(6):734–44.

192. Egashira K, Inou T, Hirooka Y, Yamada A, Urabe Y, Takeshita A. Evidence of Impaired Endothelium-Dependent Coronary Vasodilatation in Patients with Angina Pectoris and Normal Coronary Angiograms. New England Journal of Medicine. 1993 Jun 10;328(23):1659–64.

193. Quyyumi AA, Cannon RO, Panza JA, Diodati JG, Epstein SE. Endothelial dysfunction in patients with chest pain and normal coronary arteries. Circulation. 1992 Dec;86(6):1864–71.

194. Hasdai D, Gibbons RJ, Holmes DR, Higano ST, Lerman A. Coronary endothelial dysfunction in humans is associated with myocardial perfusion defects. Circulation. 1997 Nov 18;96(10):3390–5.

195. Xue H, Davies R, Brown LAE, Knott KD, Kotecha T, Fontana M, Plein S, Moon JC, Kellman. Automated Inline Analysis of Myocardial Perfusion MRI with Deep Learning. Radiology AI. 2020. In Press.

196. Wu FZ, Wu MT. 2014 SCCT guidelines for the interpretation and reporting of coronary CT angiography: a report of the Society of Cardiovascular Computed Tomography Guidelines Committee. J Cardiovasc Comput Tomogr. 2015 Apr;9(2):e3.

197. Nahser PJ, Brown RE, Oskarsson H, Winniford MD, Rossen JD. Maximal coronary flow reserve and metabolic coronary vasodilation in patients with diabetes mellitus. Circulation. 1995 Feb 1;91(3):635–40.

198. Wang L, Jerosch-Herold M, Jacobs DR, Shahar E, Folsom AR. Coronary risk factors and myocardial perfusion in asymptomatic adults: the Multi-Ethnic Study of Atherosclerosis (MESA). J Am Coll Cardiol. 2006 Feb 7;47(3):565–72.

199. Sara JD, Widmer RJ, Matsuzawa Y, Lennon RJ, Lerman LO, Lerman A. Prevalence of Coronary Microvascular Dysfunction Among Patients With Chest Pain and Nonobstructive Coronary Artery Disease. JACC Cardiovasc Interv. 2015 Sep;8(11):1445–53.

200. Yokoyama I, Momomura S ichi, Ohtake T, Yonekura K, Nishikawa J, Sasaki Y, et al. Reduced Myocardial Flow Reserve in Non–Insulin-Dependent Diabetes Mellitus. Journal of the American College of Cardiology. 1997 Nov 15;30(6):1472–7.

201. Prior JO, Quiñones MJ, Hernandez-Pampaloni M, Facta AD, Schindler TH, Sayre JW, et al. Coronary circulatory dysfunction in insulin resistance, impaired glucose tolerance, and type 2 diabetes mellitus. Circulation. 2005 May 10;111(18):2291–8.

202. Rizzoni D, Porteri E, Guelfi D, Muiesan ML, Valentini U, Cimino A, et al. Structural alterations in subcutaneous small arteries of normotensive and hypertensive patients with non-insulin-dependent diabetes mellitus. Circulation. 2001 Mar 6;103(9):1238–44.

203. Lillioja S, Young AA, Culter CL, Ivy JL, Abbott WG, Zawadzki JK, et al. Skeletal muscle capillary density and fiber type are possible determinants of in vivo insulin resistance in man. J Clin Invest. 1987 Aug;80(2):415–24.

204. Savoia C, Schiffrin EL. Vascular inflammation in hypertension and diabetes: molecular mechanisms and therapeutic interventions. Clin Sci. 2007 Jun;112(7):375–84.

205. Vogt M, Motz W, Scheler S, Strauer BE. Disorders of coronary microcirculation and arrhythmias in systemic arterial hypertension. Am J Cardiol. 1990 Apr 3;65(14):45G-50G.

206. Olsen MH, Wachtell K, Meyer C, Hove JD, Palmieri V, Dige-Petersen H, et al. Association between vascular dysfunction and reduced myocardial flow reserve in patients with hypertension: a LIFE substudy. J Hum Hypertens. 2004 Jun;18(6):445–52.

207. Kaufmann PA, Gnecchi-Ruscone T, di Terlizzi M, Schäfers KP, Lüscher TF, Camici PG. Coronary heart disease in smokers: vitamin C restores coronary microcirculatory function. Circulation. 2000 Sep 12;102(11):1233–8.

208. Kaufmann PA, Gnecchi-Ruscone T, Schäfers KP, Lüscher TF, Camici PG. Low density lipoprotein cholesterol and coronary microvascular dysfunction in hypercholesterolemia. J Am Coll Cardiol. 2000 Jul;36(1):103–9.

209. Taylor CA, Fonte TA, Min JK. Computational Fluid Dynamics Applied to Cardiac Computed Tomography for Noninvasive Quantification of Fractional Flow Reserve: Scientific Basis. Journal of the American College of Cardiology. 2013 Jun 4;61(22):2233–41.

210. van de Hoef TP, Nolte F, EchavarrÍa-Pinto M, van Lavieren MA, Damman P, Chamuleau SAJ, et al. Impact of hyperaemic microvascular resistance on fractional flow reserve measurements in patients with stable coronary artery disease: insights from combined stenosis and microvascular resistance assessment. Heart. 2014 Jun;100(12):951–9.

211. Chareonthaitawee P, Kaufmann PA, Rimoldi O, Camici PG. Heterogeneity of resting and hyperemic myocardial blood flow in healthy humans. Cardiovasc Res. 2001 Apr;50(1):151–61.

212. Duvernoy CS, Meyer C, Seifert-Klauss V, Dayanikli F, Matsunari I, Rattenhuber J, et al. Gender differences in myocardial blood flow dynamics: lipid profile and hemodynamic effects. J Am Coll Cardiol. 1999 Feb;33(2):463–70.

213. Knott KD, Seraphim A, Augusto JB, Xue H, Chacko L, Aung N, et al. The Prognostic Significance of Quantitative Myocardial Perfusion: An Artificial Intelligence-Based Approach Using Perfusion Mapping. Circulation. 2020 Apr 21;141(16):1282–91.

214. Eng CM, Fletcher J, Wilcox WR, Waldek S, Scott CR, Sillence DO, et al. Fabry disease: baseline medical characteristics of a cohort of 1765 males and females in the Fabry Registry. J Inherit Metab Dis. 2007 Apr;30(2):184–92.

215. Waldek S, Patel MR, Banikazemi M, Lemay R, Lee P. Life expectancy and cause of death in males and females with Fabry disease: findings from the Fabry Registry. Genet Med. 2009 Nov;11(11):790–6.

216. Thurberg BL, Randolph Byers H, Granter SR, Phelps RG, Gordon RE, O'Callaghan M. Monitoring the 3-year efficacy of enzyme replacement therapy in fabry disease by repeated skin biopsies. J Invest Dermatol. 2004 Apr;122(4):900–8.

217. Thurberg BL, Rennke H, Colvin RB, Dikman S, Gordon RE, Collins AB, et al. Globotriaosylceramide accumulation in the Fabry kidney is cleared from multiple cell types after enzyme replacement therapy. Kidney Int. 2002 Dec;62(6):1933–46.

218. Hughes DA, Nicholls K, Shankar SP, Sunder-Plassmann G, Koeller D, Nedd K, et al. Oral pharmacological chaperone migalastat compared with enzyme replacement therapy in Fabry disease: 18-month results from the randomised phase III ATTRACT study. J Med Genet. 2017;54(4):288–96.

219. Sado DM, White SK, Piechnik SK, Banypersad SM, Treibel T, Captur G, et al. Identification and assessment of Anderson-Fabry disease by cardiovascular magnetic resonance noncontrast myocardial T1 mapping. Circ Cardiovasc Imaging. 2013 May 1;6(3):392–8.

220. Moon JCC, Sachdev B, Elkington AG, McKenna WJ, Mehta A, Pennell DJ, et al. Gadolinium enhanced cardiovascular magnetic resonance in Anderson-Fabry disease. Evidence for a disease specific abnormality of the myocardial interstitium. Eur Heart J. 2003 Dec;24(23):2151–5.

221. Moon JC, Sheppard M, Reed E, Lee P, Elliott PM, Pennell DJ. The histological basis of late gadolinium enhancement cardiovascular magnetic resonance in a patient with Anderson-Fabry disease. J Cardiovasc Magn Reson. 2006;8(3):479–82.

222. Oliveira JP. Staging of Fabry disease using renal biopsies. Clin Ther. 2007;29 Suppl A:S15-16.

223. Namdar M, Gebhard C, Studiger R, Shi Y, Mocharla P, Schmied C, et al. Globotriaosylsphingosine accumulation and not alpha-galactosidase-A deficiency causes endothelial dysfunction in Fabry disease. PLoS ONE. 2012;7(4):e36373.

224. Bergmann SR, Fox KA, Rand AL, McElvany KD, Welch MJ, Markham J, et al. Quantification of regional myocardial blood flow in vivo with H215O. Circulation. 1984 Oct;70(4):724–33.

225. Camici P, Chiriatti G, Lorenzoni R, Bellina RC, Gistri R, Italiani G, et al. Coronary vasodilation is impaired in both hypertrophied and nonhypertrophied myocardium of patients with hypertrophic cardiomyopathy: a study with nitrogen-13 ammonia and positron emission tomography. J Am Coll Cardiol. 1991 Mar 15;17(4):879–86.

226. Tomberli B, Cecchi F, Sciagrà R, Berti V, Lisi F, Torricelli F, et al. Coronary microvascular dysfunction is an early feature of cardiac involvement in patients with Anderson-Fabry disease. Eur J Heart Fail. 2013 Dec;15(12):1363–73.

227. Kalliokoski RJ, Kantola I, Kalliokoski KK, Engblom E, Sundell J, Hannukainen JC, et al. The effect of 12-month enzyme replacement therapy on myocardial perfusion in patients with Fabry disease. J Inherit Metab Dis. 2006 Feb;29(1):112–8.

228. Elliott PM, Borger MA, Borggrefe M, Cecchi F, Charron P, Hagege AA, et al. 2014 ESC Guidelines on diagnosis and management of hypertrophic cardiomyopathy: the Task Force for the Diagnosis and Management of Hypertrophic Cardiomyopathy of the European Society of Cardiology (ESC). Eur Heart J. 2014 Oct 14;35(39):2733–79.

229. Vermes E, Childs H, Carbone I, Barckow P, Friedrich MG. Auto-threshold quantification of late gadolinium enhancement in patients with acute heart disease. J Magn Reson Imaging. 2013 Feb;37(2):382–90.

230. Germain DP, Hughes DA, Nicholls K, Bichet DG, Giugliani R, Wilcox WR, et al. Treatment of Fabry's Disease with the Pharmacologic Chaperone Migalastat. N Engl J Med. 2016 Aug 11;375(6):545–55.

231. Chimenti C, Morgante E, Tanzilli G, Mangieri E, Critelli G, Gaudio C, et al. Angina in fabry disease reflects coronary small vessel disease. Circ Heart Fail. 2008 Sep;1(3):161–9.

232. Mourad JJ, Hanon O, Deverre JR, Camici PG, Sellier P, Duboc D, et al. Improvement of impaired coronary vasodilator reserve in hypertensive patients by low-dose ACE inhibitor/diuretic therapy: a pilot PET study. J Renin Angiotensin Aldosterone Syst. 2003 Jun;4(2):94–5.

233. Neglia D, Fommei E, Varela-Carver A, Mancini M, Ghione S, Lombardi M, et al. Perindopril and indapamide reverse coronary microvascular remodelling and improve flow in arterial hypertension. J Hypertens. 2011 Feb;29(2):364–72.

234. Hittinger L, Shannon RP, Bishop SP, Gelpi RJ, Vatner SF. Subendomyocardial exhaustion of blood flow reserve and increased fibrosis in conscious dogs with heart failure. Circ Res. 1989 Oct;65(4):971–80.